ENCLOSURE 2

MFN 15-079

NEDO-33406-A, Revision 3

Non-Proprietary Information– Class I (Public)

IMPORTANT NOTICE

This is a non-proprietary version of NEDC-33406P-A, Revision 3, which has the proprietary information removed. Portions of the enclosure that have been removed are indicated by an open and closed double square bracket as shown here [[ ]].

Note the NRC's Final Safety Evaluation is enclosed in NEDO-33406-A, Revision 3. Portions of the Final Safety Evaluation that have been removed are indicated with a single square bracket as shown here. [ ].

Global Nuclear Fuel
A Joint Venture of GE,Toshiba, & Hitachi

NEDO-33406-A
Revision 3
December 2015

NON-PROPRIETARY INFORMATION – CLASS I (PUBLIC)

Licensing Topical Report

Additive Fuel Pellets for GNF Fuel Designs

INFORMATION NOTICE

This is a non-proprietary version of NEDC-33406P-A, Revision 3, which has the proprietary information removed. Portions of the document that have been removed are indicated by an open and closed double square bracket as shown here [[ ]].

Within the US NRC Safety Evaluation, the proprietary portions of the document that have been removed are indicated by an open and closed single square bracket as shown here [ ].

IMPORTANT NOTICE REGARDING CONTENTS OF THIS REPORT

PLEASE READ CAREFULLY

The design, engineering, and other information contained in this document are furnished for the purpose of obtaining Nuclear Regulatory Commission (NRC) approval of Additive Fuel Pellets for GNF Fuel Designs. The only undertakings of GNF-A with respect to information in this document are contained in contracts between GNF-A and its customers or participating utilities, and nothing contained in this document shall be construed as changing that contract. The use of this information by anyone other than that for which it is intended is not authorized; and with respect to any unauthorized use, GNF-A makes no representation or warranty, and assumes no liability as to the completeness, accuracy, or usefulness of the information contained in this document.

November 9, 2015

Mr. Jerald G. Head
Senior Vice President, Regulatory Affairs
General Electric-Hitachi
Nuclear Energy Americas, LLC
P.O. Box 780, M/C A-18
Wilmington, NC 28401-0780

SUBJECT: FINAL SAFETY EVALUATION FOR GENERAL ELECTRIC HITACHI NUCLEAR ENERGY AMERICAS, LLC TOPICAL REPORT NEDC-33406P, REVISION 2, "ADDITIVE FUEL PELLETS FOR GNF FUEL DESIGNS" (TAC NO. ME3082)

Dear Mr. Head:

By letter dated December 18, 2009 (Agencywide Documents Access and Management System (ADAMS) Package Accession No. ML093560114), GE Hitachi Nuclear Energy Americas, LLC (GEH) submitted Topical Report (TR) NEDC-33406P, Revision 2, "Additive Fuel Pellets for GNF [Global Nuclear Fuel – Americas, LLC] Fuel Designs," to the U.S. Nuclear Regulatory Commission (NRC) staff for review.

By letter dated December 11, 2014, an NRC draft safety evaluation (SE) regarding our approval of TR NEDC-33406P, Revision 2, was provided for your review and comment. By letter dated February 16, 2015, you provided comments on the draft SE. The NRC staff's disposition of the GEH comments on the draft SE are discussed in the attachment to the final SE enclosed with this letter. Please note the enclosed SE is a non-proprietary version prepared for public release.

The NRC staff has found that TR NEDC-33406P, Revision 2, is acceptable for referencing in licensing applications for nuclear power plants to the extent specified and under the limitations delineated in the TR and in the enclosed final SE. The final SE defines the basis for our acceptance of the TR.

Our acceptance applies only to material provided in the subject TR. We do not intend to repeat our review of the acceptable material described in the TR. When the TR appears as a reference in license applications, our review will ensure that the material presented applies to the specific plant involved. License amendment requests that deviate from this TR will be subject to a plant-specific review in accordance with applicable review standards.

In accordance with the guidance provided on the NRC website, we request that GEH publish approved proprietary and non-proprietary versions of TR NEDC-33406P within three months of receipt of this letter. The approved versions shall incorporate this letter and the enclosed final SE after the title page. Also, they must contain historical review information, including NRC requests for additional information and your responses. The approved versions shall include an "-A" (designating approved) following the TR identification symbol.

If future changes to the NRC's regulatory requirements affect the acceptability of this TR, GEH will be expected to revise the TR appropriately. Licensees referencing this TR would be expected to justify its continued applicability or evaluate their plant using the revised TR.

Sincerely,

/RA/

Mirela Gavrilas, Deputy Director
Division of Policy and Rulemaking
Office of Nuclear Reactor Regulation

Project No. 710

Enclosure:
Final Safety Evaluation (Non-Proprietary)

In accordance with the guidance provided on the NRC website, we request that GEH publish approved proprietary and non-proprietary versions of TR NEDC-33406P within three months of receipt of this letter. The approved versions shall incorporate this letter and the enclosed final SE after the title page. Also, they must contain historical review information, including NRC requests for additional information and your responses. The approved versions shall include an "-A" (designating approved) following the TR identification symbol.

If future changes to the NRC's regulatory requirements affect the acceptability of this TR, GEH will be expected to revise the TR appropriately. Licensees referencing this TR would be expected to justify its continued applicability or evaluate their plant using the revised TR.

Sincerely,

/RA/

Mirela Gavrilas, Deputy Director
Division of Policy and Rulemaking
Office of Nuclear Reactor Regulation

Project No. 710

Enclosure:
Final Safety Evaluation (Non-Proprietary)

DISTRIBUTION:

RidsNrrDpr	RidsResOd
RidsNrrDprPlpb	JDean
RidsNrrLADHarrison	RidsOgcMailCenter
RidsACRS_MailCTR	RidsNrrDss
RidsNrrDssSnpb	AMendiola
JGolla	MPanicker
RidsNroOd	KHsueh

ADAMS Accession Nos.: ML15195A459 (Package); ML15190A103 (Cover Letter & SE); ML15190A113 (Attachment); *concurred via e-mail NRR-106

OFFICE	PLPB/PM	PLPB/LA*	SNPB/BC	PLPB/BC	DPR/DD
NAME	JGolla	DHarrison	JDean	AMendiola	MGavrilas
DATE	10/26/2015	10/08/2015	10/26/2015	10/30/2015	11/09/2015

OFFICIAL RECORD COPY

GE-Hitachi Nuclear Energy Americas Project No. 710
cc:

Mr. Jerald G. Head
Senior Vice President, Regulatory Affairs
GE-Hitachi Nuclear Energy
P.O. Box 780 M/C A-18
Wilmington, NC 28401
Jerald.head@ge.com

Mr. James F. Harrison
GE-Hitachi Nuclear Energy Americas LLC
Vice President - Fuel Licensing
P.O. Box 780, M/C A-55
Wilmington, NC 28401-0780
james.harrison@ge.com

Ms. Patricia L. Campbell
Vice President, Washington Regulatory Affairs
GE-Hitachi Nuclear Energy Americas LLC
1299 Pennsylvania Avenue, NW
9th Floor
Washington, DC 20004
patriciaL.campbell@ge.com

Mr. Brian R. Moore
Vice President, Fuel Engineering, Acting
Global Nuclear Fuel–Americas, LLC
P.O. Box 780, M/C A-55
Wilmington, NC 28401-0780
Brian.Moore@gnf.com

SAFETY EVALUATION BY THE

OFFICE OF NUCLEAR REACTOR REGULATION

LICENSING TOPICAL REPORT

ADDITIVE FUEL PELLETS FOR GNF FUEL DESIGNS

NEDC-33406P, REVISION 2

(TAC NO. ME3082)

1.0 INTRODUCTION AND BACKGROUND

By letter dated December 18, 2009, Global Nuclear Fuel (GNF) submitted a Licensing Topical Report (LTR), "Additive Fuel Pellets for GNF Fuel Designs," NEDC-33406P, Revision 2, December 18, 2009 (Reference 1). GNF desires to introduce aluminosilicate additive fuel pellets in to GNF fuel products to increase fuel reliability and operational flexibility of GNF nuclear fuel. The scope of this LTR focuses on relevant fuel material properties and in-core behavioral characteristics that are affected by the addition of additive to the UO_2 fuel. Material properties of fuel with additive such as melting, density, thermal expansion, thermal conductivity, grain size and grain strength, stored thermal energy, creep, yield strength, elastic modulus, strain hardening coefficient and tangent modulus, plastic Poisson's ratio, and swelling are treated using the PRIME thermal-mechanical code (Reference 2).

This LTR describes the proposed introduction of aluminosilicate additive fuel pellets into normal core reloads. A nominal value of **[**

]

Pacific Northwest National Laboratory (PNNL) has supported this review as a consultant to the NRC staff. Several rounds of request for additional information questions from both the NRC staff and the PNNL staff were sent to GNF. The first round of RAIs is listed in Reference 2. All responses to the RAI questions are listed in Reference 3.

This review focused on the following major areas of the material properties (Section 2.0 of Reference 1) that includes microstructure, melting temperature, theoretical density, thermal expansion, thermal conductivity, specific heat, grain size and growth, creep, yield stress, modulus of elasticity, strain hardening coefficient and tangent modulus, plastic Poisson's ratio, and rim structure effects. The review also covers the following in-reactor performance concerns (Section 3.0 of Reference 1) from the use of additive fuel; impact of fuel oxidation resulting in fuel washout when exposed to primary coolant water in the event of fuel failure, impact of fuel melting limits, impact on reactivity

insertion accident (RIA) thresholds, impact on in-reactor densification, and impact on release of fission products and accident source terms. The review covers the in-reactor data used to verify the performance of additive fuel (Section 4.0) and the licensing criteria (Section 5.0) used to verify satisfactory performance of the additive fuel.

The PRIME code (Reference 4) was used by GNF for stored energy and rod pressure inputs to loss-of-coolant accident (LOCA), determining maximum rod internal pressure, cladding strain, cladding fatigue, and fuel melting analyses. Comparative calculations have been made with the NRC-developed FRAPCON-3 fuel performance code (References 5 and 6) for comparison to typical PRIME specified acceptable fuel design limit (SAFDL) calculations for maximum rod internal pressure, LOCA temperature (stored energy) and pressure, fuel melting, and clad strain analyses. An evaluation of the use of PRIME and design limits for these licensing applications is discussed in Sections 3.3 and 3.4. Operating experience of additive fuel is discussed in Sections 3.3 and 3.5. The conclusions and recommended limitations are presented in Section 4.2.

The NRC audit code, FRAPCON-3 (Reference 5), has been used as an aid in this review to assess the models and calculation results from PRIME. This code was originally assessed against a large volume of low and high burnup fuel performance data (Reference 6) and has been continually assessed against newer high burnup data (Reference 7) as it became available.

2.0 REGULATORY EVALUATION

The NRC staff used the guidance of Standard Review Plan (SRP), NUREG-0800, Section 4.2, “Fuel System Design” for the review of NEDC-33406P, Revision 2. SRP Section 4.2 acceptance criteria are based on meeting the requirements of General Design Criteria (GDC) 10 of Appendix A of Title 10 of the *Code of Federal Regulations* (10 CFR) Part 50.

GDC 10 states: *The reactor core and associated coolant, control, and protection systems shall be designed with the appropriate margin to assure that specified acceptable fuel design limits are not exceeded during any condition of normal operation, including the effects of anticipated operational occurrences.*

GDC 10 establishes SAFDLs to ensure that the fuel is “not damaged.” That means that fuel rods do not fail, fuel system dimensions remain within operational tolerances, and functional capabilities are not reduced below those assumed in the safety analysis.

In accordance with SRP Section 4.2, the objectives of the fuel system safety review are to provide assurance that:

a. The fuel system is not damaged as a result of normal operation and anticipated operational occurrences (AOOs), fuel system damage is never so severe as to prevent control rod insertion when it is required,

b. The number of fuel rod failures is not underestimated for postulated accidents, and

c. Coolability is always maintained.

The NRC staff reviewed the additive fuel pellet topical report to: (1) ensure that the material properties and in-core behavioral characteristics of additive fuel as analyzed using the PRIME code and supported by confirmatory calculations using the FRAPCON audit code are capable of accurately (or conservatively) ensuring the fuel system safety criteria, (2) identify any limitations on the behavioral characteristics of the additive fuel, and (3) ensure compliance of fuel design criteria with licensing requirements of fuel designs and is capable of ensuring compliance with SRP Section 4.2 guidance criteria.

3.0 TECHNICAL EVALUATION

Global Nuclear Fuels (GNF) submitted the LTR on additive fuel pellets for its fuel designs in order to increase the reliability and operational flexibility of nuclear reactor fuel bundles and cores.

This review focused on the following major areas of the material properties and in-reactor performance issues such as washout behavior, fuel melting, RIA behavior, in-reactor densification, validity of alternate source term (AST) assumptions, and long term fuel storage. The review also covered the in-reactor data used to verify the performance of additive fuel and the licensing criteria used to verify satisfactory performance of the additive fuel.

3.1 Additive Fuel Material Properties

The GNF additive fuel material properties addressed in this section are, in general, applicable to properties under normal operation and AOOs but some are also applicable to design basis accidents such as thermal conductivity, thermal expansion, specific heat, and stored thermal energy. Other properties which are unique to in-reactor fuel performance such as washout behavior that results in oxidation of the fuel upon introduction of water in to the fuel rod after a breach of fuel rod cladding, fuel melting limits, RIA failure thresholds, in-reactor densification, and release of fission products will be addressed in Section 3.2.

3.1.1 *Microstructure*

Microstructure is not usually defined as a material property, however, it can impact the properties of a material, and as a result it is included in this section. The material properties it can impact are the fuel melting temperature and may impact the fission gas release (FGR). During fabrication the aluminosilicate additive **[**

] as depicted in Figure 2-1 of the topical report. The additive has a **[**

] for this phase composition.

Therefore, [ ] can exist at the grain boundaries and will be discussed in Section 3.1.2 on fuel melting. The additive fuel microstructure is not modeled explicitly in the PRIME fuel performance code but is implicitly included in the models for fuel melting and FGR.

[
]. This will be discussed in Section 3.3.2 on the comparison of the FGR model comparisons to additive fuel FGR data.

3.1.2 *Fuel Melting*

Fuel melting is generally not allowed during normal operation nor during AOOs to ensure that the fuel does not (1) relocate within the fuel rod, (2) result in excessive FGR that could exceed the rod pressure limit, and (3) prevent deleterious reaction between the molten fuel and cladding. The intent of no fuel melting for UO_2 criteria is to assure geometric stability of the pellet and preclude the migration of liquid UO_2. For normal operation and AOOs fuel relocation is more limiting than reaction with the cladding because relocation will have to be present for the reaction with the cladding to take place.

The melting temperature for additive fuel is [

] is called the eutectic temperature. Therefore, a small amount of liquid begins just above the eutectic temperature. GNF has provided a significant amount of data to determine the eutectic temperature for their composition of additive fuel. The NRC staff finds the GNF determination of eutectic temperature acceptable.

For the purpose of additive fuel pellets, in order to define the point of melting that is acceptable for fuel performance, GNF has proposed a [

] has been determined based on experimental testing of single additive fuel pellets in a furnace under isothermal temperatures (no temperature gradients in the fuel pellet). The isothermal temperature of [

].

The NRC staff requested (Reference 3, RAI 24) information regarding whether fuel [
] has been examined in full length (12 foot) fuel rods because the weight of a 12 foot fuel column is significant compared to testing of a single fuel pellet. The staff also requested the length of time for the [ ] along with a suggestion/ question on whether there should be a time limit for an AOO event [
].

GNF responded that they do not have slumping tests for **[**

] that is above the eutectic temperature where the **[**
] for AOO events. The center region of the pellet has **[** **]** but the outer region of the pellet is well below the eutectic temperature.

The fuel pellets above and below the small number of pellets with **[** **]** will also be solid (no liquid). That will help contain the **[** **]** in the center of the pellet. GNF also stated that power ramp tests to simulate AOO events on fuel rods with additive fuel have shown a small amount of **[** **]** movement due to pellet-cladding mechanical interaction (PCMI) but the **[** **]** did not extend beyond the eutectic temperature such that the outer fuel below the eutectic temperature constrained the **[** **]** fuel. GNF further noted that for both thermal overpower (TOP) and mechanical overpower (MOP) events of **[** **]** overpower (OP) and **[** **]** OP, respectively, the **[** **]** for the nominal additive concentration of **[** **]**. It is also noted that since both conditions must be met, the TOP event is the most limiting as it provides a limit on the maximum fuel centerline temperature. GNF provided an additional analysis demonstrating that the **[**
] cannot be achieved at any axial node for a TOP event. GNF responded to the staff request regarding the limitation in time with a significant fraction of fuel above the eutectic temperature. The objective of the current additive fuel rod and core design methodologies is to assure that the licensing requirement of no fuel melting during normal operation, including AOOs, is satisfied. To meet this objective, a **[** **]** TOP limit is defined on the basis of a limiting slow transient. The duration of the transient is assumed to be **[** **]** and is based upon the expected spectrum of slow boiling water reactor (BWR) transients. To confirm the adequacy of **[** **]** time limit for the additive fuel, Table 2-1 from Reference 1 was reproduced in Reference 3 (NRC RAI 24-S01) and was expanded to include both the additive concentration and the time at temperature. This table lists additive concentration, time in minutes at temperature, liquid volume (%), and **[** **]**.
The table data confirm that for the planned GNF upper bound additive concentration of **[**
]. Therefore, the assumed **[** **]** duration for the determination of TOP limit for additive fuel is acceptable. The NRC staff finds the data and the response acceptable.

The NRC staff asked whether a limit should be placed on the amount of **[**

] during normal operation because the amount of time at temperature during normal operation could be considered longer than those tested for a TOP event (Reference 3, RAI 24-S02). GNF provided an analysis of the amount of fuel above the eutectic temperature at their thermal-mechanical operating limit (TMOL) for steady-state power operation at their **[** **]** limit. This analysis demonstrated that there may be a very small amount of additive fuel **([**
]) that will be **[**

]. GNF noted that this small amount of **[** **]** and will remain contained by the cooler radial outer solid fuel pellet and cooler solid pellets axially above and below. GNF also provided calculations of the extent of fuel melting at the TMOL as a function of burnup that demonstrated a very limited range of burnup **[** **]** and no melting above **[** **].** The NRC staff agrees that this extremely small amount of **[** **]** and should be easily contained by the cooler portions of surrounding (radial and axial) fuel. The staff finds this response acceptable but the amount of **[** **]** unless further testing at long time periods typical for steady-state operation or analyses are provided (See Section 4.2).

3.1.3 Theoretical Density

GNF has proposed to use the linear rule of mixtures to determine the theoretical density of the additive fuel. The room temperature theoretical density of the additive fuel differs from the standard UO_2 due to the higher density UO_2 displaced by the lower density additive phase. This approach of calculating the theoretical density has been used for gadolinia **[** **]** fuel previously approved by NRC in the PRIME fuel performance (Reference 4). The NRC staff finds this approach to determining fuel density acceptable.

3.1.4 *Thermal Expansion*

The thermal expansion of additive fuel below **[** **]** additive has been shown to be the same as for UO_2 when temperatures are below the eutectic temperature. Above eutectic temperature, the thermal expansion of additive fuel is slightly different than that of standard UO_2. Above the eutectic temperature there is an increasing fraction of **[** **]** in essentially no net change in density relative to standard UO_2.

Above the **[** **]** temperature there is a volume change of ~ 9.6 percent due to the change from solid to liquid phase. However, due to the very low concentration of additive fuel **[** **]** the change in thermal expansion is very small. This is illustrated in Figure 1 where the thermal expansion of UO_2 in the GNF PRIME fuel performance code and that for additive fuel is plotted versus temperature. Also, included in this figure is the thermal expansion model in the FRAPCON-3.4 fuel performance code.

[

]

Figure 1. Thermal Expansion Strains Predicted by PRIME UO_2 (non-additive), FRAPCON-3.4, and the GNF Additive Fuel Models.

It can be seen from Figure 1 that there is little difference in thermal expansion between additive fuel and the models in PRIME and FRAPCON-3.4 for UO_2 fuel up to the bulk melting temperature of additive fuel (>2750°C). This demonstrates that for the concentrations proposed by GNF for additive fuel there is little change in thermal expansion compared to that for UO_2 fuel up to the bulk melting temperature of additive fuel. Because GNF does not allow fuel melting for normal operation or AOOs, additive fuel has little impact on fuel thermal expansion for these conditions. The NRC staff agrees that for the very small additions of additive fuel there is little impact on fuel thermal expansion, i.e., it is well within the uncertainty of the UO_2 thermal expansion data. The staff finds the GNF model for thermal expansion of additive fuel acceptable.

3.1.5 *Thermal Conductivity*

The thermal conductivity variation with small aluminosilicate additions results in a very small decrease and this decrease is well within the uncertainty of the UO_2 thermal conductivity data. GNF has provided laboratory thermal conductivity measurements performed on pellets and the data are plotted for additive concentrations above [ ] in Figure 2-14 of the LTR (Reference 1). GNF has also provided plots for thermal conductivity as a function of temperature for additive concentrations ranging from 0 wt% to [ ] for various burnups ranging 0.0 GWd/MTU to 60 GWd/MTU (Reference 3, Figure RAI 6-1) and is reproduced here

as Figure 2. The model derived from the GNF data is illustrated in Figure 3 where GNF PRIME thermal conductivity model for additive fuel ([ ] additive) at a burnup of 1 GWd/MTU and fuel density of 95% TD) is plotted versus temperature (up to the bulk melting temperature of additive fuel) and compared with the FRAPCON-3.4 model for UO_2 fuel. The small difference between these two models from 1400°C to 2200°C is primarily due to the difference in the PRIME and FRAPCON-3.4 UO_2 models and not due to additive fuel. The model for determining the thermal conductivity of additive fuel is very similar to that for gadolinia fuel that was previously approved by NRC.

[

]

Figure 2. Thermal Conductivity as a Function of Temperature, Additive Concentration, and Exposure

[

]

Figure 3. Comparison of GNF PRIME Code Thermal Conductivity for Additive Fuel ([ ] Al_2O_3-SiO_2) to UO_2 Thermal Conductivity in FRAPCON-3.4

Responding to a staff question why the thermal conductivity dropped significantly at [ ], GNF responded that the additive liquid has a lower thermal conductivity than the solid phase and the volume of liquid additive becomes significant at this temperature significantly reducing the thermal conductivity. The staff finds this explanation acceptable.

The NRC staff concludes that the GNF thermal conductivity model for the additive fuel additions proposed is within the uncertainty of the UO_2 thermal conductivity data. The staff finds the GNF model for thermal conductivity of additive fuel acceptable.

3.1.6 *Specific Heat and Stored Energy*

The specific heat of additive fuel is calculated by applying the linear rule of mixtures similar to that used for fuel density. Specific heat is used in the calculation of fuel stored energy for LOCAs. The specific heat of additive fuel is nearly identical to that for UO_2 because of the small additions of Al_2O_3-SiO_2 additive to UO_2 fuel. A comparison of PRIME calculated stored energy versus fuel temperature compared to that calculated with FRAPCON-3.4 code for UO_2 fuel in Figure 4 demonstrates little difference between additive and UO_2 fuel. The NRC staff concludes that the GNF thermal conductivity model for the additive fuel additions proposed is within the uncertainty of the UO_2 specific heat data and finds the GNF model for specific heat of additive fuel acceptable.

[

]

Figure 4. Comparison of GNF PRIME Stored Energy for Additive Fuel ([ ] Al_2O_3-SiO_2) To That Calculated With The FRAPCON-3.4 Code for UO_2 Fuel

3.1.7 *Grain Size and Growth*

Grain size and growth are important in the sense that there is a tendency for larger grains to suppress FGR at low and moderate temperatures. Initial grain size and grain growth during reactor operation are conservatively assumed to be same in additive fuel as that for the standard UO_2 fuel. [

]. The GNF models for fuel densification and creep are also dependent on the initial grain size but grain growth is not used for these two parameters.

The staff requested the assumed as-fabricated grain size used for FGR calculations in the PRIME code and the coefficients used for grain growth for additive fuel (Reference 3, RAI 18). GNF responded that the assumed initial grain size for additive fuel was conservatively (the GNF FGR model predicts higher FGR with smaller grain size) assumed to be the same as used for UO_2 fuel of [ ] (based on 3-D dimensions) even though the initial as-fabricated grain size for additive fuel is [ ]. GNF also stated that the additive fuel grain growth is assumed to be the same as UO_2 grain growth, i.e., the UO_2 grain model applied to additive fuel, and they

limit the maximum grain size the same as for UO_2 fuel.

This same RAI (Reference 3, RAI 18) asked for the impact of grain growth on rod pressures (due to FGR), creep and cladding strain; and also the impact of additive fuel on LOCA stored energy and peak cladding temperature (PCT) compared to UO_2 fuel. GNF responded that grain growth and thus the grain growth model impacts the rod internal pressure (RIP) licensing calculation but not the centerline temperature and cladding plastic strain licensing calculations. Since the same initial grain size and grain growth model is used for both additive and non-additive fuel, the impact of grain growth model on the pressure calculation will be approximately identical for additive and non-additive fuel. GNF further responded that the impact of additive fuel on LOCA stored energy at the highest stored energy value was negligible ([ ] difference).

The NRC staff concludes that the assumption of initial grain size of [ ] is conservative in relation to FGR (rod pressure) and application to fuel creep and densification will be dependent on how well the PRIME code compares to measured fuel temperatures and cladding strain (see Sections 3.3.1 and 3.3.3) from additive fuel. In addition, the application of the UO_2 grain growth model to FGR will depend on the PRIME predictions of FGR data from additive fuel (see Section 3.3.2).

3.1.8 *Creep*

Experimental demonstration has shown that the creep behavior of additive fuel is significantly different from that of standard non-additive fuel at elevated temperatures. Fuel creep rate has a significant impact on cladding strain analysis. GNF performed PRIME calculations of steady state creep rates as a function of stress at various temperatures for both [ ] additive and standard UO_2 fuel (Figure 2-15 of Reference 1). GNF has determined that the creep rate for additive fuel compared to UO_2 fuel, e.g., at 1473K and 5 ksi stress additive fuel is [ ] greater creep than UO_2. The comparative study provided by GNF of predicted steady-state creep rates for several different temperatures between 1473°K to 1773°K and stresses between 1,000 psi to 18,000 psi at additive concentrations of [ ] in Figures 2-16 through 2-18 of the submittal (Reference 1) compared reasonably well to the creep data for additive fuel.

The staff's RAI (Reference 3, RAI 26) noted that the creep rates at high stresses reached values as high as [ ] and asked how these high creep rates could be verified and applied when the measured creep rates from the data were at several orders of magnitude less than those calculated. GNF responded that these high creep rates are only obtained at stresses above the yield stress and the fuel is assumed to result in immediate plastic deformation when above the yield stress, therefore, these high creep rates are not applied in fuel strain calculations.

Responding to the above mentioned RAI for a comparison of actual measured strains from three different creep measurements to those predicted by the GNF creep model for additive fuel, GNF provided only one comparison to creep data at 1813°K for 1.7 psi stress and

[ ] additive that demonstrated the GNF additive creep model over predicted fuel strains initially **[ ]** but at longer times the GNF model predicted the data well.

The same RAI asked if fuel mass is conserved when hard contact is experienced that results in the cladding pushing back on the fuel resulting in fuel movement due to creep or plastic strain above the yield strength. The staff requested that if the fuel mass is conserved, has the movement of the fuel, if any, been confirmed experimentally based on direct observation of porosity and dish filling due to creep. GNF responded that fuel volume is **[ ]**, as discussed in Section 3.1.12. The flow of material to conserve volume occurs primarily at the pellet center where temperatures are high and result in fuel movement to **[ ]**. Direct measurement of this **[ ]** has not been compared to the model predictions. However, GNF provided a comparison of observed cladding strains from **[ ]** with additive fuel to those calculated by PRIME assuming UO_2 fuel creep rates and those assuming additive fuel creep rates in Figure 21-2 of Reference 3. This comparison demonstrated that the use of additive creep model provided a much better comparison to the measured strain data that provided an indirect validation of the additive creep model for this **[ ]**.

The staff noted in an earlier draft response that the measured strains in Figure 21-2 did not match up with those quoted for this ramped rod in Table 21-1of Reference 3. GNF responded that the figure in this earlier response was in error and provided a corrected figure in a subsequent response.

The NRC staff's conclusion on the validity of the GNF creep model for additive fuel will be dependent how well the PRIME code compares to measured cladding strains from power ramping tests on additive fuel rods (see Section 3.3.3). This is because fuel creep has a significant impact on calculated cladding deformation (SAFDL strain limit) during AOO events.

3.1.9 *Yield Stress*

Additive fuel has a significant impact on yield strength above the critical temperature (the **[ ]**). Below the critical temperature the yield stress is considered same as standard UO_2.

Yield stress has an impact on the cladding strain analysis. GNF has performed mechanical testing of additive fuel with additives up to **[ ]** to determine the yield strength versus temperature. The yield strength of additive fuel has been found to be similar to that for UO_2 fuel when the temperature is below **[ ]** and then decreases to be approximately a factor of **[ ]** lower than UO_2 at **[ ]** where it is assumed to be constant at **[ ]** with increasing temperature. This **[ ]** lower limit for yield strength is used to maintain **[ ]**.

The staff's RAI (Reference 3, RAI 17(a)) noted that no data were presented to verify the yield strength for additive fuel. Also the RAI requested an explanation of why no strain rate dependence exists in the additive fuel model since the submittal (Reference 1, Section 2.9) indicated that yield stress experimental results showed strain rate sensitivity for the yield stress.

However, the strain rate dependence was not provided in the submittal. GNF responded by providing a limited amount of yield stress data for additive fuel that demonstrated the decrease compared to UO_2 fuel above a **[ ]** temperature. Additionally, GNF provided the explicit strain rate sensitivity and showed that the strain rate dependency for yield stress was small for rates in the range of **[ ]**. GNF noted that, as discussed in the response to the referenced RAI, PRIME analyses of power increases are performed using a series of **[**

].

This same RAI also asked what the assumed ductile-brittle transition temperature was for additive fuel. GNF responded that it was assumed to be the same as for UO_2 fuel because it is below the **[ ]** temperature where additive fuel yield strength deviates for that for UO_2 fuel and further claim this has little impact on fuel performance analyses.

The NRC staff conclusion on the validity of the GNF yield strength model for additive fuel will be dependent on how well the PRIME code compares to measured cladding strains from power ramping tests on additive fuel rods (see Section 3.3.3). This is because fuel yield strength has a significant impact on calculated cladding deformation (SAFDL strain limit) during AOO events.

3.1.10 *Modulus of Elasticity*

GNF calculates the modulus of elasticity for additive fuel based on the rule of mixtures similar to that used for determining fuel density and specific heat. The application of the rule of mixtures is illustrated in Attachment 17.A of Reference 3.

In response to a staff RAI (RAI 17(b), Reference 3) for data to substantiate the assumption that the rule of mixtures applies to calculating the modulus of elasticity, GNF responded that even though the elastic modulus of Al_2O_3-SiO_2 is significantly lower than that for UO_2 or for $(U,Gd)O_2$ the impact on additive fuel is not significant because of the very small concentrations of Al_2O_3-SiO_2 and within the accuracy of the measurement of elastic modulus up to the yield strength.

The staff's conclusion on the validity of the GNF modulus of elasticity model for additive fuel will be dependent on how well the PRIME code compares to measured cladding strains from power ramping tests on additive fuel rods (see Section 3.3.3).

3.1.11 *Strain Hardening Coefficient and Tangent Modulus*

The strain hardening coefficient and tangent modulus both impact the cladding strain analysis

for AOO events (power ramping). GNF has a small adjustment on the strain hardening coefficient and tangent modulus that they note provides only slight effect on PRIME analysis results.

The NRC staff conclusion on the validity of the GNF strain hardening coefficient and tangent modulus for additive fuel will be dependent how well the PRIME code compares to measured cladding strains from power ramping tests on additive fuel rods (see Section 3.3.3).

3.1.12 *Plastic Poisson's Ratio*

The plastic Poisson's ratio impacts the cladding strain analyses for AOO events (power ramping). GNF has assumed that there is **[**

]. GNF noted that they have incorporated this effect to better predict the cladding strains during power ramp tests on additive fuel.

The staff conclusion on the validity of the GNF plastic Poisson's ratio model for additive fuel will be dependent how well the PRIME code compares to measured cladding strains from power ramping tests on additive fuel rods (see Section 3.3.3).

3.1.13 *Effect of Additive on the High Burnup Fuel Pellet Rim Structure*

Irradiation of fuel to high burnup results in changes to the structure of UO_2 pellets. These changes begin when the local burnup exceeds around 60 GWd/MTU and occur in the lower temperature region or near the periphery of the pellet and result in a structure known as the high burnup structure (HBS) or rim structure. Formation of the HBS is attributed to recrystallization which starts at grain boundaries and propagates into the affected grains and to the formation of small pores on and within grains.

The staff requested a comparison of fuel rim formation data from high burnup additive fuel to the standard fuel for rim formation identifying concentration and ratio of $Si:Al_2O_3$ (RAI 17(c) Reference 3). Also the staff requested data to show that the structure and chemical composition of additive does not change on the old grain boundaries in the rim due to restructuring. In its response, GNF stated that the impact of alumina-silica additive effect on the HBS was evaluated relative to standard and large grain UO_2 fuel in test rods that operated to average exposures of the standard fuel to **[ ]**. The 3-dimensional grain size of the standard large grain non-additive and additive pellets were **[ ]**, respectively. The fuel samples were irradiated in the Halden reactor at linear hear generation rates (LHGRs) that ranged from **[ ]** at the beginning of life (BOL) to **[ ]** at the end of life (EOL). The additive concentration range of **[ ]** and the composition of aluminosilicate was **[ ]**. The resulting pellet structure was examined after irradiation. As Figure RAI 17-3 (Reference 3) illustrates, the HBS formed at the edge of both standard UO_2 and additive pellets and extended radially inward to a greater extent in the standard pellet than in the additive pellet.

For normal operation and AOOs, the primary concern arising from the formation of the HBS is the impact on fuel temperature that in turn impacts FGR and thermal expansion, and thus RIP and cladding strain. The thickness of the HBS is lower for additive fuel than UO_2 fuel and High Burnup Effects Program (HBEP) results indicate that the structure is similar in terms of porosity and retained fission gas. Thus the thermal impact of the HBS rim for additive fuel is expected to be lower than for UO_2 fuel.

The area where the rim could impact behavior important to safe operation is in the dispersal of fission products and fuel during LOCA and RIA events because the strength of the grain boundaries may change due to the additive precipitated on these boundaries during fabrication, however, there is no data to determine these effects. There is some proprietary evidence that larger grain sizes suppress the high burnup rim formation but this data has not been presented by GNF. If the rim formation was suppressed it could possibly reduce the amount of fuel dispersal during a LOCA or RIA event.

In summary, GNF has proposed that the high burnup rim structure in additive will not change the in-reactor performance from that in UO_2 fuel including the following: 1) the formation or properties of the rim with the exception of a different initial as-fabricated grain size, 2) the thermal or mechanical properties, 3) the storage or dispersal of fission products and fuel material in postulated accidents (LOCA or RIA), and 4) the microstructural stability and chemical properties of the rim.

The NRC staff concludes that the additive is not expected to affect the HBS or alter the behavior of the HBS with respect to in-reactor and post irradiation performance. The licensing impacts of HBS for additive fuel will be conservatively assessed using the HBS rim formation model for UO_2 fuel. The staff concludes that the impact of additives on rim structure is conservative and acceptable.

3.2 In-Reactor Performance Assessment

The use of additive fuel could potentially impact the following in-reactor fuel performance issues; fuel oxidation and washout as a result of fuel failure, lower fuel melt limits, RIA failure threshold, fuel densification, FGR, and accident source terms.

3.2.1 *Fuel Oxidation and Washout Due to Fuel Rod Failure*

Washout behavior can be described as that after a breach of the fuel rod cladding. Water is introduced in to the fuel rod interior and can interact with the fuel inside. At BWR conditions, water is mildly corrosive to UO_2. Corrosivity depends on several factors, mainly, the grain structure of the fuel.

GNF has performed a significant amount of testing of the effect of water at BWR conditions on the possible washout of additive fuel due to fuel oxidation with the BWR water. Past testing has shown that the oxidation due to water proceeds along the grain boundaries such that the **[ ]** could impact oxidation and washout. These oxidation tests have demonstrated that the oxidation for additive fuel is similar

to UO_2 fuel with the exception of one set of data which had a higher oxidation rate than UO_2. GNF has presented data that is convincing that the fuel with the higher oxidation rate was due to surface defects not typically found in their production of additive fuel. GNF was not able to determine definitively the cause of these surface defects.

The NRC staff (RAI 25, Reference 3) requested GNF to provide details of corrections made to the fuel oxidation data to account for the effect of surface defects with respect to the number of additive pellets that underwent reactor operation and were examined. This RAI also asked GNF to confirm whether sampling be performed on production of fuel batches of additive fuel and to confirm that no surface defects exist. GNF responded that the pellets with the surface defects were fabricated before GNF was facilitized to produce additive fuel and thus this earlier additive fuel had uncertainties in additive concentration, powder pressing, and sintering; such that these uncertainties would be minimized in batch production of additive fuel. In addition, GNF noted that they will be performing qualification tests on additive fuel before full production begins that will include **[** **]** to verify that no surface defects exist. GNF further noted that once full production begins, microstructure examination is also part of the standard monitoring of pellet quality to determine that pellet characteristics do not change from the earlier qualification tests. This examination includes **[** **]** measurements that may detect surface defects.

The NRC staff requested GNF to address the production qualification and how on-going monitoring will ensure that the pellets meet specifications and whether the qualification and quality monitoring will be sufficient to detect surface defects. GNF responded that the qualification includes **[** **]**. For the production qualification of additive fuel, pellets from press-feed blends of **[** **]** were subjected to extensive microstructure examination to assure that additive distribution is uniform and that grain size and structure are as expected. **[** **]** to assure that pellet characteristics do not change, although to a lesser extent. GNF production pellets have closed, stable pores, and as a result have very low open porosity. For the additive pellet production qualification, the nominal measured open porosity is reported to be approximately **[** **]**. Examination of **[** **]** lead use assembly (LUA) pellets reveal surface flaws equivalent to approximately **[** **]** of pellet volume. Since open porosity testing **[** **]** of pellet quality, open porosity is expected to identify the presence of surface flaws such as those in some of the **[** **]** additive pellets if they were to occur in production pellets.

An extension of RAI 25 requested GNF to provide information on any specification for **[** **]** and how the flaws will be detected if the flaw is outside of normal distribution. The estimate of **[** **]** surface defect of pellets is based on an assumed defect geometry and distribution. Since this volume is at the surface of the pellet it will be included as open porosity resulting from the normal fabrication process and additional porosity due to anomalous surface defects. GNF has shown that pellets with the anomalous open porosity will have much higher

oxidation in a corrosion test **[**

].

The staff reviewed the GNF responses on detection of surface defects similar to those in the additive fuel with high oxidation and concludes that due to the small size of these defects, it may be difficult to identify these defects in production batches based on standard testing done on these batches.

However, the staff notes that if washout were to occur in additive fuel rods, the release activity will be quickly detected in plant offgas systems. Past experience with fuel washout in commercial plants have shown that a plant can detect this activity and shutdown before exceeding coolant and offgas activity limits.

3.2.2 *Fuel Melting*

In addition to fuel melting behavior described in Section 3.1.2, few other considerations for fuel melting behavior during its in-reactor performance is described in this section. One such aspect of melting behavior is evolution of the fuel microstructure upon thermal cycling that causes repeated increases and decreases in **[** **]** in the pellets. During testing of pellets at high additive concentrations up to **[**

]. This indicates the possibility of microstructural evolution due to thermal cycling. In factory-produced pellets **[**

], thus resulting in a microstructure that is indistinguishable from that present before thermal cycling. Because of this, thermal cycling is not considered to have any new effect on additive fuel properties or performance. The NRC staff accepts this conclusion.

3.2.3 *Reactivity Insertion Accident (RIA) Characteristics*

An RIA is an important postulated accident for the design of LWRs. This postulated accident results from an inadvertent insertion of reactivity due to the ejection of a control rod assembly in a PWR or the drop of a control blade in a BWR. In the unlikely event that sufficient reactivity is inserted into the reactor core by the ejected/dropped control rod, prompt energy deposition into the fuel can occur, which when sufficiently high can lead to fuel rod failure.

GNF has presented RIA testing performed in the Nuclear Safety Research Reactor (NSRR) at the Japan Atomic Energy Research Institute (JAERI) from 30 fuel rods with different additive compositions and concentrations. These tests were all performed on unirradiated fuel rods. Those with concentrations near those proposed by GNF for their additive fuel demonstrated a higher failure level than for UO_2 fuel rods. PNNL has performed an evaluation of failure threshold of MOX fuel compared to UO_2 fuel (Beyer and Geelhood 2013, Reference 11) that concluded no difference in failure threshold between these two fuel types. MOX fuel is similar to

additive fuel in a couple of areas such as higher creep rate than UO_2 fuel for both and higher storage of fission gas on grain boundaries. Therefore, the failure threshold for additive fuel may be similar to that for UO_2 fuel.

An RAI (RAI 23, Reference 3) noted that the higher content of fission gas on grain boundaries and the higher creep rate than for UO_2 fuel, the additive fuel has the potential to increase the dispersal of additive fuel if fuel rod failure is experienced during a RIA event.

This RAI also noted the additional gas on the grain boundaries could result in higher fission product release when the grain boundaries are fractured during the RIA. This may result in higher radiological releases than for UO_2 fuel. GNF states that since the GNF additive **[**

]. Also, the dispersal of MOX fuel during an RIA is impacted by increased gaseous swelling relative to UO_2 due to increased fission gas bubbles on grain boundaries. Since the additive fuel has **[**

].
GNF has responded that there are currently no in-reactor nor prototypical ex-reactor heating tests of high burnup additive fuel to determine whether fuel dispersal is similar or different than for the UO_2 or MOX fuel tested at high burnup.

GNF's response to RAI 17 indicates that since the additive **[** **]**, the impact of additive is expected to cause a **[** **]** HBS for additive fuel with similar thermal-mechanical properties as for UO_2 pellets. The impact of additive on HBS has been studied by Post Irradiation Examination (PIE) of 9x9 LUAs with additive and standard pellets. Rapid heating of the pellets caused cracks in the pellets at around **[** **]** which is higher than the temperature required to generate cracks in high burnup of **[** **]** UO_2 during rapid heating with no restraint. From the results of these tests, it is concluded that no major impacts of the additive on the HBS have been observed to date.

The NRC currently does not have a limit on fuel dispersal during a RIA event other than it should be considered if the fuel fails during this event. In the event the failure threshold is exceeded, fuel dispersal in additive fuel will be considered using the same basis as standard UO_2 fuel.

In regards to a higher radiological release in additive fuel during a RIA event, GNF has responded that this should also be less than or similar to that for UO_2 fuel based on the fact that they conclude FGR during steady-state power operation and AOOs is similar to UO_2. The staff notes that an evaluation of release from MOX fuel has concluded that it has a higher release than for UO_2 fuel due to the higher fission gas on grain boundaries in MOX fuel (Reference 8). The issue of radiological release of additive fuel will be addressed in Sections 3.2.6 and 3.3.2 on FGR during normal operation and AOOs.

3.2.4 *Fuel Densification and Swelling*

GNF proposes to use the previously approved UO_2 densification and swelling models in PRIME for application to GNF additive fuel (Reference 9). With the approval of TR NEDE-33241P-A, the requirement for routine densification was replaced by qualification of densification for a new design or fabrication process followed by density monitoring of 100 percent of pellet lots. GNF has stated that the in-reactor densification and swelling of additive fuel is expected to be unchanged with respect to standard UO_2 fuel. They state the evidence for similar densification is based on ex-reactor densification tests on unirradiated additive fuel pellets and a limited amount of in-reactor tests.

However, no data were provided in the submittal to verify the above conclusions of similar behavior to standard UO_2 fuel. The staff requested GNF (RAI 17(d), Reference 3) provide in-reactor densification and swelling data to confirm the similar behavior of additive fuel to standard UO_2 fuel. GNF confirmed that they conducted a 10 year program to irradiate additive fuel in the Halden reactor with six instrumented fuel assemblies (IFAs) that included two UO_2 rods, two additive rods with **[** **]** additive, and 2 additive rods with **[** **]** additive. **[**

]. These rods were operated in the range **[** **]** to burnups of **[** **]**. The results listed in Table RAI 17-1 (Reference 3) show that the densification response of UO_2 and additive fuel within the range of data used in the development of the PRIME model and are similar. Table RAI 17-2 lists the fuel swelling rates for UO_2 and additive fuel for a limited number of rods. Results indicate that the swelling rates for both UO_2 and additive fuel are similar.

The staff notes that GNF provided a limited amount of data that confirmed more or less similar behavior with respect to densification (**[** **]** for additive than for UO_2 fuel). The application of the previously approved UO_2 densification model to GNF additive fuel is conservative if additive fuel has **[** **]**. The NRC staff concludes that the application of the previously approved UO_2 densification model to GNF additive fuel is acceptable. The very small amount of additive fuel swelling data that was within the range of UO_2 fuel swelling from Halden tests at burnups less than 75 GWd/MTU was compiled by PNNL staff for developing the FRAPCON-3.4 swelling model (Reference 10). The staff concludes that

the application of the previously approved UO_2 swelling model to GNF additive fuel is acceptable.

3.2.5 *Fission Gas Release (FGR)*

GNF proposes to use the previously approved UO_2 FGR model in PRIME for application to GNF additive fuel. GNF has provided FGR data from additive fuel with PRIME predictions of this data to verify that the UO_2 FGR model adequately predicts this data. The staff evaluation of the PRIME FGR model predictions to the additive fuel data will be discussed in Section 3.3.2 below.

3.2.6 *Alternate Source Term (AST)*

The AST used in plant licensing should apply equally well to additive and non-additive fuel. NRC's NUREG-1465 (Reference 12) provides a realistic estimate of the radiological species released to the containment in the event of a severe reactor accident involving substantial meltdown of the core. Of specific interest for additive fuel is the reaction of Cesium (Cs) with the **[ ]** in the additive fuel and its effect on Cs release under accident conditions. The alternate source term assumes 95 percent of the released iodine is in the chemical form of cesium iodide (CsI) with the remainder elemental iodine (I) and organic iodide (Reference 13).

The CsI is soluble in water and since the source term assumes the pH of water within the containment above 7.0, this minimizes the irradiation-induced conversion of ionic iodine in pools of water and wet surfaces to elemental iodine. Cs can form a relatively stable compound with **[ ]** from additive and fission generated Cs co-resides on the grain boundaries with the additive phase. **[ ]**. The combination of the residence of Cs within the grain boundary and the CsI solubility property in pools of water contribute to the total quantity of Cs to be substantially less than the core-wide inventory of fission-generated Cs. The fact that there is an adequate quantity of Cs expected to reside in the pellet-cladding gap during the initial stage of an accident to react with all of the iodine, and the Cs has sufficient instability at later accident conditions to maintain availability of Cs, the alternate source term assumptions used in design of plant systems should not be affected by the use of additive fuel. The NRC staff accepts the fact that the source term is not affected by the additive fuel.

3.3 <u>In-Reactor Data to Verify Qualification of Additive Fuel</u>

GNF has performed several experiments to investigate additive fuel behavior. The qualification data base for additive fuel includes fuel temperature, FGR, cladding deformation (strain), and RIP measurements in-reactor. The sections below reflect these four different data measurements.

3.3.1 *Fuel Temperature*

The PRIME predicted temperatures for the small additive concentrations proposed results in a very small change in fuel thermal conductivity (see Section 3.1.5) from UO_2 fuel. This should result in very similar temperatures to those for UO_2 fuel because the maximum additive concentration is only **[ ]**. GNF has provided validation of the PRIME code temperature predictions of additive fuel by demonstrating that the code adequately predicts additive fuel temperatures of in-reactor temperature measurements for additive fuel from Halden Reactor tests. The code data comparisons are provided in Figures 4-1 and 4-2 of the submittal that demonstrate the predictions of additive fuel are within those for UO_2 fuel up to a burnup of **[ ]**. The thermal conductivity burnup dependence of additive fuel should be the same as for UO_2 fuel because the additive fuel is **[ ]** UO_2, this similar burnup dependence with UO_2 is also consistent with UO_2 fuel with small gadolinia additions up to 8 wt%.

PNNL concludes the PRIME code predicts temperatures of additive fuel adequately up to the burnups requested.

3.3.2 Fission Gas Release (FGR)

FGR and resulting internal pressure is an important aspect of fuel behavior and it can be a limiting factor for fuel thermal-mechanical limit. The FGR is dependent on the fuel microstructure and chemistry, and the fuel temperature that is highly dependent on the power history and burnup.

The prediction of FGR is very important in the rod pressure analysis. GNF has provided FGR data for both steady-state power operation and power ramping to simulate fuel power changes due to control rod movement and AOOs in the submittal. In addition, GNF added additional power ramped rods from the Segmented Rod Program (SRP) in their response to RAIs. The power ramped rods were irradiated in commercial reactors for base steady-state power operation to accumulate burnup and then transported to the Halden or R2 test reactors for the power ramping and then punctured to measure the FGR following the ramp test. The power ramp tests were performed at relatively low to moderate burnups between **[ ]** some of which (Duane Arnold/Halden data) were ramped to relatively low powers resulting in low FGR. The power ramp tests were identified as the Duane Arnold/Halden, **[ ]**/Halden, and Segmented Rod Program tests with FGR values in the range **[ ]**. GNF has provided PRIME predictions of these **[ ]** FGR power ramped data using the previously approved UO_2 FGR model.

The steady-state power tests were from 5 different irradiation tests identified as IFA-537, IFA-538, **[ ]**. These steady-state power tests ranged in burnup from **[ ]** with FGR values between **[ ]**. GNF has provided PRIME predictions of these **[ ]** steady-state FGR data from additive fuel using the previously approved UO_2 FGR model. PNNL's evaluation of this data noted that the PRIME code under predicted all **[**

].
This was of concern because the GNF rod pressure analyses assumes that the fuel rod runs at the TMOL for steady-state power operation out to the burnup limit to demonstrate that the SAFDL for rod pressure is met for a given reactor core, this usually results in FGR values above 9 percent at end-of-life (EOL) rod average burnups (≥ 55 GWd/MTU). In addition, GNF also performed rod pressure analyses with power ramps above the TMOL. Therefore, it is important to be able to adequately predict data at high rod powers (near or above the TMOL) and high release values up to the approved GNF burnup limit of **[** **]**. As a result, past NRC reviews of FGR models within the last 15 years have concentrated on verifying that the proposed vendor FGR models adequately predict data with measured values greater than 5 percent FGR. This was also the focus by NRC (model verification against FGR values greater than 5%) in the previous review and approval of the UO_2 FGR model in PRIME.

An RAI (RAI 20, Reference 3) requested more background information on those fuel rods with high release values that included information on the terminal peak rod powers achieved in the ramped power tests and the power histories of the steady-state tests. This rod power information was needed to verify that GNF had FGR data that operated near or at their TMOL power limit for steady-state power operation used in their rod pressure analyses. In addition, AOO events are evaluated by GNF above the TMOL powers such that power ramp data above the TMOL are needed to verify FGR predictions for AOO events. The first GNF response provided addition FGR data at low burnups between **[** **]** from power ramped rods (identified as SRP ramped rods).

GNF initially did not provide the rod powers for either the ramped nor steady-state power tests, such that a follow up request was made to obtain this information.

GNF provided the rod power histories in follow up responses. In these follow up responses GNF suggested that certain data from **[**

] GNF based the suggestion on the fact that the **[**

] Staff noted that if the **[** **]** data were eliminated from Figure 5, there would only be **[** **]** at a burnup of 53 GWd/MTU that operated near or above the GNF TMOL. GNF recognized the staff concern about lack of data in the power/exposure range where rod internal pressure is limiting and accepted the staff position that the **[** **]** data be considered in the evaluation of the acceptability of the proposed additive fuel FGR model.

The staff evaluated the rod powers supplied by GNF and made a plot of predicted-minus-measured FGR versus fuel burnup for those data with greater than 5 percent FGR in Figure 5. The data is differentiated on whether rod powers were near or above the GNF TMOL powers and those significantly below the TMOL. Examination of this figure demonstrates that the PRIME code provides a relatively good prediction (even distribution of under predictions and over predictions) of FGR at burnups below **[** **]** that operated near the TMOL but at burnups above **[**

]

GNF proposed to include all of the additive FGR data including those at low FGR and low rod powers (significantly below the TMOL). GNF has noted that when all of the data is used, the mean predicted-minus-measured of all the data is nearly zero suggesting no bias in the predictions. However, as noted earlier when additive data at high FGR values are examined there appears to be a [

]can be explained in Figure 6. Figure 6 is a copy of Figure 4.3 from the submittal with trend lines drawn by the staff. This plot demonstrates that the additive FGR model [

].

In order to concentrate on those additive FGR data applicable to the rod pressure analyses performed at their TMOL at higher burnups where rod pressure becomes limiting, staff has selected only those FGR data that operated ≥ 0.85 TMOL and burnups ≥ 40 GWd/MTU based on the power histories supplied to PNNL/staff in RAI 20 (S02). This has resulted in [ ] additive fuel FGR data that meet this criterion. The [ ] FGR data points selected from additive fuel rods are the following: [

].

There are three primary reasons why the staff used only these [ ] data:

1) From examination of Figure 4-3 (see Figure 6 below) of submittal it is obvious that the FGR model over predicts the FGR additive fuel at low LHGRs and/or low burnup.

2) Low power and/or low burnup (< 40 GWd/MTU) conditions are not within the operating range where rod pressures are limiting.

3) From Figure 6 it is obvious that the FGR model [

]. The red line in Figure 6 is the trend in additive fuel

predictions of additive data while the dark dashed line is the trend in the predictions of UO_2 data. The solid dark line is the 2σ upper bound of the predictions of the **[ ]** additive fuel FGR data at ≥ 0.85*TMOL and burnups > 40 GWd/MTU.

GNF has proposed to use the same bounding analysis methodology used for UO_2 fuel to bound the additive fuel FGR data for rod pressure analyses. This bounding analysis includes using a bounding power perturbation of **[ ]** and a bias to the FGR model (lowers the temperature-exposure dependent term for earlier grain boundary gas interlinkage and release). A follow up RAI to RAI 20 of Reference 3 requested that GNF provide a prediction of the **[ ]** additive FGR data using this bounding analysis methodology to demonstrate that this bounds the additive fuel FGR data applicable to rod pressure analyses at a 2σ level. GNF provided a prediction using a power perturbation of **[ ]**, rather than the **[ ]** power perturbation used for licensing, and the FGR model bias used for UO_2 licensing. The results indicated that **[ ]** of the **[ ]** data points were under predicted (**[ ]**) and **[ ]** data point (**[ ]**) was on the bounding line. All of these additive FGR data should have been bounded in order to provide a 2σ bounding prediction.

As a follow up to RAI 20, the staff requested GNF to provide FGR predictions of the **[ ]** selected additive FGR data using a **[ ]** power perturbation and the FGR model bias used for UO_2 fuel to determine if this would bound this additive FGR data. Using this increased power perturbation, the predictions bounded the **[ ]** but the **[ ]** datum remained under predicted.

Examination of the power history of the **[ ]** experimental fuel rod revealed that the LHGRs of this rod remained significantly higher over the entire exposure range of this rod (**[ ]**) than the TMOL versus exposure used by GNF. In addition, the measured value of FGR for this rod is much higher than what would be expected in a commercial fuel rod. Therefore, the staff concludes that this rod operated outside of the rod power range of interest for GNF fuel and this fuel rod FGR datum does not need to be bounded. Therefore, the staff concludes that the bounding prediction of the **[ ]** remaining additive fuel FGR data using a **[ ]** bounding power perturbation is acceptable.

As an alternative, GNF has proposed that instead of using the **[ ]** bounding power perturbation that they continue using the **[ ]** power perturbation used for UO_2 licensing analyses **[ ]** to achieve the same or more bounding predictions as those using a **[ ]** bounding power perturbation for the **[ ]** additive FGR data identified above. The staff concludes that this is also acceptable.

[

]

Figure 5. Predicted-Minus-Measured Fission Gas Release by PRIME Code of Additive Data with Measured Releases Greater Than 5%, Data is Differentiated in Terms of Rod Powers Near or Above the GNF Thermal-Mechanical Operating Limit (TMOL and Those with Rod Powers Less Than the TMOL.

[

]

Figure 6. GNF Predicted versus Measured for UO_2 and Additive Fuel with Trend Lines Drawn by PNNL.

3.3.3 *Cladding Deformation (Strain)*

GNF performed cladding strain analyses with the PRIME code to establish a MOP limit for AOO events (involving power transients). GNF initially provided very little measured cladding strain data from power ramping of additive fuel to validate the PRIME code strain predictions for AOO events with additive fuel and the various additive fuel models in PRIME used to predict cladding strain. As a result, RAI 21 of Reference 3 requested additional information on the power ramp testing that was performed on additive fuel to assess the applicability to PRIME and the MOP limits.

GNF responded with cladding strain data from [ ] power ramps, however, two of these power ramps were at very low burnups ([ ]) where cladding strains were negligible because the fuel cladding gap was relatively large at this burnup. The other

[ ] power ramp data were from rods with burnups between **[ ]** (close to the burnup at which margin to MOP limit is the smallest) with PRIME under predicting cladding strains for **[ ]** rods. In addition, the power ramps of this data were below the rod powers of the MOP limit. The NRC staff's evaluation concluded that the PRIME code appeared to have an **[ ]** in cladding strain for additive fuel based on the small amount of cladding data near the burnup and rod power where margin to the MOP limit is minimum. The NRC staff further recommended that **[**

]. The NRC staff concludes that this is acceptable and notes it is very conservative because GNF has provided data (Section 6.3 of Reference 1 and Figure RAI 21-3 of Reference 3) to show that the failure limit during a power transient for additive fuel is noticeably **[ ]** than for UO_2 fuel at equivalent burnup levels.

3.4 Impact of Additive Fuel on Licensing Criteria

This section will address the review results of the effect of additive on the design bases for each of the fuel system damage, failure, and coolability criteria established in Section 4.2 of NUREG-0800 relative to standard fuel. Specifically, this section addresses the impact of the additive fuel on the following fuel licensing criteria for fuel melting, rod internal pressure, cladding strain, cladding fatigue, cladding creep collapse, and LOCA/stability/core transients.

3.4.1 *Fuel Melting*

The impact of additive on fuel melting limit is addressed in Sections 3.1.2 and 3.2.2 of this evaluation.

3.4.2 *Rod Internal Pressure (RIP)*

Fuel RIP is limited by the licensing requirement that there is **[**
] due to high fuel RIP at operating power levels. The RIP limit is dependent on cladding creep and fuel swelling.

The cladding type has not been altered in this submittal and the cladding creep model was previously found to be acceptable in PRIME. The effect of additive in the PRIME calculation of fuel RIP is demonstrated by analyzing the GNF2 fuel design with and without additive. The fuel swelling model for additive fuel was found to be acceptable in Section 3.2.4. The staff concludes that the RIP limit for additive fuel is acceptable.

The RIP calculation is used to demonstrate that the peak operating rod in a core will remain below RIP limit. RIP is dependent on FGR (addressed in Section 3.3.2) and internal void volume calculations. FGR has the largest impact on RIP calculations; the FGR model is discussed in Section 3.3.2. The internal void volume calculation is dependent on cladding creep, fuel thermal expansion, and fuel swelling. As noted above the cladding type has not been altered in this submittal and the cladding creep model was previously found to be

acceptable in PRIME. The thermal expansion model for additive fuel was found to be acceptable in Section 3.1.4. As noted above, the fuel swelling model for additive fuel was found to be acceptable in Section 3.2.4.

In addition, GNF has presented predicted versus measured rod internal pressures that demonstrated a best estimate prediction of rod internal pressures. However, it should be noted that experimental rods have a much larger internal void volume to fuel volume than commercial fuel rods such that these comparisons are not prototypical of commercial rods. In addition, lead test assembly (LTA) rods do not operate at limiting power conditions and, therefore, typically have low FGR such that these rods are not prototypical of peak power rods in the core that will be limiting in terms of rod internal pressure.

The NRC staff concludes that the RIP calculation is acceptable based on the acceptability of those models in PRIME used in this analysis.

3.4.3 Cladding Plastic Strain

GNF performed analyses for each rod type to determine the maximum overpower magnitudes for which the cladding circumferential strain does not exceed 1 percent cladding **[ ]** strain limit. Analyses to determine the **[ ]** circumferential strain were performed at several exposure points during the fuel rod lifetime. The MOP is determined as the maximum permissible overpower for which the cladding circumferential strain does not exceed the limit. For the cladding strain analysis, GNF considered the **[ ]** that produces the most severe result.

Figure 5-3 of the submittal (Reference 1) indicates that the presence of additive greatly increases the margin to **[ ]** strain for same overpower (**[ ]** in the limiting exposure range). An RAI (RAI 21(g), Reference 3) noted that the submittal did not include the **[ ]** for MOP events, as approved in the PRIME review. GNF responded and showed that additive fuel met the **[ ]** strain limits at high burnup approved in the PRIME code review. These strain limits are only dependent on the cladding and not the fuel type. Therefore, these strain limits at low and high burnup are found to be applicable to additive fuel. The prediction of cladding strain is addressed in Section 3.3.3 above.

3.4.4 *Cladding Fatigue plus Creep Rupture Limit*

GNF demonstrated the effect additive on the fatigue life by performing PRIME analyses of additive and standard fuels. The analysis by GNF included creep rupture damage added to the fatigue damage which applies conservatism to the results.

The limit on cladding fatigue is only dependent on the cladding type, and the amount of cladding oxidation and irradiation damage. The additive fuel does not impact any of these cladding properties. Therefore, the cladding fatigue limits are found to be applicable to additive fuel. The

higher creep rate (discussed in Section 3.1.8 above) in additive fuel as compared to UO_2 fuel will result in lower cladding stresses and strains that should result in more margin to cladding fatigue. However, GNF will continue to use UO_2 properties for bounding cladding fatigue analyses.

3.4.5 *Cladding Creep Collapse*

The only fuel property that impact cladding creep collapse is densification, e.g., higher densification may result in a higher probability for collapse. As noted in Section 3.2.4 above, the use of the UO_2 fuel densification model for additive fuel may be conservative because the small amount of data on densification of additive fuel suggests that **[**

]. Lower FGR could potentially impact cladding creep collapse because RIPs are lower, however, past GNF creep collapse analyses for UO_2 fuel have conservatively assumed no FGR or only athermal FGR, this removes the concern of lower FGR for additive fuel. Previous creep collapse analyses for UO_2 fuel are found to be applicable to additive fuel.

3.4.6 *LOCA/Stability/Core Transients*

The LOCA limits of PCT and cladding oxidation are not impacted by the additive fuel. An RAI (RAI 18 (c), Reference 3) requested that GNF provide example stored energy analyses for additive and non-additive (UO_2) fuel for a PCT limited plant. This comparison demonstrated that additive fuel made little difference in stored energy as compared to non-additive fuel. This is because the change in specific heat and thermal conductivity from UO_2 fuel are negligible. The LOCA limits on PCT and cladding oxidation are found to be applicable to additive fuel.

The LOCA, transient, and stability analyses use gap conductance for both a high power and lower power case. The gap conductance for the high power case is significantly lower early in exposure due to decrease in thermal conductivity of additive fuel. The impact of additive fuel on fuel rod failure during a RIA event is addressed in Section 3.2.3 above.

3.4.7 *Impact of Nuclear Design Requirements*

To confirm compliance with GDC 11, GNF analyzed the impact of introducing additive fuel on the key reactivity coefficients; results of the evaluation confirmed that the introduction of additive at the planned concentration does not impact the nuclear dynamic parameters/reactivity coefficients. For BWR fuel, the key reactivity coefficients are: 1) the moderator void coefficient, 2) the moderator temperature coefficient, 3) the Doppler coefficient, and 4) the prompt power coefficient. Since the neutron absorption cross section of aluminosilicate is very small relative to the fuel, the additive does not make the reactivity coefficients less negative.

GDC 26 requires that the reactivity control system shall be capable of maintaining the reactor subcritical under cold conditions with sufficient margin to account for equipment malfunctions such as stuck control rods. GNF's 3D analysis assures adequate cold shutdown margin.

In summary, the staff concludes that the impact of additive fuel on licensing analysis for the

GNF fuel designs are negligible and do not significantly impact the fuel behavior or characteristics.

3.5 Operating Experience

GNF has been irradiating additive fuel in power reactors starting with segmented rod bundle (SRB) with up to **[ ]** additive and up to approximately **[ ]** exposure. The irradiated fuel segmented rods were retrieved for hot cell examination and further ramp testing. Restricted LTAs were inserted into US commercial reactor core and achieved up to **[ ]** exposure. These LTAs consisted of segmented and full-length rods. LUAs with segmented and full-length rods were irradiated in European reactors and achieved approximately **[ ]** exposure. The rods were retrieved for hot cell examination and further ramp testing and followed by re-insertion in reactors.

Section 3.2 of this safety evaluation provides detailed discussion of the specific in-reactor operating experience related to measured fuel temperatures, fission gas release, and cladding deformation.

Several rod segments, both standard and additive and without an inner zirconium liner or barrier, were ramped and few of them re-ramped in test reactors with a range of additive concentrations **[ ]** with peak power of **[ ]**. GNF reports that the standard rods failed and none of the additive rods failed during testing. Tests have shown that the additive fuel provided additional margin to pellet-cladding-interaction (PCI) failure compared to barrier alone. The staff requested information (RAI 21(c), Reference 3) on whether additive fuel with and without barrier cladding have different LHGR operating limits than non-additive fuel with and without barrier cladding to prevent PCI failures. GNF responded that even though currently, LHGR operating limits for non-additive fuel are identical for barrier and non-barrier cladding, due to the susceptibility of fuel with non-barrier to PCI failures during rapid power increases, GNF provides **[ ]** for fuel with non-barrier cladding to minimize the risk of PCI failures. GNF stated that based upon currently available test results **[ ]** may be offered for additive fuel with barrier cladding relative to non-additive fuel with barrier cladding.

The ramp test program of additive rods base irradiated in **[ ]** provided a valid assessment of PCI performance. GNF reports that the principal factor in PCI resistance appears to be a **[ ]**. The NRC staff has determined that GNF has demonstrated there is adequate margin for additive fuel with respect to PCI failure compared with non-additive fuel.

The staff concludes that GNF has provided sufficient operating experience for additive fuel.

4.0 CONCLUSIONS, LIMITATIONS, AND CONDITIONS

4.1 Conclusions

GNF has tested additive fuel (aluminosilicate in UO_2) over a wide range of concentrations and compositions. GNF used the NRC-approved PRIME fuel performance code to evaluate the key material properties of the additive fuel. The impact of additive fuel on in-reactor fuel performances such as washout characteristics, RIA behavior, FGR, RIP, and fuel melting have been adequately analyzed. The licensing criteria assessment per SRP 4.2 (NUREG-0800) of additive fuel relative to standard fuel with respect to fuel melting, fuel RIP, cladding strain, and cladding creep has been adequately addressed.

The NRC staff concludes that thermal-mechanical performance of the proposed additive fuel design is adequately addressed in the GNF submittal with the application of the PRIME fuel performance code. Fuel melting and fuel creep rate are found to have significant effects from addition of aluminosilicate. Theoretical density is deemed to have been affected only slightly. Fuel properties such as thermal conductivity, FGR, and fuel washout have been insignificantly impacted.

The staff's safety evaluation of the additive fuel is subject to the limitations and conditions listed in Section 4.2.

4.2 Limitations and Conditions

1. Ratio of silica-to-alumina shall be within the range **[ ]**. (Section 1.0)

2. The maximum concentration of aluminosilicate shall be **[ ] ([ ]**). (Section 1.0)

3. The time for AOO events with fuel near the **[ ]** criterion shall be limited to less than or equal to **[ ]**. (Section 3.1.2)

4. Steady-state power operation shall be limited to less **[ ]** of liquid unless further testing at long time periods typical for steady-state operation or analysis are provided. (Section 3.1.2)

5. For licensing analyses, the initial grain size for additive fuel shall be no greater than **[ ]**, based on 3-D dimensions. (Section 3.1.7)

6. The rim thickness model for additive fuel shall be the same used for UO_2 fuel. (Section 3.1.13)

7. For the additive fuel the currently approved peak pellet burnup limit of **[ ]** shall be applied.

8. Until sufficient cladding strain data from power ramps can be used to determine a higher limit, the MOP limits for UO_2 fuel shall be applied to additive fuel. (Section 3.3.3)

9. The FGR model uncertainty for UO_2 with additives as proposed in NEDE-33406P shall be modified for additive fuel licensing analyses by biasing the rod power by **[ ]** in order to bound the limited additive fuel FGR data that operated near the thermal mechanical operating limit (TMOL). This limitation is imposed due to the fact that the 2σ upper bound determined using a power perturbation of **[ ]** under predicts **[ ]** out of **[ ]** FGR data from additive fuel (data that operated greater than 0.85% TMOL). This limitation can be removed or modified based on additional data analysis that satisfies the concern that the limited amount of additive fuel FGR data is not bounded for licensing analyses. The uncertainty used for licensing analyses for UO_2 without additives is unchanged with a **[ ]** model uncertainty and a **[ ]** power perturbation (Section 3.3.2).

   OR

   The interlinkage temperature threshold for additive fuel **[ ]** to achieve the same or more bounding predictions as those using a **[ ]** bounding power perturbation for the **[ ]** additive fuel data discussed in Section 3.4.2 above. (Section 3.3.2)

   The staff is providing the above option for Limitation number 9 to the applicant since the revised interlinkage temperature will achieve the same or more bounding predictions as those using a **[ ]** power perturbation for the **[ ]** additive FGR data identified in Section 3.3.2 of the safety evaluation.

8.0 REFERENCES

1. NEDC-33406P, Revision 2, “Additive Fuel Pellets for GNF Fuel Designs,” Global Nuclear Fuel, December 2009. (ADAMS Accession No. ML093560114)

2. Letter from Stephen Philpott (US NRC) to Brian Moore (GNF-Americas), “Request for Additional Information RE: Global Nuclear Fuel – Americas, LLC (GNF) Topical Report (TR) NEDC-33406P, Revision 2, Additive Fuel Pellets for GNF Fuel Designs (TAC No. ME3082)” US NRC, May 14, 2013. (ADAMS Accession No. ML11077A011)

3. Letter MFN 13-101 to USNRC from Brian Moore (GE-Hitachi), “GNF Response to NRC RAIs for NEDC-33406P, Revision 2, Additive Fuel Pellets for GNF Fuel Designs,” Global Nuclear Fuel, December 16, 2013.

4. NEDC-33256P-A, NEDC-33257P-A & NEDC-33258P-A, Revision 1, Licensing Topical Reports, “The PRIME Model for Analysis of Fuel Rod Thermal-Mechanical Performance, Part 1 – Technical Bases, Part 2 – Qualification, Part 3 – Application Methodology,” Global Nuclear Fuel, September 2010.

5. Geelhood KJ, WG Luscher, and CE Beyer, NUREG/CR-7022, Vol. 1, PNNL-19418, Vol. 1, FRAPCON-3.4: A Computer Code for the Calculation of Steady-State, Thermal-Mechanical Behavior of Oxide Fuel Rods for High Burnup, Pacific Northwest National Laboratory, Richland, Washington, 2011

6. Geelhood KJ, WG Luscher, and CE Beyer, NUREG/CR-7022, Volume 2, PNNL-19418, Volume 2, "FRAPCON-3.4: Integral Assessment, Pacific Northwest National Laboratory, Richland, Washington, 2011.

7. Geelhood KJ, and CE Beyer. "Hydrogen Pickup Models for Zircaloy-, Zircaloy-4, M5™ and ZIRLO™", Water Reactor Fuel Performance Meeting, Chengdu, China, September 11-14, 2011.

8. Lanning, DD, CE Beyer and K. J. Geelhood. 2005. FRAPCON-3 Updates, Including Mixed-Oxide Fuel Properties," NUREG/CR-6534, Vol. 4, PNNL-11513, Pacific Northwest National Laboratory.

9. NEDE-33214P-A, "Densification Testing – Licensing Topical Report," Global Nuclear Fuel, September 2005.

10. Luscher, WG and KJ Geelhood. 2011. Material Property Correlations: Comparisons between FRAPCON-3.4, FRAPTRAN 1.4 and MATPRO, NUREG/CR-7024, PNNL-19417) Pacific Northwest National Laboratory, Richland, Washington.

11. C. E. Beyer, K.J.Geelhood, "PNNL-22549, Pellet-Cladding Mechanical Interaction Threshold for Reactivity Initiated Accidents for Pressurized Water Reactors and Boiling Water Reactors," DOE Contract DE-AC05-76RL01830, Pacific Northwest National Laboratory, June 2013.

12. NUREG-1465, "Accident Source Terms for Light Water Nuclear Power Plants," US Nuclear Regulatory Commission, February 1995.

13. Regulatory Guide 1.183, "Alternate Radiological Source Terms for Evaluating Design Basis Accidents at Nuclear Power Reactors," USNRC, July 2000.

Attachment: Resolution of Comments

Principal Contributors: PNNL Staff
Mathew M. Panicker

Date: November 9, 2015

**Comment Summary for Safety Evaluation for
GE Hitachi Nuclear Energy Americas, LLC Licensing Topical Report
NEDC-33406P, Revision 2, "Additive Fuel Pellets for GNF Fuel Designs"**

Location	Comment	NRC Disposition
General	Global Nuclear Fuel – Americas, LLC (GNF) proprietary information in the Draft SE has been marked in the pattern consistent with the description on the cover page of Enclosure 1 and in the Enclosure 3 affidavit.	No action needed.
General	There were issues with section breaks and page flow so the extra section breaks were removed and in some cases figures and figure titles moved so the title and figure would be together. Therefore, the page number references used herein are those in the Enclosure 1b and not in the Draft SE that was received.	No action needed.
Page 1 Section 1.0	Line 18 Add comma between creep and yield strength to clarify they are separate phenomena …energy, creep, yield strength, elastic modulus.…	Comment accepted. Change incorporated in final SE.
Page 4 Section 3.1.2	Lines 31 and 33 Insert the word liquid to clarify the statements. The melting temperature for additive fuel is **[** **]**	Comment accepted. Change incorporated in final SE.

ATTACHMENT

Location	Comment	NRC Disposition
Page 5 Section 3.1.2	Line 5 Insert the word liquid to clarify the statements. **[** **]** Line 15 and 18 Suggested Clarifications GNF responded that they do not have slumping tests for **[** **]** that is above the eutectic temperature where the **[** **]** for AOO events. Line 25 Word change for clarity … have shown a small amount of **[** **]** movement due to pellet-cladding…. Line 27 Word change for clarity …eutectic temperature such that the outer fuel below the eutectic temperature constrained the…. Lines 32-35 Clarifications to MOP and TOP statements In GNF methodology, the MOP provides a limit on the allowable change in LHGR while TOP provides a limit on the allowable peak LHGR during an AOO. Therefore, the peak temperature is limited by TOP. …It is also noted that since both conditions must be met the TOP event is the most limiting, as it provides a limit on the maximum fuel centerline temperature. GNF provided an additional analysis demonstrating that the 0.20 volume fraction for liquid cannot be achieved at any axial node for a TOP event.	All comments accepted. Changes incorporated in final SE.

Location	Comment	NRC Disposition
Page 6 Section 3.1.3	Line 34 Delete paragraph marks to put Theoretical Density on the section number line.	Comment accepted. Change incorporated in final SE.
Page 7 Section 3.1.4	Line 16 Add a word for clarity …additive fuel **[ ]** the change in thermal expansion is very small. Line 21 Figure 1 is Proprietary to GNF except for the FRAPCON results.	Comment accepted. Change incorporated in final SE. Comment accepted. Change incorporated in final SE.
Page 10 Section 3.1.5	Line 2 Figure 3 is Proprietary to GNF except for the FRAPCON results. Line 11 Delete extra word …than the solid phase and the volume of liquid additive becomes significant at this.	Comment accepted. Change incorporated in final SE. Comment accepted. Change incorporated in final SE.
Page 10 Section 3.1.6	Line 24 Word modification …because of the small additions of Al_2O_3-SiO_2 additive to UO_2 fuel.	Comment accepted. Change incorporated in final SE.
Page 11 Section 3.1.6	Line 7 Figure 4 is Proprietary to GNF except for the FRAPCON results.	Comment accepted. Change incorporated in final SE.
Page 13 Section 3.1.8	Lines 20-21 Add words for clarity …or plastic strain above the yield strength. The staff requested that if the fuel mass is conserved, has the movement of the fuel, if any, been confirmed experimentally…. Lines 23-26 Modify statements for clarity …volume is **[ ]**, as discussed in Section 3.1.12. The flow of material to conserve volume occurs primarily at the pellet center where temperatures are high and result in fuel movement to **[ ]**	All comments accepted. Changes incorporated in final SE.

Location	Comment	NRC Disposition
Page 14 Section 3.1.9	Lines 29-39 These changes are based on the RAI 17 response which addresses yield stress. …decrease compared to UO_2 fuel above a **[ ]** temperature. Additionally, GNF provided the explicit strain rate sensitivity and showed that the strain rate dependency for yield stress was small for rates in the range of **[ ]**. GNF noted that, as discussed in the response to the referenced RAI, PRIME analyses of power increases are performed using a series of **[ ]**.	All comments accepted. Changes incorporated in final SE.
Page 16 Section 3.1.12	Line 2 Add words for clarification …ramping). GNF has assumed that there is **[ ]**.	Comment accepted. Change incorporated in final SE.
Page 16 Section 3.1.13	Line 26 Add words for clarification …fuel in test rods that operated to average exposures of the standard fuel to **[ ]**.	Comment accepted. Change incorporated in final SE.
Page 17 Section 3.1.13	Line 7 Add words for clarification. …of the grain boundaries may change due to the additive precipitated on these boundaries during fabrication, however…	Comment accepted. Change incorporated in final SE.

Location	Comment	NRC Disposition
Page 19 Section 3.2.2	Line 34 Modified word for clarity **…[** **]**,	Comment accepted. Change incorporated in final SE.
Page 20 Section 3.2.3	Line 6 Deleted what appeared to be extra words. …lead to fuel rod failure. Lines 33-34 Clarify the effect of additive …has **[** **]**.	Comment accepted. Change incorporated in final SE. Comment accepted. Change incorporated in final SE.
Page 21 Section 3.2.3	Lines 9-13 Clarify statements regarding dispersal with additive fuel. …it should be considered if the fuel fails during this event. In the event the failure threshold is exceeded, fuel dispersal in additive fuel will be considered using the same basis as standard UO_2 fuel.	Comment accepted. Change incorporated in final SE.
Page 22 Section 3.2.4	Lines 11-12 Add parentheses for clarity …respect to densification ([ ] for additive than for UO_2 fuel).	Comment accepted. Change incorporated in final SE.
Page 23 Section 3.2.6	Line 9 Add clarifying words …conditions to maintain availability of Cs, the alternate source term assumptions used…	Comment accepted. Change incorporated in final SE.

Location	Comment	NRC Disposition
Page 25 Section 3.3.2	Lines 13-29 Modified to clarify the position stated in RAI 20 (S-02) GNF provided the rod power histories in follow up responses. In these follow up responses GNF suggested that certain data from **[** **]** GNF based the suggestion on the fact that the **[** **]** Staff noted that if the **[** **]** data were eliminated from Figure 5, there would only be **[** **]** at a burnup of 53 GWd/MTU that operated near or above the GNF TMOL. GNF recognized the staff concern about lack of data in the power/exposure range where rod internal pressure is limiting and accepted the staff position that the **[** **]** data be considered in the evaluation of the acceptability of the proposed additive fuel FGR model.	All comments accepted. Changes incorporated in final SE.
Page 26 Section 3.3.2	Lines 20-21 Clarify sentence **[** **]** Lines 26-27 Change word for clarity and correct RAI citation ≥ 40 GWd/MTU based on the power histories supplied to PNNL/staff in RAI 20 (S02).	Comment accepted. Change incorporated in final SE.
Page 27 Section 3.3.2	Entire Page The term uncertainty in the context of the proposed bounding FGR methodology should be changed to perturbation. See Page 27 markup for other suggested clarifications.	All comments accepted. Changes incorporated in final SE.

Location	Comment	NRC Disposition
Page 28 Section 3.3.2	Lines 2-7 The term uncertainty in the context of the proposed bounding FGR methodology should be changed to perturbation. As an alternative, GNF has proposed that instead of using the **[ ]** bounding power perturbation that they continue using the **[ ]** power perturbation used for UO2 licensing analyses **[** **]** to achieve the same or more bounding predictions as those using a **[ ]** bounding power perturbation for the **[ ]** additive FGR data identified above. The staff concludes that this is also acceptable.	Comment accepted. Change incorporated in final SE.
Page 30 Section 3.3.3	Line 10-11 Edits to improve clarity …of cladding data near the burnup and rod power where margin to the MOP limit is minimum.	Comment accepted. Change incorporated in final SE.
Page 32 Section 3.4.3	Line 3 Add clarifying statement …the PRIME review. GNF responded and showed that additive fuel met the….	Comment accepted. Change incorporated in final SE.
Page 32 Section 3.4.4	Line 21 Add clarifying word …UO_2 properties for bounding cladding fatigue analyses.	Comment accepted. Change incorporated in final SE.
Page 32 Section 3.4.5	Line 31 The currently approved creep collapse topical report, Cladding Creep Collapse Licensing Topical Report, NEDC-33139PA, July 2005, allows for the use of athermal fission gas release (FGR). Since July 2005, the creep collapse analysis for new fuel products has utilized the athermal FGR approach. Therefore, Line 31 is modified to reflect that option. …conservatively assumed no FGR or only athermal FGR, this removes….	Comment accepted. Change incorporated in final SE.

Location	Comment	NRC Disposition
Page 33 Section 3.4.6	Line 4 Clarifying statement …The gap conductance for the high power case is…	Comment accepted. Change incorporated in final SE.
Page 33 Section 3.4.7	Lines 12 - 13 Clarify statement To confirm compliance with GDC 11, GNF analyzed the impact of introducing additive fuel on the key reactivity coefficients; results of the evaluation confirmed that the introduction of additive at the planned concentration does not impact the nuclear dynamic parameters/reactivity coefficients. …	Comment accepted. Change incorporated in final SE.
Page 34 Section 3.5	Line 17 Add word for clarity …**[** **]** may be offered for additive fuel with…	Comment accepted. Change incorporated in final SE.
Page 35 Section 4.1	Line 1 Add clarifying words The NRC staff concludes that thermal-mechanical performance of the proposed…. Lines 3-5 The statements in these lines are the same as statements in the TR. The statement regarding the theoretical density is not correct. The effect aluminosilicate has on the theoretical density is characterized as slight in Section 2.3.1 of the TR. Therefore, the following changes are proposed for both the SE and the –A version of the TR. …Fuel melting and fuel creep rate are found to have significant effects from addition of aluminosilicate. Theoretical density is deemed to have been affected only slightly. Fuel properties such as thermal conductivity, FGR, and fuel washout have been insignificantly impacted.	Comment accepted. Change incorporated in final SE. Comment accepted. Change incorporated in final SE.

Location	Comment	NRC Disposition
Page 35 Section 4.2-3.	Lines 20-21 Add clarifying words The time for AOO events with fuel near the **[ ]** criterion shall be limited to less than or equal to **[ ]**. (Section 3.1.2)	Comment accepted. Change incorporated in final SE.
Page 35 Section 4.2-5.	Lines 28-29 Add clarifying words and correct Section reference to 3.1.7. For licensing analyses, the initial grain size for additive fuel shall be no greater than **[ ]**, based on 3-D dimensions. (Section 3.1.7)	Comment accepted. Change incorporated in final SE.
Page 36 Section 4.2-9.	Entire Sub-Paragraph The term uncertainty in the context of the proposed bounding FGR methodology should be changed to perturbation. See Page 36 markup for other suggested clarifications.	Comment accepted. Change incorporated in final SE.

TABLE OF CONTENTS

Page

LIST OF TABLES

LIST OF FIGURES

EXECUTIVE SUMMARY

GNF desires to introduce aluminosilicate additive fuel pellets into GNF fuel products to increase fuel reliability and operational flexibility of nuclear fuel bundles and cores. This document provides the technical justification to deploy additive fuel in [[ ]] using [[ ]] additives at concentrations of up to [[ ]] by weight and SiO_2:Al_2O_3 ratios in the range of [[ ]] by weight. Ramp testing has demonstrated additive is effective at concentrations as low as [[ ]] by weight UO_2 and that additive fuel can survive in the range in which 95% of non-barrier standard fuel would fail. At the small concentrations being proposed, the additive has minimal effect on the thermal-mechanical properties of the fuel at normal operating conditions.

REVISIONS

Number	Purpose of Revision
0	Initial Issue.
1	Corrected significant figures for ASTM concentration in Table 1-1, corrected composition low end in Table 1-1 and Section 7.
2	Editorial changes and clarifications for sections 2.1, 2.2, 3.2 and 5.1. Added section 2.14 on High Burn-up Structure (HBS). Inserted new section 5.7 on nuclear licensing effects and renumbered remaining section. Added discussion to section 6.3 on fuel operation above eutectic.
3	Created “-A” version by adding the NRC’s Final Safety Evaluation (Reference 7) and GNF’s responses to the NRC's Requests for Additional Information (RAIs) (Reference 6). Revised Sections 2.2.1, 2.2.2, 2.2.3, 2.5.2 and 2.9 consistent with the response to RAI 17-S01 in GNF’s letter MFN 13-101, dated December 16, 2013 (Reference 6). Revised Section 7.0, third paragraph, to make the statements in the conclusion consistent with other sections of the report and the NRC Final Safety Evaluation. Added References 6 and 7.

1.0 INTRODUCTION

Additive fuel pellet technology has been investigated since 1976. At that time, a comprehensive program was initiated to characterize and test additive fuel, with a specific focus on conditions where pellet clad interaction (PCI) occurs. As part of this program, additive fuels were characterized, and material properties were determined for implementation into thermal-mechanical methods. Several lead test assemblies and segmented rods were inserted into power reactors in both the US and abroad. Instrumented fuel assemblies were inserted into a test reactor to develop thermal and mechanical data to support design and licensing. A series of tests were performed to characterize the reactivity initiated accident performance of additive fuels. More recently, additive fuel Lead Use Assemblies (LUAs) have been deployed in two foreign reactors to provide irradiated material for studying high exposure effects. [[

]]

[[

]] The table below summarizes the range of concentration, composition and product applicability of additive fuel to be approved by acceptance of this LTR.

	Additive Fuel Range of Applicability		
	Concentration wt%	Composition SiO_2 : Al_2O_3 by wt	Fuel Design
Derived from ASTM C776-00 Impurity Limit	[[ ]]	[[ ]]	N/A
Target Range	[[ ]]	[[ ]]	GE14, GNF2, new

Table 1-1 Additive Fuel Range to be Licensed

The scope of this licensing topical report will focus on relevant fuel material properties and in-core behavioral characteristics that are affected by the addition of additive and demonstrate the negligible effects on licensing safety limits with additive fuel pellets. This document will serve as a supplement to the PRIME licensing topical reports [References 1, 2, and 3] previously submitted to further support the models technical basis and qualification to data not shown in the previous submittals. By agreement with NRC staff, the submission and review of PRIME was

limited to non-additive fuel and it is this topical report that requests approval of PRIME use with additive fuel. No changes to any of the additive fuel models in PRIME previous submittals are proposed with this topical report.

2.0 MATERIAL PROPERTIES

In the planned additive concentration and composition ranges, the material properties of additive fuel and standard, non-additive fuel are generally similar and in some cases the same. However, several fuel material properties differ between additive fuel and standard, non-additive fuel and these properties are outlined in this section. This section also includes a description of how these properties are handled in the PRIME thermal-mechanical code. Some calculations in the PRIME methodology require gadolinia content as an input. [[

]]

The properties discussed in this section are melting, density, thermal expansion, thermal conductivity, grain size and grain growth, stored thermal energy, creep, yield strength, elastic modulus, strain hardening coefficient and tangent modulus, plastic Poisson's ratio, and swelling. Due to the importance of microstructure to the material properties and irradiation behavior, a general description of the microstructure of additive fuel will also be discussed.

2.1 MICROSTRUCTURE

Although microstructural evolution, other than grain growth, is not explicitly modeled in PRIME, the microstructure of additive fuel can differ from that of standard UO_2 fuel, and those differences prove to be the primary driver of the materials properties that differ in PRIME.

As shown in Figure 2-1, the as-fabricated pellet microstructure consists principally of a single phase UO_2 with a minor additive "phase" residing at the UO_2 grain boundaries. This additive phase can consist of additional phases [[

]] For simplicity, these non-UO_2 grain boundary-resident phases are collectively called the additive phase.

[[

]]

Figure 2-1 As-Fabricated Pellet Microstructural Comparison

During fabrication, the additive phase uniformly covers the grain boundaries, with excess additive tending to accumulate preferentially at grain edges and corners, an effect seen in Figure 2-1. The thickness of additive phase coating grain boundary faces [[

]], as shown in Figure 2-2.

[[

]]

Figure 2-2 TEM Micrograph of [[ ]] Additive Fuel Grain Boundary

This microstructure evolves further upon significant heating in operation. Typically, single-phase ceramic materials such as UO_2 of reasonably high purity exhibit what can be considered discrete melting temperatures, above which the material is all or nearly all liquid and below which the material is all or nearly all solid. [[

]]

The effect is that, during a temperature increase, at a critical temperature (the eutectic temperature) below the UO_2 melting temperature, any crystalline silica vitrifies. Upon further increase in temperature a larger volume fraction of the fuel becomes vitreous as the solubility of alumina and urania in this phase increases, dissolving more alumina and urania into the vitreous solution until the liquidus temperature is reached and the vitreous fraction of additive fuel is

100%, at which point the fuel can accurately be described as fully liquid. Such behavior is typical for any vitreous or low melting point impurity which forms a eutectic with UO_2, a category which includes both pure alumina (Al_2O_3) and silica (SiO_2) as well as other impurities routinely found in fuel pellets at small but measurable levels. Such behavior can be conceptualized with equilibrium phase diagrams, though they fail to capture some of the complexities introduced with non-equilibrium vitreous phases. Figures 2-3 and 2-4 show these binary phase diagrams. In these diagrams, equilibrium vitreous phases are described as "liquid" in reference to their long range crystalline order, in contrast to their viscosity or mechanical properties. This distinction is clarified here because it is a fuel's viscosity and mechanical properties, rather than long-range order, that most affect safety related behavior.

[[ ]]

Figure 2-3 Al_2O_3 – UO_2 Binary Phase Diagram

[[ ]]

Figure 2-4 SiO_2 – UO_2 Binary Phase Diagram

Each of the binary phase diagrams in Figures 2-3 and 2-4 are represented on one of the three edges of the ternary phase diagram in Figure 2-5. The interior of the ternary phase diagram contains contour lines showing the liquidus surface, with the heavy lines denoting the ternary loci of binary eutectic points.

[[ ]]

Figure 2-5 Al_2O_3 – SiO_2 – UO_2 Phase Diagram

A pseudo-binary diagram similar to those of Figures 2-3 and 2-4 can be determined for the additive – UO_2 system for any discrete additive composition (silica:alumina ratio). Such a diagram is a slice through the ternary diagram of Figure 2-5 connecting the additive composition of interest on the Al_2O_3 - SiO_2 line to the UO_2 corner point. Figures 2-6 and 2-7 are two such phase diagrams, presented in schematic form, which represent the compositions with which GNF has the most experience and approximating the bounding compositions under consideration. Figure 2-6 shows the phase diagram for additive fuel at a silica:alumina ratio of [[

]]

[[ ]]

Figure 2-6 Additive – UO_2 Pseudo-Binary Phase Diagram [[ ]]

[[ ]]

Figure 2-7 Additive – UO_2 Pseudo-Binary Phase Diagram [[ ]]

[[

]] The peritectic temperature, at which vitreous aluminosilicate becomes thermochemically stable upon heating, is described in PRIME (Section 2.2.2) and is [[ ]], above which only the vitreous additive and crystalline UO_2 phases are assumed to exist for the purposes of the calculation. [[

]] While this critical temperature has been verified experimentally (see Section 2.2.3) there is some solid mullite phase predicted to exist between the peritectic temperature and approximately [[ ]] in the case of the targeted composition region for which no credit is taken for decreased total vitreous phase content. In practice, the melting transition occurs over the temperature range from the ternary peritectic of [[ ]] to the liquidus, the temperature of which varies as a function of additive content and at a concentration of zero is equal to the melting point of pure

UO_2. For this reason, the peritectic temperature is referred to as the eutectic temperature throughout the text of this Report and in PRIME documentation.

2.2 MELTING TEMPERATURE

2.2.1 OVERVIEW

Fuel melting properties are considered in this section, while predictions of melting during normal operating conditions is addressed in Section 3.2 and during AOOs in Section 5.1. Melting of the fuel pellet is avoided to ensure that fuel does not relocate within the fuel pin under the force of gravity; that excess fission gas release does not occur; and that there is no deleterious reaction between molten fuel and the fuel rod cladding. Because the additive phase does not exhibit a congruent melting phase transition, a melting point definition is provided to ensure that each of these requirements are met at any temperature below the melting point so defined.

Of the above requirements, fuel relocation is most limiting for additive fuel. As shown in Section 3.2, the region of pellets exposed to cladding material is not hot enough during operation to permit contact of molten material with cladding. [[

]] As discussed in Section 2.1, the melting temperature of additive fuel is not a clearly defined phase transition point as in pure UO_2, and is not associated with the distinct phase transition of melting. Rather, with increasing temperature, there is a gradual dissolution of fuel volume into a vitreous phase and a gradual decrease in the viscosity of the vitreous phase. This transition occurs over the temperature range from the eutectic temperature to the liquidus temperature that defines the temperature where the material is 100% liquid for a given composition. The mechanical properties, which govern the ability of the fuel to relocate, change gradually over this temperature range and the risk of fuel relocation is expected somewhere within it. Thus, for the purposes of additive fuel pellets, an effective melting temperature is defined to ensure the fuel pellets do not relocate during normal operations including postulated AOOs. This effective melting temperature is a temperature below the liquidus where the fuel pellet deforms similar to melting for pure UO_2 [[

]] Because this occurs at a lower temperature than the liquidus limit and widespread relocation (as used in standard UO_2), [[

]] Furthermore, the resistance of the vitreous phase to deformation varies with temperature, but in PRIME it is assumed to have no contribution to the resistance to deformation at temperatures above the eutectic temperature. Because of this, at temperatures above the eutectic the vitreous phase is conservatively considered a liquid for mechanical purposes and in that context the terms are used interchangeably.

[[ ]] was investigated experimentally (see section 2.2.3) for additive fuel, and it was found that [[

]]. The corresponding temperature can in turn be derived by [[ ]]

[[ ]]

Figure 2-8 Fuel Melting Point Calculation Example

An example is given below to illustrate. Consider a pellet containing [[

]] additive with zero exposure. In this example [[

]]. The melting point can then be calculated using [[ ]], the PRIME value of which is plotted in Figure 2-8 in black, at [[ ]] additive, yielding a result of [[ ]]. In this example, the presence of [[ ]] additive results in a depression of [[ ]] from the non-additive melting point. In the proposed implementation, [[ ]], which can be converted to [[ ]] such as that used above by using the relationships in the following section. This approach yields a melting point curve, varying with temperature, as shown in Figure 2-9. This figure, plotted for zero exposure and no gadolinia content, shows the melting point depression at additive concentrations of interest, as well as the conservative nature of the defined melting point with respect to the liquidus. In this case, the melting point refers not to the crystallinity of the fuel but to a conservative assessment of the pellet resistance to macroscopic deformation; as such it is an effective melting point, though not the temperature at which fully-liquid behavior is observed.

[[ ]]

Figure 2-9 Additive Fuel Melting Temperature

2.2.2 PRIME APPROACH

In PRIME, the fuel melting temperature model is developed similarly to the fuel thermal conductivity model (see Section 2.5). The relation for the melting temperature of UO_2 is developed and then extended to include the effects of burn up, gadolinia and additive, based upon thermal arrest measurement data for UO_2, $(U,Gd)O_2$ and UO_2 containing additive. The resulting fuel melting temperature relation is described in detail below.

[[

]].

[[ ]]

Figure 2-10 Additive Fuel Phase Diagram (Schematic)

2.2.3 MODEL CORRELATION TO EXPERIMENTAL DATA

Determination of the melting point [[

]] Because of the importance of these components, [[

]]

[[

]]

Figure 2-11 PRIME Liquidus / Eutectic Temperature and Experimental Data

[[

]]

Figure 2-12 PRIME Liquidus / Eutectic Temperature and Data / Error Bars

Figure 2-12 shows the same data as Figure 2-11, but includes average values for each point along with error bars corresponding to the sum of the standard deviation of the individual measurements and the estimated temperature measurement error based on testing against calibration standards. The correlation shown in these two figures represents the ability of PRIME to provide an accurate prediction of [[

]]

The second component, [[ ]], was determined experimentally. The assumption in PRIME [[

]]

[[

]]

Table 2-1 Isothermal Additive Fuel Pellet Deformation Test Results

Clearly the fuel retains resistance to slumping at temperatures well in excess of the eutectic temperature because all fuel is sintered above the eutectic temperature and the pellets exhibit no measurable deformation. However, more detailed studies were conducted to determine more precisely how much higher than the eutectic the temperature can go before resulting in macroscopic deformation. In these studies additive test pellets were exposed [[

]]

These data show that [[

]]

The [[

]]

2.3 THEORETICAL DENSITY

2.3.1 OVERVIEW

The room temperature theoretical density of additive fuel differs slightly from standard UO_2 due to the higher density UO_2 displaced by the lower density additive phase. The theoretical density is calculated based [[ ]].

2.3.2 PRIME APPROACH

The theoretical density of $(U,Gd)O_2$ additive fuel is given by [[

]] (2-7)

2.4 THERMAL EXPANSION

2.4.1 OVERVIEW

[[

]] This difference is insignificant for the proposed additive formulations

[[

]], as shown in Section 2.4.2.

[[

]] Above the eutectic temperature there is an increasing fraction of lower density liquid phase present, but this liquid phase increases in

[[

]] This is calculated on an *a priori* basis using fundamental properties of the additive phase. [[

]], the net effect is generally negligible or very small.

2.4.2 PRIME APPROACH

The thermal expansion equivalent strain of a fuel pellet ring is assumed isotropic and given by

[[

]]

Figure 2-13 shows a comparison of the PRIME outputs for thermal expansion of unirradiated additive fuel at a concentration of [[ ]] versus that of standard UO_2 fuel.

[[

]]

Figure 2-13 Thermal Expansion of Additive Fuel from Room Temperature

2.5 THERMAL CONDUCTIVITY

2.5.1 OVERVIEW

Because the thermal conductivity of the additive phase is lower than that of pure UO_2, the thermal conductivity of additive fuel is slightly lower than that of conventional fuel. This effect is highly dependent on the concentration of additive, and has been measured for high additive concentrations [[ ]], though at the concentrations of interest there is very little effect. The thermal conductivity decrease is most pronounced at lower temperatures and low burn ups. At higher temperatures, the phonon scattering penalty suffered by the additive phase becomes less important as radiative heat transfer predominates, and at higher burnups the addition of phonon scattering sites and features has a greater influence on the previously low entropy UO_2 lattice than the glassy additive phase. Thus, at high temperatures and higher burn up the additive fuel thermal conductivity further approaches that of standard UO_2.

2.5.2 PRIME APPROACH

In PRIME, the fuel thermal conductivity model is developed for UO_2 and then extended to include the effects of burn up, gadolinia and additive. To permit explicit treatment of the observed burn up dependency, the phonon contribution to the thermal conductivity of UO_2 is based upon the Klemens model. The burn up dependency is included by modifying the phonon term to account for the defect concentration due to burn up. The modification includes the effect of defect recovery due to thermal annealing. The gadolinia dependency is similarly addressed by additionally modifying the phonon term to account for the defect concentration due to gadolinia. Finally, the effects of addition of additive are explicitly addressed. The resulting fuel thermal conductivity relation is described in detail below.

[[

]]

The results of these tests are reflected in PRIME through the following thermal conductivity relations. These relations are presented in SI units for convenience. The relations are converted to English units for use in PRIME (1 BTU=0.2931 Watt-hr, 1 ft=0.3048 m, and 1 °R=0.5556 K).

For $T \leq T_{EUT}$

$$K = [[\quad\quad]] \qquad (2\text{-}11)$$

For $T > T_{EUT}$

$$K = [[\quad\quad]] \qquad (2\text{-}12)$$

Where

K = Fuel thermal conductivity (W/mK)

[[

]]

2.5.3 MODEL CORRELATIONS TO EXPERIMENTAL DATA

Laboratory measurements of thermal conductivity were performed on test pellets using [[
]] and the results are plotted in Figure 2-14 against the corresponding PRIME predictions. These pellets were fabricated with [[
]] at the concentrations indicated.

[[

]]

Figure 2-14 Thermal Conductivity Data for Additive Fuel

The effect of additive on the thermal conductivity of fuel is small, even at the tested concentrations, which are greater than those under consideration for use.

2.6 GRAIN SIZE AND GROWTH

2.6.1 OVERVIEW

Grain size and growth are important because of the tendency for larger grains to suppress fission gas release at low and moderate exposures. Both the initial grain size and grain growth during operation [[

]] The initial grain size for additive fuel can be significantly larger than that of standard UO_2, and this phenomenon is reflected in the generic grain growth approach and implemented by having separate design basis values for the grain sizes of additive fuel and non-additive fuel. [[

]]

2.6.2 PRIME APPROACH

Grain growth is given by

[[

]]

For application in PRIME, grain growth is calculated for each pellet ring. An arithmetic mean of the temperatures at the inner and outer ring boundaries is used. Additionally, a limiting grain size is defined to avoid a potential non-conservative under prediction of fission gas release fraction. No grain growth is calculated when the current grain diameter is equal to or larger than [[ ]].

2.7 STORED ENERGY

2.7.1 OVERVIEW

The fuel stored thermal energy is modified slightly by the presence of additive using [[ ]] reflecting the stored energy of pure UO_2 and that of pure additive phase. Because the range of relative quantities of additive phase under consideration is very small, the effect is small. This approach is used up to the melting point, [[ ]]. Above the melting point it is assumed that there is a step change in the heat capacity [[ ]]. While this only approximates the complex melting behavior of additive fuel, because the model is weighted by the annular ring volume and the total liquid fraction in a pellet is very small in even the most extreme AOOs intended to be analyzed by PRIME (see Section 3.2), the error introduced by the approximation is negligible.

2.7.2 PRIME APPROACH

In PRIME, stored energy is calculated for each pellet ring and then weighted by the annular ring volume to obtain the pellet-stored energy. For each ring the stored energy is given by

[[

]]

2.8 CREEP

2.8.1 OVERVIEW

The steady-state creep behavior of additive fuel is [[

]] is shown in Figure 2-15, which shows PRIME calculations of steady state creep rates as a function of stress at various temperatures for both [[

]] The inputs include a fission rate of 0, [[

]]

[[

]]

Figure 2-15 Steady State Creep Rates of Additive Fuel vs. Standard UO_2

2.8.2 PRIME APPROACH

Uniaxial compression tests have been performed to determine the creep characteristics [[

]]

The results of these tests are reflected in the PRIME model through the use of a fuel pellet creep model of the form

[[

]]

2.8.3 MODEL CORRELATIONS TO EXPERIMENTAL DATA

Uniaxial compression testing was performed on unirradiated additive fuel samples and some of the results are plotted in Figure 2-16 through Figure 2-18.

[[ ]]

Figure 2-16 Prime Creep Calculations Vs. Data for 0.25 wt% Additive

[[ ]]

Figure 2-17 Prime Creep Calculations Vs. Data for 1.0 wt% Additive

Figure 2-16 and Figure 2-17 show the steady state creep rate plotted against applied uniaxial stress at a variety of temperatures, and cover additive at concentrations of [[

]] Figure 2-18 shows the steady state creep rate plotted against temperature at a variety of applied stresses. In all of these tests, the test pellets were unirradiated fuel and the data were normalized to 95% theoretical density. The PRIME outputs use the same input parameters discussed in Section 2.8.1.

[[

]]

Figure 2-18 Prime Creep Calculations Vs. Data for 0.5 wt% Additive

2.9 YIELD STRESS

[[

]] The yield stress models described below have been developed based on mechanical testing of unirradiated additive fuel [[

]] Based upon the results, the fuel yield stress in PRIME is given by

[[

]]

2.10 MODULUS OF ELASTICITY

In modeling additive fuel there is an adjustment made to the modulus of elasticity of standard non-additive fuel to compensate for the effect of the glassy and/or liquid phase present. [[

]]

2.11 STRAIN HARDENING COEFFICIENT AND TANGENT MODULUS

In modeling additive fuel there is an adjustment made to the strain hardening coefficient and tangent modulus of standard non-additive fuel to compensate for the effect of the glassy and/or liquid phase present. [[

]]

In PRIME, the fuel material stress-strain curve is given by the relation

[[

]] (2-31)

2.12 PLASTIC POISSON'S RATIO

In general, plastic deformation is assumed to be nondilatational, i.e. plastic deformation does not include an associated volume change. In PRIME, this assumption is applied [[

]]

2.13 CUMULATIVE EXPOSURE

Cumulative exposure is not a material property but is a parameter that affects material properties like [[

]]

2.14 EFFECT OF ADDITIVE ON THE HIGH BURN-UP FUEL PELLET RIM STRUCTURE

The additive consists of a combination of glassy and crystalline phases after sintering. It has a very high viscosity at temperatures below ~1200°C so that the as-sintered additive is essentially rigid despite the presence of a glassy phase. The additive remains on the grain faces during in-reactor operation, does not combine chemically with UO_2 or (U, Pu)O_2 and is immobile at temperatures in the range where High Burn-up Structure (HBS) has been observed to form. The consequence of these conditions is that the additive is expected to remain on the boundaries of the as-sintered grains in the region of the HBS, Figure 2-19, and not diffuse into or react chemically with the recrystallized grains that comprise the HBS.

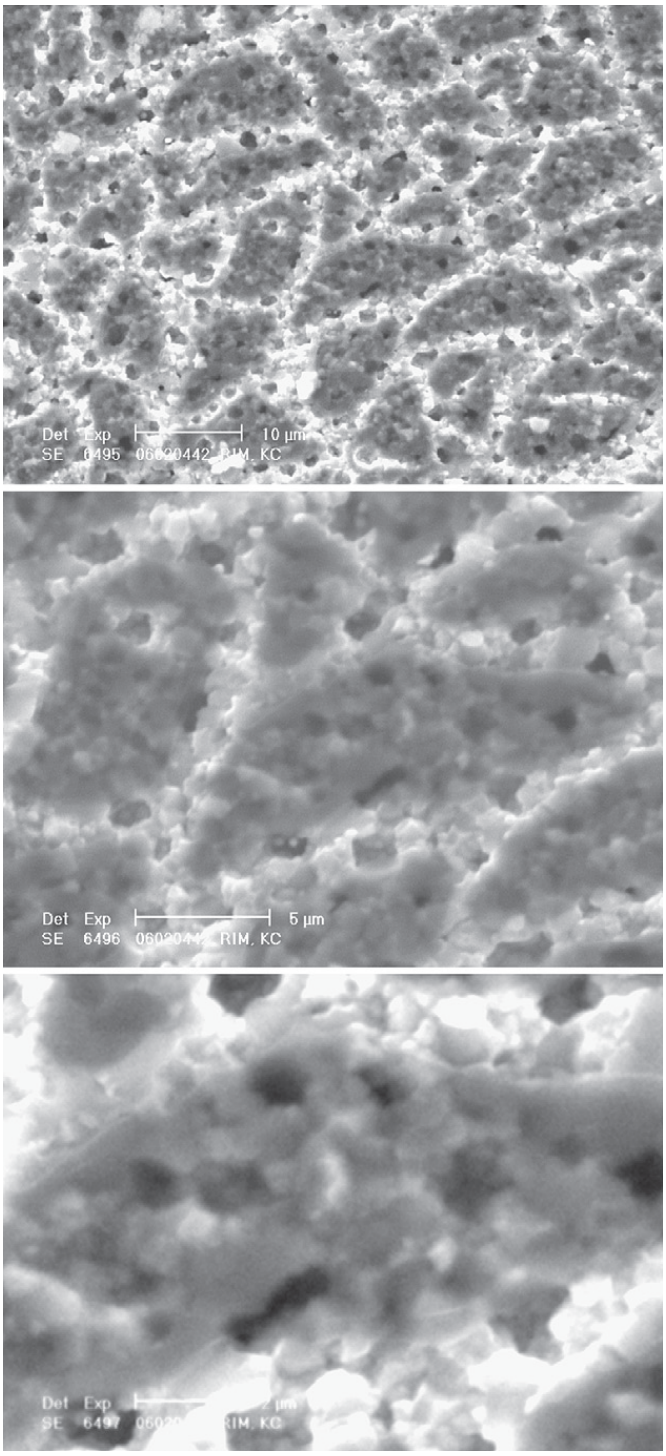

Figure 2-19 SEM images of the amorphous-appearing structure within the initial UO2 grains and the presence of the initial grain boundaries in the HBS

The implications of the expected behavior of the Al-Si-O additive on the HBS structure are:

1. The formation of the rim structure will be suppressed by the presence of large as-sintered grains as observed in Japanese tests to pellet average exposures in excess of 80 GWd/MTU,

2. The Al-Si-O additive will not affect the formation or the properties of the HBS except as related to the size of as-sintered grains,

3. The effect of the HBS on thermal and mechanical properties will be the same in fuel with the Al-Si-O additive as in fuel without the additive and as modeled in the PRIME computer code,

4. The Al-Si-O additive is not expected to alter the storage in or the dispersal from the HBS of fission products and fuel material in the event of postulated accidents; e.g., Loss-of-Coolant-Accident (LOCA) or Reactivity Insertion Accident (RIA),

5. The post-irradiation microstructural stability and chemical properties of the HBS in pellets with the Al-Si-O additive is expected to be the same as in pellets without the additive.

In conclusion, as noted above the Al-Si-O additive of GNF resides on the as-sintered boundaries of UO_2 grains and is expected to alter the formation of the HBS structure only through the presence of larger grains; i.e., slightly suppress the formation of a HBS. The additive is insoluble in UO_2 and the mixed $(U, Pu)O_2$ that forms during irradiation. The mobility of the additive is sufficiently low at temperatures where the HBS has been observed that it will not diffuse or otherwise migrate into the porosity of the HBS. As a result, the Al-Si-O additive is not expected to affect the HBS or alter the behavior of the HBS with respect to in-reactor and post-irradiation performance.

3.0 BEHAVIORAL ASSESSMENT

Based upon the effects of additive on fuel pellet microstructure, at the preferred GNF additive composition and concentrations, as discussed in Section 2.0, the following characteristics are potentially impacted: washout behavior, fuel melting, RIA behavior, in-reactor densification, validity of alternate source term assumptions, and long-term fuel storage. Each effect is discussed below.

3.1 WASHOUT CHARACTERISTICS

Pellet susceptibility to oxidation in the presence of water at BWR conditions has been closely examined by GNF to evaluate the propensity for fuel washout. Over a period of more than a decade, testing has been performed on laboratory and factory produced pellets with a wide variety of additive compositions and concentrations. For those covered under the scope of this Report the test results support a conclusion that washout behavior for additive fuel is comparable to that of standard UO_2.

The standard view of washout behavior is that after a breach of the fuel rod cladding, water is introduced to the fuel rod interior and can interact with the fuel inside. Water at BWR conditions proves mildly corrosive to UO_2, and that corrosivity is dependent on several factors, principally the grain structure of the fuel. Testing shows that the grain boundaries are more susceptible to corrosion than grain faces, so corrosion begins at grain boundaries and proceeds along them at a faster rate than through bulk grains. For this reason, there is typically greater corrosion rates for small-grained fuel than for large grained fuel, which has a lower density of grain boundaries. Based upon this understanding of the washout phenomenon, the solubility of any material residing at the grain boundaries has the potential to have an important influence on the corrosion resistance properties of the fuel.

For the purposes of this evaluation, pellet susceptibility to oxidation was tested by [[

]] The results indicate that for the additive variation being considered, the behavior is similar to that of non-additive fuel. This

is consistent with the current understanding of the washout phenomenon. UO_2 fuel with large grains has been shown to exhibit enhanced corrosion resistance relative to standard UO_2 fuel with smaller grains due to the lower grain boundary area-to-volume ratio. The addition of additive to UO_2 fuel can result in larger grains. Accordingly, additive fuel corrosion resistance would be expected to be better than standard UO_2 fuel due to the grain size effect alone. [[

]] At the concentrations being considered, the additive glassy phase tends to accumulate in significant quantities only at the grain boundary edges and corners, with the grain boundary planes containing only a thickness [[

]] as shown in Figure 2-2. [[

]] support the experimental observations that the corrosion performance is comparable to that of standard UO_2 fuel.

In tests of laboratory-prepared pellets [[

]]

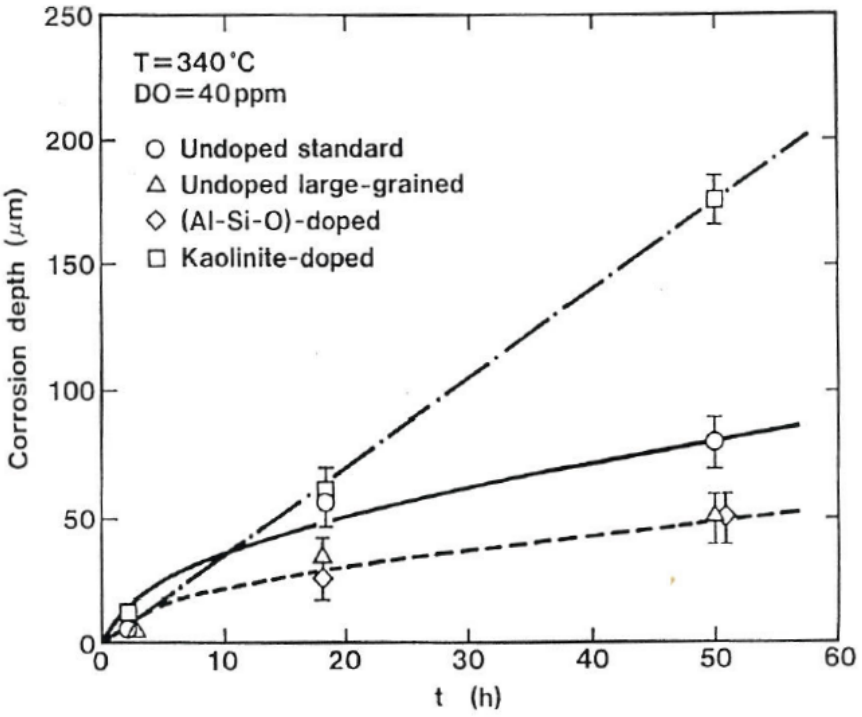

Figure 3-1 Comparison of Corrosion Behavior of Synthetic vs. Natural Additives
(Taken from K. Une, Corrosion Behavior of unirradiated Oxide Fuel in High Temperature Water, May 1995)

In addition to testing performed on laboratory pellets, archive pellets from additive LUA programs have also been evaluated. For the [[ ]], additive pellets were made with [[

]] There was no significant difference between the corrosion resistance of additive vs. non-additive fuel once this effect was accounted for. For the original evaluation of the [[ ]], unirradiated archive pellets were tested [[ ]], and the results are shown in Table 3-1.

[[

]]

Table 3-1 [[ ]] Pellet Oxidation Testing Results

[[

]] several types of sample pellets were prepared by GE Corporate Research and Development (GE-CRD) in a laboratory using [[

]]

[[ ]]

Figure 3-2 Circumferentially Oriented Flaws in [[ ]]

[[

]]

A final test of laboratory prepared pellets was performed on pellets prepared by Nippon Fuel Development (NFD) and tested by GNF. These samples were tested in the same way as the GE-CRD pellets discussed above, and the two sets of tests combine to represent the most comprehensive and carefully prepared and measured evaluation of pellet oxidation available for additive types similar to those to be used by GNF. [[

]] The results are presented in Table 3-2. Note that the GE-CRD and NFD pellets were [[

]], though the trends evident within a group of pellets are valid.

[[

]]

Table 3-2 Oxidation Testing Results

From Table 3-2, it can be seen that [[

]], and the

samples representative of the GNF-targeted additive composition [[ ]] and concentration [[ ]] actually showed improved corrosion resistance over standard UO_2.

The most recent set of oxidation tests was performed on unirradiated archive pellets fabricated for the [[ ]]. These pellets were the most recently factory-produced pellets tested for oxidation and are the most representative of the current GNF pellet production process. The data are presented in Table 3-3.
[[

]]

Table 3-3 Oxidation Testing Results from [[ ]] Archive Pellets

The additive used for the [[ ]] with a [[
]], and corrosion testing was performed using the same [[

]] method as used for the GE-CRD, NFD, and [[ ]] pellets. The results of the corrosion testing are consistent with prior work [[
]] in that they show that the corrosion resistance of additive fuel made with [[ ]] additives is comparable to that of standard UO_2.

The laboratory tests as described here indicate that additive fuel pellets of the type to be used by GNF are not intrinsically more susceptible to corrosion-assisted washout than are standard UO_2 pellets.

[[

]]

Table 3-4 Summary of Oxidation Testing Performed on Additive Fuel

Table 3-4 summarizes the results of GNF testing of additive fuel corrosion behavior. It is apparent that [[ ]] additives offer superior oxidation resistance over [[ ]] additives, driving GNF's design to use only [[ ]] additives. [[ ]] additives offer comparable corrosion resistance to standard UO_2.

3.2 FUEL MELTING

In addition to the fuel melting behavior description of additive fuel contained in Sections 2.1 and 5.1, there are other considerations of the expected fuel melting behavior. One such aspect of the unique melting behavior of additive fuel is evolution of the fuel microstructure upon thermal cycling which repeatedly increases and decreases the liquid fraction in the pellets. Upon heating above the eutectic temperature, UO_2 dissolves into the vitreous phase, which then precipitates back out as UO_2 upon subsequent cooling. In laboratory testing of pellets at high additive concentrations (5000 ppm), UO_2 particles have been observed to precipitate from large islands of additive on the pellet surface upon cooling from temperatures above the eutectic temperature, indicating the possibility of microstructural evolution due to thermal cycling. However, in factory-produced pellets these additive islands at the pellet surface are not observed, nor have any UO_2 precipitates in the additive phase otherwise been observed in such pellets. Any surface

layer of additive that would be present are removed by surface grinding of the pellets, and additive islands in the pellet interior are not large enough to support this precipitation mechanism. The precipitation mechanism observed occurs by accretion of UO_2 on a nearby grain, the inverse of the dissolution process, thus resulting in a microstructure that is indistinguishable from that present before thermal cycling. Because of this, thermal cycling is not considered to have any new effect on additive fuel properties or performance.

Also of note is that the melting behavior of additive fuel exhibits similarities to that of non-additive fuel. For example, the ASTM impurity limits for aluminum and silicon are 250 and 500 wppm respectively for sintered UO_2 pellets, which corresponds to an equivalent [[

]] additive concentration of about [[

]] Even at impurity concentrations well below the ASTM impurity limit, at purity levels comparable to those seen in typical standard UO_2 pellets, there is some aluminosilicate present, and the same behavior of partial melting above the eutectic temperature is exhibited through the full range of silica:alumina ratio compositions For example, for a "non-additive" pellet at 10% of the ASTM specification limit for aluminosilicate impurities, or an "additive" concentration of 105 wppm, the fuel melting point is depressed by 1.8 ˚C according to the PRIME model, [[ ]] and approximately [[

]]

Another relevant consideration is that [[ ]] described in Section 2.1, is considered conservative because temperatures [[

]] are confined to the pellet center, which makes up only a small fraction of the overall pellet volume, while the outer, cooler, region of the pellet [[ ]] including the additive phase. [[

]] Even at the limits of normal operation, only a small fraction of fuel is exposed to temperatures above the [[ ]] To illustrate this, PRIME was used to model the case of a full length rod fuel column with 10 axial nodes, subjected to the typical operating limits at the edge of the thermal-mechanical operating envelope, shown in Figure 3-3.

[[

]]

Figure 3-3 Representative Thermal-Mechanical Envelope for GNF2

In this case, [[ ]] At each of three limiting points on the envelope of Figure 3-3, the volume % of the fuel column that exceeds the eutectic temperature was calculated, assuming a parabolic radial temperature distribution for each node, and the results are shown in Figure 3-4.

[[

]]

Figure 3-4 Limiting Case of Fuel Fraction Above Eutectic Temperature

It can be seen from these results that even at the maximum anticipated operational LHGR, only a small fraction of the fuel column, [[ ]] in this case, is [[

]] Of that [[ ]], only a small fraction thereof is [[ ]] at these limiting conditions. Figure 3-5 illustrates to scale the regions of the fuel that experience temperatures [[ ]] at the limiting exposure of [[ ]].

[[

]]

Figure 3-5 Region of Fuel Above Eutectic at Limiting LHGR and Exposure

To further illustrate the conditions at the predicted highest temperature node at the highest temperature condition, the maximum centerline temperature predicted at that location is [[ ]], at which temperature the corresponding wt% liquid is approximately [[ ]], and about [[ ]] of the volume of this node is above the eutectic temperature. Even in this worst-case node, the total amount of liquid predicted is [[

]]

Furthermore, the liquid phase (more accurately called the vitreous phase) retains some resistance to deformation at temperatures above the eutectic temperature. Because the as-fabricated fuel pellets contain some vitreous phase even at room temperature, there is a continuous change in the material properties of the additive phase with increasing temperature, and the eutectic temperature, while representing the temperature at which a pure crystalline additive would melt, has no such meaning with a vitreous additive. Instead, the eutectic temperature represents the temperature at which UO_2 is expected to have any solubility in the vitreous phase, and there is not an associated step change in the material properties of the aluminosilicate itself.

The preceding examples are illustrations intended to show that in aluminosilicate additive fuel the high temperature mechanical stability is not exceptionally dissimilar to standard UO_2 fuel, and there is little risk of significant geometric redistribution of the fuel column due to the liquid that can be present in additive fuel.

3.3 REACTIVITY INSERTION ACCIDENT (RIA) CHARACTERISTICS

Reactivity Insertion Accident (RIA) testing of additive fuel has demonstrated that additive fuel meets applicable licensing requirements and furthermore shown there is no measurable RIA fuel performance penalty suffered by additive fuel compared to standard non-additive fuel. A total of 30 rods, including standard fuel as well as fuel with a variety of additive compositions and concentrations, were tested in the Nuclear Safety Research Reactor (NSRR) at the Japan Atomic Energy Research Institute. In these tests, the fuel evaluated included high and low additive concentrations [[ ]] and A and B additive compositions [[ ]] These additive types apply to the range of additive compositions considered in this Report, and the "low" additive concentration is equal to the [[ ]] for licensing in this Report. The deposited energy examined in this testing program ranged from [[ ]] and the results summarized in Figure 3-6.

[[

]]

Figure 3-6 RIA Testing Results

All of the additive fuel tested, as well as the GE non-additive fuel tested, exceeded the NSRR standard rod failure threshold of 260 cal/gUO_2 and was at least comparable to the GE standard rod threshold of [[ ]] The failure threshold was shown with certainty to be at [[ ]] for fuel with the highest kaolin additive concentration and for standard fuel, and was shown to be around [[ ]] Testing of rods with [[ ]], resulted in better resistance to rod failure than identical failed tests for higher concentrations, indicating that the failure thresholds indicated above for [[ ]] additive are conservative assessments of the RIA resistance of additive fuel of the type proposed. Additive fuel was also observed, where readily comparable, to exhibit less fragmentation than standard fuel.

3.4 IN-REACTOR DENSIFICATION

Additive fuel pellet in-reactor densification (and swelling) behavior is expected to be unchanged with respect to standard UO_2 fuel. Prior manufacturing experience indicates that there is little difference in the sintering kinetics and therefore densification behavior of additive fuel. A limited amount of in-reactor testing also supports this conclusion. [[

]], so it is also expected that, much like GNF non-additive fuel [Reference 4], additive fuel will be inherently resistant to significant in-reactor densification.

Because the additive fuel densification behavior is so similar to that of standard UO_2 fuel, the methodology for densification testing and qualification of additive fuel will follow the same approved methodology for standard UO_2 fuel as described in NEDE-33214P-A. [[

]]

3.5 EFFECT ON ALTERNATE SOURCE TERM

The alternate source term used in plant licensing should apply equally well to additive and non-additive fuel. The source term is detailed in NUREG-1465, which was introduced in 1995 to provide for a more realistic estimate of the radiological species released to containment in the event of a severe reactor accident involving substantial meltdown of the core. That document describes the specific nuclide types, quantities, chemical form, phase and timing of release into containment. The resulting source term is used in safety analyses for the design of plant systems and for plant licensing. [[

]] The alternate source term assumes that 95% of the released iodine is in the chemical form of CsI, with the remainder as volatile elemental iodine (I_2) and

organoiodides, e.g. CH_3I. These assumptions reduce the total amount of volatile iodine available to leave containment because CsI is highly soluble in water. Additionally, the source term model assumes the pH of water within the containment to be above 7. This constraint minimizes the irradiation-induced conversion of ionic iodine present in pools of water and on wet surfaces to elemental iodine. The analysis of such containment water assumes that the released Cs forms CsOH, which contributes to maintaining the pH at values greater than 7. This analysis assumes only a portion of the released Cs is converted to CsOH. Therefore, a significant amount of Cs needs to be released from the fuel to the containment for these assumptions to remain valid. [[

]]

- The amount of silica to be added is [[

]]

- The additive resides on the grain boundaries and is essentially insoluble in the grain matrix. The intergranular silica may [[

]] satisfy the NUREG-1465 criteria in the event of an accident because:

[[

]]

Therefore, the alternate source term assumptions used in design of plant systems and plant licensing should not be affected by the use of additive fuel.

3.6 LONG TERM FUEL STORAGE

For long-term storage, the concerns are the initial conditions at the start of storage (i.e. end of reactor operation), response during storage, and response to a cladding failure during storage. The initial conditions of interest include: the rod internal pressure, cladding corrosion and crud (impacts decay heat transfer and thus temperature during storage), cladding hydrogen concentration and morphology, and cladding strain. The presence of additive will have no impact on these parameters.

The response during storage includes possible additional cladding creep and corrosion and changes in hydride morphology resulting in hydrogen assisted or delayed hydrogen-cracking failure or reduced ductility or more specifically reduced seismic margin. Again, for the same initial conditions, the presence of additive will have no impact on these responses.

Fuel temperatures in the spent fuel pool will be near the temperature of the spent fuel pool water or very low. Fuel temperatures in dry storage are dictated by the specific loading of the dry storage cask, which depend on burnup and time after shutdown. The current regulations require the fuel temperatures to remain below 400°C in dry storage (Reference 5). For both of these cases, the fuel temperatures are below the melting temperature of additive fuel, so neither fuel relocation nor other phenomena associated with fuel melting are concerns for long term storage.

The concern after failure is fuel dispersal. For dry storage, including cask drying for transportation, dispersal will be negligible due to the relatively low temperatures and lack of water flow over the fuel. Because the temperatures are below the eutectic temperature of additive fuel, additive fuel will have no impact on this already negligible dispersal. Similarly, for wet storage, dispersal will be negligible due to the very low temperatures and very slow flow velocities (driven by convection only). Additive fuel will have no affect on this negligible dispersal.

4.0 QUALIFICATION DATA

GNF has conducted several experimental programs to investigate additive fuel behavior. These investigations were performed in commercial BWRs as well as test reactors. The experimental measurements include fission gas release, cladding diametral deformation and fuel temperature and rod internal pressure. Comparison of the PRIME code predictions with these measured data are discussed in the following subsections.

4.1 QUALIFICATION DATASET

GNF additive fuel rods have been successfully irradiated in power reactors since 1977, first in low-power segmented rod bundles and later in unrestricted LTAs. The experimental programs selected for PRIME additive fuel model qualification are briefly described in the following subsections.

4.1.1 [[ ]] – HALDEN RAMP TESTS

Five Lead Use Assemblies (LUAs) were fabricated by GE in 1984 and loaded into [[ ]] for irradiation. To achieve segment exposures in the target range, the LUAs were irradiated in [[ ]] The segments were generally representative of GE8 (8x8) fuel rods. All segments were comprised of nominally 0.483 inch outside diameter cladding. The nominal active fuel length was 26.29 inches, and the nominal plenum volume was 0.696 in^3. Some of the segments contained 8 w/o Gd_2O_3-UO_2 with low levels of aluminosilicate additive.

After the [[ ]], some segments were transported to the Halden test reactor in Norway for bump testing. In this case, the segments were placed in a test assembly and incubated for ~2-20 days at relatively low power levels (~6.0 - 7.5 kW/ft). After the incubation period, the power level in the test assembly was increased to elevate the segment power levels to values near the design and licensing basis power-exposure envelope. The test segments were then held at the bump power levels for ~30 days to ensure that equilibrium fission gas release conditions were achieved. At the end of Halden bump testing, segments were punctured for fission gas release measurements. The results from segments used for PRIME03 additive model qualification are summarized in Table 4-1.

Segment ID	Exposure, GWd/tU	GD_2O_3 Concentration, w/o	Additive Concentration, w/o	Measured FGR, %	PRIME03, FGR %
[[					
					]]

Table 4-1 Model Qualification Cases from [[ ]] –Halden Ramp Tests

4.1.2 HALDEN STEADY-STATE (THERMAL RIGS) TESTS

Standard UO_2 fuel and 2500 wppm or 0.25 wt.% natural clay additive fuel rods were irradiated in Halden in the [[ ]]. Test variables were pellet-clad gap, additive type and power. Test rods were instrumented with fuel centerline thermocouples, fuel column elongation sensors and gas pressure sensors. The rigs were inserted in 1985 and the last one was discharged in 1996. Table 4-2 summarizes the cases selected for PRIME03 additive model qualification with measured and calculated FGR.

Tests	Exposure, GWd/tU	Additive Concentration, w/o	Fuel Centerline Temperature	Measured Fission Gas Release, %	PRIME03 FGR, %
[[					
					]]

Table 4-2 Model Qualification Cases from Halden Steady-State (Thermal Rigs) Tests

4.1.3 [[ ]]-HALDEN RAMP TESTS

Fuel rod segments containing [[ ]] aluminosilicate additives at the [[ ]] (by weight) levels, as well as standard UO_2, in non-barrier cladding were base irradiated [[ ]] The PCI resistance of the additive fuels, relative to

that of standard UO_2 was determined by power ramp tests performed in the Halden Reactor. Power ramp testing of the segments was started in May 2001 in the Halden reactor in the assembly [[ ]]. All testing was completed by the end of June 2001. Candidate rods selected for PRIME03 additive model qualification are summarized in Table 4-3.

Segment Serial Number	Halden Test	Pre/Post Ramp Test Exposure, GWd/tU	Additive Concentration, ppm	Measured Fission Gas Release, %	PRIME03 FGR, (%)	Max. Cladding Strain, %
[[						
						]]

Table 4-3 Model Qualification cases from [[ ]]-Halden Ramp Tests

4.1.4 NFD HALDEN THERMAL RIG TESTS

GNF participated in a joint research program, termed the NFD Halden thermal rig tests, with the Japanese Utility Group to understand additive fuel behavior. Table 4-4 summarizes for selected rods, measured and calculated fission gas release (FGR) and end-of-life (EOL) rod internal pressure for these tests.

Fuel Type	Exposure (MWd/t)	Measured FGR (%)	PRIME03 FGR(%)	Measured EOL Pressure, psia	PRIME03 EOL Pressure, psia
[[					]]

Table 4-4 Model Qualification cases from NFD-Halden Thermal Rig Tests

4.1.5 NUPEC(JNES) STEP3 LUA TESTS

PRIME03 additive model qualification candidate rods from NUPEC(JNES) STEP3 LUA Tests are summarized in Table 4-5. Measured and PRIME03 calculated FGR data are also summarized in Table 4-5

Fuel Type	EOL Rod Average Exposure (GWd/t)	Measured FGR (%)	PRIME03 FGR (%)	Measured ΔD/D, %	PRIME03 ΔD/D, %
[[					
					]]

Table 4-5 Model Qualification cases from NUPEC(JNES) STEP3 LUA Tests

4.1.6 [[ ]]-LUA TESTS

Eight LUAs representative of GE14 fuel and designed for high burnup exposures started irradiation in [[ ]] The LUAs included both full and segmented rods with aluminosilicate additive fuel pellets and utilized improved cladding and spacer materials. Three full-length rods and four segmented rods (9 total rod segments) from this LUA program were transported from [[ ]] for rod puncturing and fission gas release measurements. The rods contained UO_2 plus aluminosilicate additive at concentrations of either [[ ]]

The results used for PRIME03 additive model qualification are summarized in Table 4-6.

Rod/Segment ID	Exposure, GWd/tU	Additive Concentration, w/o	Measured FGR%	PRIME03 FGR%
[[				
				]]

Table 4-6 Model Qualification Cases from [[ ]]

4.1.7 PRIME QUALIFICATION RESULTS

Fuel centerline temperature, fission gas release, rod internal pressure and cladding diametral strain for additive fuel were compared with non-additive cases previously used to qualify PRIME03. PRIME03 additive qualification results are discussed in the following subsections.

4.1.7.1 FUEL CENTERLINE TEMPERATURE QUALIFICATION

Additive fuel centerline data are compared with the PRIME03 non-additive qualification dataset to identify any significant bias in the additive data. An overall comparison of predicted and measured fuel centerline temperature for both the additive and non-additive cases is shown in Figure 4-1. The ratios of predicted/measured fuel centerline temperature as a function of exposure are presented in Figure 4-2. Fuel centerline temperature for the additive cases is well within the scatter of the PRIME03 non-additive qualification data and independent of fuel exposure.

[[

]]

Figure 4-1 Predicted versus Measured Fuel Temperature

[[

]]

Figure 4-2 Predicted/Measured Fuel Temperature versus Exposure

4.1.7.2 FISSION GAS RELEASE QUALIFICATION

Figure 4-3 and Figure 4-4 compares predicted and measured values of fission gas release for the PRIME03 dataset and the additive fuel dataset. The additive fission gas release data are well within the scatter of the non-additive data. Figure 4-4 shows no bias with exposure for the additive fuel fission gas release when compared with non-additive fuel.

[[

]]

Figure 4-3 Predicted versus Measured Fission Gas Release

[[

]]

Figure 4-4 Predicted/Measured Fission Gas Release versus Exposure

4.1.7.3 FUEL ROD INTERNAL PRESSURE QUALIFICATION

Comparisons of predicted and measured rod internal pressure for additive and non-additive fuel are presented in Figure 4-5 and Figure 4-6. No substantive deviation in PRIME03 prediction for the additive fuel internal pressure is observed when compared with non-additive fuel.

[[

]]

Figure 4-5 Predicted versus Measured Fuel Rod Internal Pressure

[[

]]

Figure 4-6 Predicted-Measured Rod Internal Pressure versus Exposure

4.1.7.4 FUEL CLADDING STRAIN QUALIFICATION

PRIME03 predictions of cladding strain for both the non-additive case and additive fuel rods are shown in Figure 4-7 and Figure 4-8. No significant difference in PRIME03 predictions for additive and non-additive fuel is observed.

[[

]]

Figure 4-7 Predicted versus Measured Cladding Diametral Strain

[[

]]

Figure 4-8 Predicted-Measured Cladding Diametral Strain

4.2 PRIME QUALIFICATION CONCLUSIONS

Fuel centerline temperatures, fission gas release and rod internal pressure prediction for the additive fuels are well within the scatter of non-additive data, and no significant bias with exposure is observed. The addition of additive cases does not change PRIME03 model uncertainties.

5.0 LICENSING CRITERIA ASSESSMENT

The material properties discussed in Section 2.1 have been implemented into the GNF thermal mechanical engineering computer code PRIME. PRIME has been submitted to the NRC for review and approval. The intent of this section is to show the effect of additive on the design bases for each of the fuel system damage, failure and coolability criteria, established in the Standard Review Plan 4.2 in NUREG-0800, relative to standard fuel by analyzing the limiting fuel design characteristics with the proposed range of additive and comparing the results to standard fuel with methodologies defined in GESTAR II. It will be shown for each licensing criterion that additive fuel is equivalent to or better than current UO_2 fuel. This assessment forms the basis for demonstrating that GESTAR II is also applicable to additive fuel.

The demonstration calculations included herein are based on the GNF2 fuel design analyzed using PRIME. The GNF2 fuel design is chosen because the design has the highest licensed linear heat generation rate (LHGR) in the current GNF fuel product line. The values shown in this section are representative of additive fuel and not the actual limits. The analysis reflects the current criteria, and it should be noted that other criteria changes may require the limits to be modified to insure compliance. The methodology described is consistent with the previously submitted PRIME application report.

5.1 FUEL MELTING

As described in Section 2.1 the fuel melting behavior of additive fuel is different than for standard fuel. However, the method of analysis used to protect standard fuel can be conservatively applied to additive fuel by [[

]]

[[

]]

Figure 5-1 Effect of Additive on Fuel Melting

[[

]]

5.2 FUEL ROD INTERNAL PRESSURE

Fuel rod internal pressure is limited by the licensing requirement that there [[

]]

To demonstrate the effect of additive in the PRIME calculation of fuel rod internal pressure, the GNF2 fuel rod design was analyzed with and without additive. Input parameters that affect the fission gas model have been conservatively chosen. For example, [[

]]

[[

]]

Figure 5-2 Effect of Additive on Fuel Rod Internal Pressure

5.3 CLADDING PLASTIC STRAIN

Analyses are performed for each rod type to determine the values of maximum overpower (Mechanical Overpower) magnitudes [[

]]

Additive fuel will be much more compliant than standard fuel during AOOs due to the high fuel temperatures, and will reduce the cladding strain and enhance margin relative to this licensing criterion. To demonstrate the impact, a typical mechanical overpower analysis, as described above, was performed for fuel with and without additive to compare the levels of permanent cladding strain as a function of exposure. Figure 5-3 shows the results.

[[

]]

Figure 5-3 Effect of Additive on Cladding Permanent Strain

As can be seen by the figure, the presence of additive [[

]]

5.4 CLADDING FATIGUE PLUS CREEP RUPTURE LIMIT

The cladding fatigue analysis also reflects operation [[

]]

To demonstrate the effect of additive on the fatigue life, additive and standard fuels were analyzed with PRIME. The standard analysis used at GNF by procedure also includes [[

]] Table 5-1 shows the results for both the standard fuel and additive fuel case.

[[

]]

Table 5-1 Fraction of Allowable Fatigue Lifetime Expended

[[

]] Additive fuel has minimal impact relative to the margin for non-additive fuel and satisfies the cladding fatigue design/licensing limit of [[

]] In general, additive will reduce cladding strains associated with pellet cladding mechanical interaction and improve fatigue life.

5.5 CLADDING CREEP COLLAPSE

Historically, GNF has performed a cladding creep collapse analysis for each new fuel design. This calculation was deliberately conservative to address uncertainties in GNF fuel rod performance that existed at the time the methodology was reviewed and approved by the NRC. [[

]] An LTR documenting the revised methodology, together with a bounding calculation intended to address GNF2 and future fuel designs, was submitted to and approved by the NRC (NEDC-33139P-A). Upon approval of the LTR, a creep collapse analysis was no longer required for a new fuel design unless the bounding analysis in the LTR did not apply to that design.

Based upon the characterized densification and fission gas release performance of GNF additive fuel relative to non-additive fuel, the revised methodology is applicable to additive fuel. Since additive fuel is otherwise identical to non-additive fuel, the bounding analysis in NEDC-33139P-A is applicable to additive fuel and additional consideration of creep collapse is not required.

5.6 LOCA\STABILITY\CORE TRANSIENTS

As discussed above additive fuel at the concentrations being considered has been shown to have only a small effect on the fuel thermal mechanical response. This suggests evaluation of core events such as LOCA, various transient events associated with reload licensing, and core stability are essentially insensitive to the differences as calculated by PRIME and therefore do not necessarily require explicit treatment in those analyses. The claim of insensitivity can be made on the basis of the magnitudes of the changes due to the presence of the additives relative to the stated uncertainties of the analysis codes.

For example LOCA evaluations using PRIME plus TRACG analysis codes require [[

]]

[[

]]

Table 5-2 Uncertainty in Melt Margin Analysis

Similarly, LOCA, transient, and stability analyses use the input [[

]], respectively.

[[

]]

Table 5-3 Effect of Additive on High-Power Gap Conductance

[[

]]

Table 5-4 Effect of Additive on Low-Power Gap Conductance

[[

]]

[[

]]

Table 5-5 Effect of Additive on Fuel Centerline Temperature

This section has demonstrated that the magnitude of the differences due to the addition of a small amount of additive to UO2 fuel is insignificant to parameters affecting LOCA, Transient, and Stability analysis. For this reason, explicit analysis of those transients for additive fuel is not included in this report. Fuel designs containing additive will be licensed following the normal new fuel and reload licensing procedures.

5.7 IMPACT ON NUCLEAR DESIGN REQUIREMENTS

General Design Criterion (GDC) 11 stipulates that the reactor core and associated coolant systems shall be designed so that in the power operating range the net effect of the prompt inherent nuclear feedback characteristics tends to compensate for a rapid increase in reactivity. To confirm compliance with GDC 11, key nuclear dynamic parameters, or reactivity coefficients, are evaluated when new fuel designs are developed. For BWR fuel, the key reactivity coefficients are: 1) the moderator void coefficient, 2) the moderator temperature coefficient, 3) the Doppler coefficient and 4) the prompt power coefficient. The impact of introducing additive fuel on these key reactivity coefficients has been evaluated and confirmed to not impact the nuclear dynamic parameters.

The absorption cross section for aluminosilicate additive is very small in relation to the fuel. The primary effect of introducing additive is to displace a small amount of UO_2 which does tend to make reactivity coefficients less negative. Infinite lattice studies were performed to examine the impact on the change in reactivity associated with a change core state (e.g. moderator void) due to the reduced fuel density. The impact on reactivity change is small and does not affect a fuel assembly's inherent compliance with GDC 11 in light of the large margins.

General Design Criteria 26 stipulates that the reactivity control system shall be capable of maintaining the reactor subcritical under cold conditions with sufficient margin to account for equipment malfunctions such as stuck control rods. Adequate cold shutdown margin (CSDM) is assured through cycle specific 3D analyses. Here again, the primary effect of introducing additive fuel is to reduce the fuel density slightly which has a small effect on core reactivity and control rod worth in the cold condition; however, the reduced fuel density will be explicitly modeled in generating nuclear libraries as part of cycle specific reload analysis for fuel

containing aluminosilicate additive. As such, compliance with GDC 26 is assured on a cycle-specific basis.

5.8 LICENSING CRITERIA CONCLUSION

The assessments above confirm that the impact of additive fuel on licensing analysis for GNF fuel designs are negligible and do not impact the relevant behavior or characteristics. Furthermore, the same application methodologies used for licensing standard fuel as defined in GESTAR II are applicable to additive fuel, and no changes in the criteria are required, [[

]]

6.0 OPERATING EXPERIENCE

6.1 BACKGROUND

GNF additive fuel has been irradiated in power reactors in the United States and abroad since 1977. In that time, data relating to pellet properties and operating characteristics has been obtained. Figure 6-1 summarizes this experience.

	Reactor	Description	Exposure GWd/MTU
Test Reactors	GETR	66 rods	80 (max)
	R2		
	Halden		
	NSRR		
Power Reactors (SRB, LTA, LUA)	Millstone	54 rods	25
	Monticello		
	QC-1		
	Caorso	5 bundles	35
	Duane Arnold	5 bundles	40
	Forsmark-1	4 bundles	40
	Fukushima-1	2 bundles	50
	Gun-C	8 bundles	68
		(4 bundles)	(80)
Reload Fuel	BWRs-Japan	All $(U,Gd)O_2$ rods	---

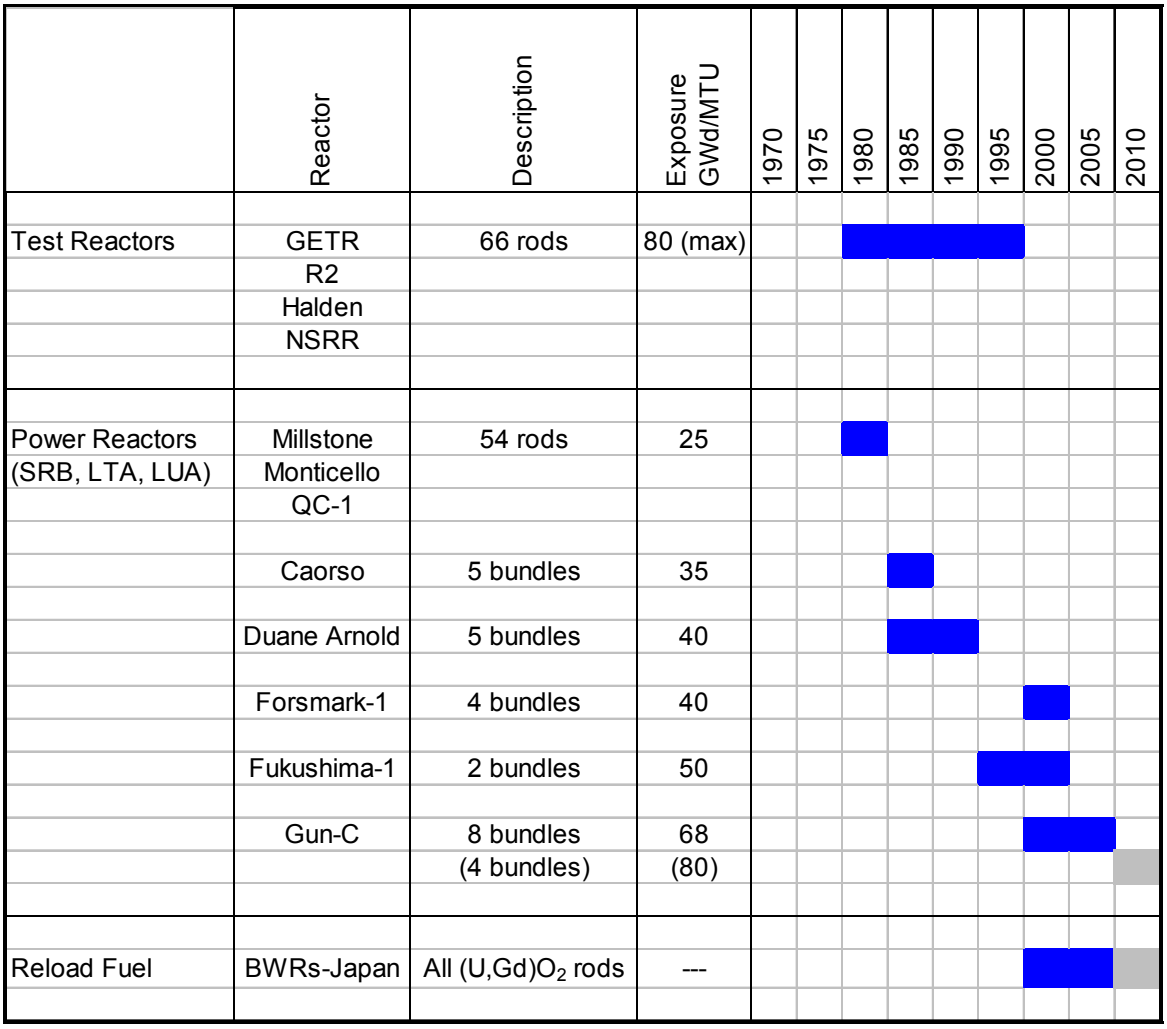

Figure 6-1 Additive Fuel Operating History Summary

Of the additive fuel rods that have operated in power reactors, the earliest of rods were part of the segmented rod bundle (SRB) program and consisted of specially designed segmented rods with up to [[ ]] These early rods attained up to approximately

[[ ]] exposure and were retrieved for hot cell examination and further testing (e.g. ramp testing). Later, restricted lead test assemblies (LTAs) were inserted into [[ ]] and achieved approximately [[ ]] exposure. The LTAs contained segmented rods and full-length rods. The segmented rods were retrieved for hot cell examination and further testing. Most recently, 10x10 designs, GE12 and GE14, containing from [[ ]] have operated as unrestricted lead use assemblies (LUAs) in the [[ ]] These LUAs contained segmented and full-length rods. The [[ ]] have achieved approximately [[ ]] exposure. Seven rods from those LUAs have been retrieved for hot cell examination and further testing in 2009. Some of the [[ ]] bundles have been re-inserted into the reactor to accumulate more exposure before examination. Fuel rod segments retrieved from the SRB bundles and [[ ]] have been ramp tested.

6.2 STEADY STATE IRRADIATION

The goal of the Lead Use and Lead Test (LUA/LTA) program was to provide irradiated fuel rods material for subsequent ramp testing to determine the minimum amount of additive that is still effective in guarding against PCI. The additive displaces uranium, so, there is economic incentive to limit the amount. More importantly, though, lower concentrations will reduce the impact on fuel fabrication and fuel properties making the transition to additive fuel more simple. As discussed above the LUAs contained segmented rods having concentrations ranging from [[ ]] fabricated from a [[ ]] The bundles operated as standard 10x10 bundles with the exception that power was kept low to preclude any pre-conditioning effects that could contribute enhanced performance in subsequent ramp testing. The exposure of the tested segments ranged from [[ ]]

In addition to the ramp testing described in section 6.3, examinations of the fuel and cladding structure were performed. These examinations confirm that [[

]]

Both the additive and non-additive pellets contained [[

]]

The most recent LUA application of additive fuel was as part of an ongoing ultra-high burn up program being conducted at [[ ]]. Eight fuel bundles were manufactured in 1999 containing additive UO2 fuel rods consisting of [[ ]] at concentrations of [[ ]] The fuel was fabricated at the GNF Wilmington fuel plant and exhibited characteristics similar to additive fuel produced in the past for properties characterization and performance testing. Specifically, the fuel density and grain size are consistent with past additive fuel and the composition and

concentration range encompass the proposed limit to be licensed in this LTR. Extensive pre-characterization of the additive fuel pellets was completed and documented. The bundles were inserted into the reactor at the beginning of cycle 14 and operated to end of cycle 19 achieving an exposure of [[ ]] At various times throughout the operation the bundles were inspected. The inspections consisted of visual examination of the bundles and individual fuel rods as well as measurements of length, rod-to-rod gap, cladding liftoff (corrosion). All measurements were indicative of normal stable behavior and the fuel bundles were recommended for continued operation.

Further hot cell examinations are planned for some of the material removed from the core after cycle 19. The examinations will include visual and ceramography of the additive pellets to confirm anticipated behavior to high exposures as well as fission gas release measurements. It is expected these examinations will be conducted in 2009. Four of the bundles have been returned to the core for at least one additional cycle of operation. At completion of that cycle the bundles will be evaluated for possible return for one last cycle of operation. The criterion for return is not related to the use of additive fuel, but will be determined primarily by the condition of the fuel rod cladding as well as other structural non-heat transfer surface components. Nonetheless, valuable confirmation of acceptable performance of additive fuel to the extremes of the licensed exposure was gained from this program. It is expected that additive fuel will not be the limitation to continued operation.

The high burn-up program demonstrates the capability of additive fuel to perform as expected to the limits of licensed exposures common to current day GNF fuel designs.

6.3 RAMP TESTING AND DEMONSTRATED PCI RESISTANCE

[[

]]

Figure 6-2 Additive Fuel Ramp Testing Results

The SRB rods were ramp tested in the Studsvik R2 test reactor. The peak power achieved during testing was limited to 18 kW/ft due to the capabilities of the reactor. [[

]] The rod segments tested contained additive concentrations of [[ ]] The [[ ]] rods were ramp tested in Halden test reactor. The peak power achieved during testing was approximately 16 kW/ft, again limited by the capability of the test reactor. A total of twelve rods were tested (all without an inner Zirconium liner or barrier). Eight rods contained additive [[ ]] and 4 rods with standard UO_2. The four standard rods failed during testing, but none of the eight 10x10 additive rods failed. Figure 6-2 shows the additive PCI ramp test data results from the SRP and [[

]] programs superimposed over the standard UO2 failure probability lines. [[

]]

Measurements of cladding diameter were made to determine the strain produced by the power ramps. [[

]]

[[

]]

The ramp test program of additive rods [[ ]] provided a valid assessment of PCI performance. The tests demonstrated the PCI resistance of additive fuel at [[

]] In other aspects, the behavior of additive and non-additive pellets were essentially equal.

Results of the ramp testing also demonstrated the outcome of operation of the additive fuel [[ ]] Following ramp testing, SEM investigation of transverse samples from three unfailed ramped additive rods were prepared and examined. [[

]]

In addition to the SEM examinations, the corresponding peak centerline and surface temperatures associated with each axial location were calculated using the PRIME model. The inputs required for the PRIME model were based on the power history of the fuel segments. All of the segmented fuel rods were base irradiated in the Forsmark-1 power reactor prior to insertion into the Halden Reactor for ramp testing. The power histories modeled in PRIME simulated the incubation period as well as the power ramp tests.

A summary of the segmented test rods can be seen below in Table 6.1.

	[[		
Position from rod bottom (mm)			
Additive Concentration (ppm)			
Peak Exposure (MWd/MTU)			
LHGR (kW/ft)			
Peak Surface Temperature (°C)			
Peak Centerline Temperature (°C)			
Time Above 1550 °C (hours)			]]

Table 6-1 Summary of Segmented Rods from Halden Ramp Testing

Furthermore, Figures (6-3) through (6-5) show the calculated temperature gradients as function of the pellet radius for each unfailed rod. [[

]]

[[

]]

Figure 6-3 Temperature Gradient of Rod Segment [[ ]]

[[

]]

Figure 6-4 Temperature Gradient of Rod Segment [[ ]]

[[

]]

Figure 6-5 Temperature Gradient of Rod Segment [[ ]]

[[

]]

7.0 CONCLUSION

GNF desires to introduce aluminosilicate additive fuel pellets to increase fuel reliability and operational flexibility of nuclear fuel bundles and cores. Additive fuel has been successfully tested over a wide range of concentrations and compositions. In order to eliminate any deleterious effects on fuel economics or fuel properties, the amount of additive and the composition range proposed will be limited to the ranges indicated below.

	Additive Fuel Range of Applicability		
	Concentration wt%	Composition SiO_2 : Al_2O_3 by wt	Fuel Design
Target Range	[[ ]]	[[ ]]	GE14, GNF2, new

As described in this report additive in the stated concentration range has a negligible effect on licensing limits as demonstrated by PRIME. Fuel designs incorporating additive can be licensed to the same or improved limits as designs with standard fuel with greater margin to failure mechanisms associated with pellet clad interaction. This additional margin will lead to more robust fuel that is more resistant to systemic in-core fuel failures.

In the proposed range, significant effects from the addition of aluminosilicate additive to the fuel pellet are limited to fuel melting and fuel creep rate. Theoretical density is deemed to have been affected only slightly. The remaining fuel properties or behaviors such as fuel thermal conductivity, fission gas release, fuel wash out are insignificantly affected by additive. [[

]]

GNF has operated additive fuel in irradiation programs ranging from single rod segments to full bundle LUAs. The in-core experience has been valuable to provide fuel rods for property development as well as understanding in-core behavior. Average bundle exposures of up to [[

]] have been obtained. Fuel inspections at various points in exposure have indicated satisfactory operation. The LUA programs demonstrate the capability of additive fuel to perform as expected to the limits of licensed exposures common to current GNF fuel designs.

8.0 REFERENCES

1. The PRIME Model for Analysis of Fuel Rod Thermal – Mechanical Performance Part 1 – Technical Bases, Global Nuclear Fuel, Wilmington, NC: 2007 NEDC-33256P
2. The PRIME Model for Analysis of Fuel Rod Thermal – Mechanical Performance Part 2 – Qualification, Global Nuclear Fuel, Wilmington, NC: 2007 NEDC-33257P
3. The PRIME Model for Analysis of Fuel Rod Thermal – Mechanical Performance Part 3 – Application Methodology, Global Nuclear Fuel, Wilmington, NC: 2007 NEDC-33258P
4. Densification Testing, Global Nuclear Fuel, Wilmington, NC:2007 NEDE-33214P-A
5. Spent Fuel Project Office, Interim Staff Guidance – 11, Revision 3, Cladding Considerations for the Transportation and Storage of Spent Fuel
6. Letter from Brian R. Moore (GNF) to NRC Document Control Desk, Subject: GNF Responses to NRC RAIs for NEDC-33406P, Revision 2, Additive Fuel Pellets for GNF Fuel Designs, MFN 13-101, December 16, 2013
7. Letter from Mirela Gavrilas (NRC) to Jerald G. Head (GEH), Subject: Final Safety Evaluation for General Electric Hitachi Nuclear Energy Americas, LLC Topical Report NEDC-33406P, Revision 2, “Additive Fuel Pellets for GNF Fuel Designs” (TAC No. ME3082), MFN 15-095, November 9, 2015

APPENDIX A GNF RESPONSES TO NRC RAIS ON NEDE-33406P REVISION 2

NRC RAI 1

Section 1.0 – Introduction

Table 1-1 indicates that the target range of concentration in percent by weight (wt%) [[ ]] and composition of SiO_2:Al_2O_3 by weight (wt) [[ ]] are [[ ]] for the American Society for Testing and Materials (ASTM) C776-00 impurity limits [[ ]]. Please explain the discrepancy between this and your statement that the impurity level "[[ ]]"

GNF Response

The purpose of the statement quoted from NEDC-33406P, Revision 2 (Reference 1.1), which compares the targeted additive concentration to the ASTM specification for impurities, is to provide some perspective regarding the amount of additive being added to Global Nuclear Fuel (GNF) fuel. This comparison demonstrates the magnitude of the proposed additive concentration relative to impurity levels that the ASTM consider inconsequential. The statement was not intended to imply that GNF's additive fuel would be compliant to the ASTM specifications over the entire range of concentration and composition.

The composition of Al and Si, in elemental µg /gU, for the maximum additive concentration and composition range specified in Reference 1.1 is shown in Table RAI 1-1. Table 1 of ASTM C776-00 (and -06), specifies impurity levels of <250 µg Al/gU and <500 µg Si/gU, respectively for Al and Si in UO_2 fuel. At greater than [[ ]] ppm UO_2 or at compositions differing from [[ ]], the ASTM impurity limit for Al and/or Si may be exceeded up to the values shown. GNF has demonstrated additive fuel performance covering the entire range specified within Reference 1.1.

Table RAI 1-1 Elemental Composition (µg/gU) for Additive Concentrations and Composition Ranges

Additive Concentration (µg SiO_2+Al_2O_3 /gUO_2)	Composition Range (wt% SiO_2:Al_2O_3)	SiO_2 (µg /gUO_2)	Al_2O_3 (µg /gUO_2)	Si (µg /gU) (ASTM Limit: 500)	Al (µg /gU) (ASTM Limit: 250)
[[					
					]]

Reference:

1.1 Global Nuclear Fuel, "Additive Fuel Pellets for GNF Fuel Designs," NEDC-33406P, Revision 2, December 2009.

NRC RAI 2

Section 2.0 - Material Properties

The opening paragraph of this section states that "some calculations in the PRIME methodology require gadolinia content as an input. [[

]]

Please clarify whether [[

]]

GNF Response

[[

]]

Reference:

2.1 Global Nuclear Fuel, "Additive Fuel Pellets for GNF Fuel Designs," NEDC-33406P, Revision 2, December 2009.

NRC RAI 3

Section 2.2.1 - Melting Temperature Overview

The LTR states, "[[ ]]" Please provide the test methods, test results, and corresponding database to support GNF's claim that [[ ]] Please explain the meaning of [[ ]]

GNF Response

For UO_2 fuel, 100% fission gas release is anticipated in the molten region and high release is anticipated in the restructured zone due to grain boundary sweeping and enhanced interlinkage and release from grain boundaries. [[

]]

To ensure that sudden shifting of molten fuel in the interior of fuel rods, and subsequent potential cladding damage, can be positively precluded, current fuel design specified acceptable fuel design limits (SAFDLs) require no fuel melting during normal operation, including anticipated operational occurrences (AOOs). However, to fully address concerns about melting, Global Nuclear Fuel (GNF) has irradiated test fuel to very high powers in the R2 and GETR test reactors. The test rods in R2 were irradiated to high exposure and high power. Significant melting occurred for this fuel. Direct temperature measurements are not available from these tests. However, fuel melting results in a molten region at the center of the fuel surrounded by a region in which grain restructuring occurs. These changes can be used to infer temperature. Melt radius, grain growth data and fission gas release data is available for the tests rods. The test database is summarized in Table RAI 3-1. The test rods in GETR were irradiated to low exposure and very high power. The objective of the GETR tests was to demonstrate that fuel rod failure due to contact of molten fuel with the cladding does not occur even for rods with melt radii exceeding [[ ]] of the pellet radius. Fission gas release data is available for these rods. The test database is summarized in Table RAI 3-2.

For UO_2 fuel, 100% fission gas release is anticipated in the molten region and high release is anticipated in the restructured zone due to grain boundary sweeping and enhanced interlinkage and release from grain boundaries. [[ ]] Figures RAI 3-1 and RAI 3-2 show PRIME predictions of fission gas release for the test rods noted above. These results show that the fission gas release due to fuel melting is well understood and well predicted. [[

]]

GNF does not have fission gas release for additive fuel subjected to powers that would produce melting to the extent noted above. However, on the basis of the discussion below, the conclusion

for UO_2 rods that [[ ]] does not occur, even if significant melting occurs, is considered applicable to additive fuel.

As discussed in NEDC-33406P, Revision 2 (Reference 3.1), the UO_2-additive phase diagram shows a relatively low temperature eutectic occurring at about [[ ]]. Above this temperature additive fuel will be in the solid plus liquid region of the phase diagram and thus some portion of liquid phase will be present. The fraction of liquid phase increases between the eutectic temperature and reaches 100% at the melting (liquidus) temperature. Some fraction of this liquid phase will be UO_2. Thus even below the melting temperature of UO_2, additive fuel will be subjected to 100% fission gas release from some fraction of the UO_2. As noted above, the intent of the no fuel melting criterion is to assure geometric stability of the pellet and preclude migration of liquid UO_2 to the fuel cladding. Testing has demonstrated acceptable geometric stability for additive fuel with up to [[ ]]. As discussed in Reference 3.1 and the responses to RAI 24, 24-S01, and 24-S02, the concept of [[

]]

Now consider the difference in fission gas release between UO_2 and additive fuel pellets subjected to high power and thus high temperature. For portions of the pellets below the additive eutectic temperature, fission gas release will be very similar. For portions of the pellets between the additive eutectic temperature and the additive slump temperature, the additive pellet will release slightly more fission gas because a small fraction of the UO_2 phase will be molten. For portions of the pellets between the slump temperature and the UO_2 melting temperature, the additive pellet will release more fission gas because the fraction of molten UO_2 increases. However, the size of this fraction of the pellets will be determined by the difference between the additive slump temperature and the UO_2 melting temperature, which is small, so this fraction will be a very small fraction of the total pellet volume. Above the UO_2 melting temperature the fission gas releases will be similar. The conclusions above will be impacted by the following considerations. In general, release for the additive pellet will be reduced relative to the UO_2 pellet due to (1) less U and thus reduced generation of fission products, including fission gases, (2) [[ ]], and (3) [[ ]] .

In summary, it is concluded that the fission gas release for GNF additive pellets with additive concentration less than the planned upper bound concentration that are subjected to high power and experience significant melting will be very similar to that for UO_2 rods. Thus [[ ]] will not occur.

Reference:

3.1 Global Nuclear Fuel, "Additive Fuel Pellets for GNF Fuel Designs," NEDC-33406P, Revision 2, December 2009.

Table RAI 3-1 Test Rods Irradiated in R2

ROD ID	Exposure (MWd/MTU)	Peak Power (kW/ft)
[[		
		]]

Table RAI 3-2 Test Rods Irradiated in GETR

ROD_ID	Exposure (MWd/MTU)	Peak Power (kW/ft)
[[		
		]]

[[

]]

Figure RAI 3-1: PRIME Predicted versus Measured Fission Gas Release (FGR) for Rods with Significant Melting

[[

]]

Figure RAI 3-2: PRIME Predicted/Measured FGR versus Exposure for Rods with Significant Melting

NRC RAI 4

Sections 2.2.1 and 2.2.3

(a) Please explain in detail the "[[ ]]" that is referred to in these sections.

(b) Please provide the database that is the basis for Figure 2-9.

(c) Figure 2-9 is plotted for zero exposure and no gadolinia content. Please explain in detail, the impact of exposure and gadolinia content on the behavior of UO_2 fuel with additives (aluminosilicate compounds).

(d) Please provide details of the experiment that determined "[[ ]]" and its associated database.

GNF Response

(a) The intent of the no fuel melting criterion for UO_2 is to assure geometric stability of the pellet and preclude migration of liquid UO_2. The concept of slump temperature is introduced for additive fuel to assure geometric stability of additive fuel at high temperature. The UO_2-additive phase diagram reveals a relatively low temperature eutectic occurring around [[ ]]. Above this temperature fuel will be in the solid plus liquid region of the phase diagram and thus some portion of liquid phase will be present. The portion of liquid phase increases with temperature and reaches 100% at the melting temperature of UO_2. Testing has demonstrated acceptable geometric stability with up to [[ ]] The slump temperature is defined as the temperature below which the portion of [[

]], is contained in NEDC-33406P, Revision 2 (Reference 4.1), and the responses to RAI 24, 24-S01, and 24-S02.

(b) Figure 2-9 of Reference 4.1 is generated from the data shown in Figure 2-11 of Reference 4.1. As discussed in Section 2.2.2, in the PRIME code the phase diagram for the system containing UO_2 and aluminosilicate additive is used in conjunction with the fuel slump temperature to determine when fuel melting occurs. The phase diagram, which represents the liquidus curve, is based upon thermal arrest measurements. The correlation of the phase diagram with the thermal arrest data is presented in Section 2.2.3 of Reference 4.1.

(c) The effect of exposure on UO_2 is to lower the melting temperature. The reduction is proportional to exposure. In the PRIME code, this reduction is incorporated into the determination of fuel melting by reducing the phase diagram by the same amount.

The effect of gadolinia on UO_2 is to lower the melting temperature by an amount proportional to the gadolinia concentration. This reduction could be addressed similarly to

that of exposure. [[

]]

(d) The testing performed to assess the volume % where slumping occurs is a relatively simple test. The description of this test and the subsequent results have been described in Section 2.2.3 of Reference 4.1, where additive pellets were heated isotropically in an oven to a temperature determined by the phase diagram to produce a significant liquid phase, then visually examined for geometric changes. The data from this test has been fully disclosed in Table 2-1 of Reference 4.1. Although simple in nature, the test results clearly demonstrate the additive fuel retains some resistance to slumping at temperatures in excess of the eutectic temperature.

Reference:

4.1 Global Nuclear Fuel, "Additive Fuel Pellets for GNF Fuel Designs," NEDC-33406P, Revision 2, December 2009.

NRC RAI 5

Section 2.4 - Thermal Expansion

Figure 2-13 illustrates the strain as a function of temperature for non-additive fuel and additive fuel with an additive concentration of [[ ]].

(a) Please discuss the behavior of the additive fuel at other concentrations of additive above and below the [[ ]].

(b) What is the effect of adding gadolinia to the additive fuel with regard to thermal expansion?

GNF Response

(a) As discussed in Section 2.4 of NEDC-33406P, Revision 2 (Reference 5.1), thermal expansion of UO_2-additive fuel is essentially unchanged from standard UO_2 for additive concentrations in the planned range. Above the eutectic temperature, the thermal expansion of additive fuel is slightly different than that of standard UO_2. [[

]]

In PRIME, for non-additive fuel, if the local temperature is above the fuel melting temperature, the local (fuel ring) thermal strain will be calculated as the sum of the thermal strain plus an additional strain resulting from the phase change volumetric increase due transition from the solid to liquid phase. For additive fuel, when the local temperature exceeds the eutectic temperature, the fuel ring thermal strain is calculated as the sum of the thermal strain plus an additional thermal strain resulting from the phase change volumetric increase. This phase change volumetric increase is treated similarly to the phase change volumetric increase due to melting in non-additive fuel.

Figure RAI 5-1 shows thermal expansion as a function of local temperature for standard UO_2 fuel and UO_2 additive fuel with concentrations of [[ ]] and [[ ]], which bound the planned nominal concentration of [[ ]], and the planned upper bound concentration of [[ ]]. The effect of additive in the planned concentration range is negligible except in the range between [[ ]] and bulk melting.

(b) [[

]]

Reference:

5.1 Global Nuclear Fuel, "Additive Fuel Pellets for GNF Fuel Designs," NEDC-33406P, Revision 2, December 2009.

[[

]]

Figure RAI 5-1: Thermal Expansion of Additive and Non-Additive Fuel

NRC RAI 6

Section 2.5 - Thermal Conductivity

(a) Figure 2-14 of Section 2.5 illustrates the behavior of thermal conductivity of unirradiated non-additive and additive fuel as a function of temperature from PRIME and experiments. Please provide the results for irradiated non-additive and additive fuel for various concentrations of additive (aluminosilicate).

(b) If [[ ]], what is the impact on thermal conductivity of unirradiated and irradiated fuel?

GNF Response

(a) The impact of exposure is to lower the thermal conductivity of UO_2 and additive fuel relative to unirradiated fuel. The impact increases nonlinearly with exposure. Fuel pellet thermal conductivity as a function of temperature for various additive concentrations at 0, 15 and 60 GWd/MTU is shown in Figure RAI 6-1. The results for 0 GWd/MTU are taken from Figure 2-14.

(b) [[

]]

Reference:

6.1 Global Nuclear Fuel, "Additive Fuel Pellets for GNF Fuel Designs," NEDC-33406P, Revision 2, December 2009.

[[

]]

Figure RAI 6-1: Thermal Conductivity as a Function of Temperature, Additive Concentration, and Exposure

NRC RAI 7

Section 2.6 - Grain Size and Growth

Section 2.6.1 of NEDC-33406P describes the grain growth model for gadolinia ((U, Gd)O_2) . Please provide data comparisons for this model that predicts grain growth for UO_2 and UO_2 – Gd_2O_3. If this model is applied explicitly to additive UO_2 fuel with Al_2O_3-SiO_2, provide the results to show how well the grain growth model will predict the grain growth.

GNF Response

As discussed in the subject section of NEDC-33406P, Revision 2 (Reference 7.1), in the PRIME code, separate grain growth models are applied for UO_2 and (U,Gd)O_2 fuel. Data comparisons for the PRIME grain growth model are shown in Figures RAI 7-1 and RAI 7-2 for UO_2, (U,Gd)O_2 and aluminosilicate additive fuel. Figures RAI 7-1 and RAI 7-2 also contain grain growth data for Global Nuclear Fuel (GNF) UO_2 fuel rods included in the RISO III ramp tests. This data was included in the final response to PRIME RAI 5 (Reference 7.2). [[

]]

Reference:

7.1 Global Nuclear Fuel, "Additive Fuel Pellets for GNF Fuel Designs," NEDC-33406P, Revision 2, December 2009.

7.2 A. Lingenfelter (GNF) to Document Control Desk (NRC), "Request for Additional Information Response for the PRIME Model for Analysis of Fuel Rod Thermal-Mechanical Performance (TAC# MD4114)," MFN 09-106, dated February 27, 2009.

[[

]]

Figure RAI 7-1: Predicted versus Measured Grain Growth

[[

]]

Figure RAI 7-2: Calculated/Measured Grain Growth versus Nodal Exposure

NRC RAI 8

Section 2.7 - Stored Energy

Please provide detailed results from the model that calculates the fuel stored energy in the presence of aluminosilicate additive for various additive concentrations. How are the results from this model [[ ]] in addition to aluminosilicate?

GNF Response

As noted in the subject section of NEDC-33406P, Revision 2 (Reference 8.1), in the PRIME code, the fuel stored energy is obtained by integrating the specific heat from 298°K to the local fuel temperature and then integrating over the pellet volume. For additive fuel, the specific heat is obtained by using [[ ]] to combine the specific heats for fuel and additive components. The fuel stored energy for UO_2-additve fuel as a function of additive concentration and (local) temperature is shown in Figure RAI 8-1. The effect of additive on fuel density is incorporated when the local stored energy is integrated over the pellet volume.

[[

]]

Reference:

8.1 Global Nuclear Fuel, "Additive Fuel Pellets for GNF Fuel Designs," NEDC-33406P, Revision 2, December 2009.

[[

]]

Figure RAI 8-1: Fuel Stored Energy as a Function of Fuel Temperature and Additive Concentration

NRC RAI 9

Sections 2.8 through 2.14

(a) Some sections state that uniaxial compression and other tests have been performed to determine creep and other characteristics of [[ ]]. Also this section states that [[

]]. Has GEH tested UO_2 fuel with [[ ]]? If not, what are the plans to test the fuel with both additives?

(b) *Please provide results from tests and the related database that will confirm the implications of the expected behavior of the Al-Si-O additive in UO_2 fuel on the High Burnup Structure stated in points 1 through 5 in Section 2.14 of NEDC-33406P, Revision 2.*

GNF Response

(a) [[

]]

(b) The effect of the aluminosilicate additive on the high burnup structure (HBS) was evaluated relative to standard and large grain UO_2 fuel in test rods that operated to average exposures of 86 GWd/MTU in the Halden reactor. Details of the test and the results are provided in Reference 9.2 below. The fuel was sintered to densities in the range of 96.8 – 97.8% Theoretical Density (TD), with 3-dimensional grain sizes of the standard, large grain non-additive and additive pellets of 9-12, 51–63 and 37–58 μm, respectively. Linear heat generation rates for the tests ranged from 47 kW/m at the beginning of life to 17 kW/m at the end of life. After irradiation, the fuel was examined to characterize the resulting pellet structure.

Visual examination of the large grain non-additive and standard grain non-additive pellets in comparison with the large grained additive pellets demonstrated that the effect of the aluminosilicate on HBS formation and the thermal-mechanical performance of the fuel correlated [[ ]]. Additional discussion of these issues is provided in the response to RAI 17c.

References:

9.1 Global Nuclear Fuel, "Additive Fuel Pellets for GNF Fuel Designs," NEDC-33406P, Revision 2, December 2009.

9.2 Une, K., Hirai, M., Nogita, K., Hosokawa, T., Suzawa, Y., Shimizu, S., Etoh, Y., "Rim structure formation and high burnup fuel behavior of large-grained UO_2 fuels," Journal of Nuclear Materials, Volume 278, pp. 54 – 63, February 2000.

NRC RAI 10

Section 3.3 - Reactivity Insertion Accident Characteristics

(a) This section indicates that the additive compositions tested include [[ ]]. Please provide information to show that these additives are similar to the aluminosilicate that is the subject of LTR NEDC-33406P, Revision 2.

(b) Please provide complete details of the tests discussed in this section, including the procedures, type of additive fuels tested, and the results obtained from the tests. Show that the test results clearly simulate the behavior of aluminosilicate as an additive.

GNF Response

(a) The testing performed and documented in Figure 3-6 of NEDC-33406P, Revision 2 (Reference 10.1), included [[ ]] – Additive Type A) and [[ ]] – Additive Type B) as the aluminosilicate additives. Table RAI 10-1 provides representative compositions observed for the [[ ]] and [[ ]] additives used in the tests. The compositions tested were, nominally [[ ]] SiO_2:Al_2O_3 and [[ ]] SiO_2:Al_2O_3 for [[ ]] and [[ ]] respectively. Test results indicate the sensitivity to the differences in SiO_2:Al_2O_3 composition is not significant. Global Nuclear Fuel's targeted composition range [[ ]] SiO_2:Al_2O_3 is based on this observation.

(b) Testing in the Nuclear Safety Research Reactor (NSRR) in Japan was performed on additive fuel rods to address reactivity insertion accident (RIA) concerns for additive fuel. See Reference 10.2 for a description of the applicability of the NSRR testing and methods of testing. Two types of fuel assemblies were used. The first assembly contained three rods located triangularly at 120° intervals at a pitch radius of 18 mm. This assembly was used to determine failure thresholds. The second assembly contained a single rod and was used primarily to investigate fuel fragmentation and mechanical energy generation. This assembly included pressure sensors to measure the pressure pulse within the assembly generated by fuel fragmentation. All rods were instrumented with outer surface thermocouples and a water level sensor in the test rig to measure the water slug ejected upwards by a steam explosion.

The NSRR pulse half width can be varied from ~4.4 ms to ~20 ms depending on the inserted reactivity. The effects of variations in pulse width are negligible since the pulse width is much smaller than the thermal time constant of the fuel. The deposited energy in the test rods was estimated based on the integral value of the reactor power. All tests were performed at ~20°C and 1 atm pressure inside the (sealed) fuel assemblies.

Thirty samples (24 triplets and six singles) of five different fuel types, as shown in Table RAI 10-2, were built using [[

]]

and tested at energy depositions between [[ ]].

The failure thresholds from these tests are shown in Figure 3-6 of Reference 10.1 in comparison to standard UO_2 [[ ]] fuel designs where failures have been observed at energy depositions of [[ ]] cal/gUO_2 and above. No failures were observed below [[ ]] cal/gUO_2 for any fuel type tested. Mechanical energy generation and release thresholds, determined by measuring the velocity of the water slug after the steam explosion and by results from the pressure sensors, indicate no appreciable differences between the additive fuel and standard UO_2 fuel. Similarly, cladding diametral changes and fuel grain growth, measured after pulsing, indicate no appreciable differences between the additive fuel and standard UO_2 fuel. These results confirm that the failure threshold for aluminosilicate additive fuel is not substantially different than that observed for standard UO_2 fuel, even for concentrations above the targeted upper bound value of [[ ]] ppm.

References:

10.1 Global Nuclear Fuel, "Additive Fuel Pellets for GNF Fuel Designs," NEDC-33406P, Revision 2, December 2009.

10.2 Saito, S., Inabe, T., Fujishiro, T., Ohnishi, N., Hoshi, T., "Measurement and Evaluation on Pulsing Characteristics and Experimental Capability of NSRR," Journal of Nuclear Science and Technology, Volume 14, Issue 3, pp. 226-238, 1977.

Table RAI 10-1 Composition of [[ ]] and [[ ]]

[[

]]

Table RAI 10-2 Additive Types and Concentrations Used in RIA Tests

Sample	Additive Type & Concentration
HA	[[
LA	
HB	
LB	]]
Non-Additive	Standard UO_2 Fuel

NRC RAI 11

Please provide the results from PRIME analysis of theoretical density of UO_2, and $(U,Gd)O_2$ fuel with and without aluminosilicate additive at different concentrations.

GNF Response

In the PRIME code, the theoretical density of UO_2 and $(U, Gd)O_2$ fuel is given by a relationship dependent upon gadolinia concentration. The theoretical density of additive fuel is obtained by combining this relationship with the theoretical density of the additive component using [[
]].

The theoretical density of UO_2-additive fuel as a function of additive concentration is shown in Figure RAI 11-1. [[

]]

Reference:

11.1 Global Nuclear Fuel, "Additive Fuel Pellets for GNF Fuel Designs," NEDC-33406P, Revision 2, December 2009.

[[

]]

Figure RAI 11-1: Fuel Theoretical Density as a Function of Aluminosilicate Concentration

NRC RAI 12

Section 3.4 - In-Reactor Densification

GEH states that the methodology for densification testing and qualification of additive fuel will follow the approved methodology for standard UO_2 fuel as described in LTR NEDE-33214P-A, "Densification Testing," dated February 2007. NRC approval of NEDE-33214 is subject to a condition that "GNF continue the established monitoring program to assure that the pellet density criteria are met using a qualified measurement technique on 100 percent of pellet lots." Please describe how this condition is met for the additive fuel and provide the details of the test measurements and the results from these measurements.

GNF Response

As discussed in Section 3.4 of NEDC-33406P, Revision 2 (Reference 12.1), until the approval of NEDE-33214P (Reference 12.2) by the NRC, GEH performed routine densification testing on UO_2 fuel pellets. Based upon the evolution of Global Nuclear Fuel (GNF) fuel pellet design and fabrication, current GNF pellets are very stable with low densification. In Reference 12.2 it is shown for current fuel [[

]].

[[

]], as shown in the response to RAI 11. Additionally, prior manufacturing experience indicates that there is little [[

]] A limited amount of in-reactor testing supports this conclusion. Thus GNF concludes the methodology, testing and qualification techniques and requirements described in Reference 12.2 for UO_2 fuel are applicable to, and will be applied to, UO_2-additive fuel.

Specifically, when batch production of UO_2-additve begins, densification will be characterized by [[ ]] (or other approved test methodology) followed by 100 percent density monitoring using the same density measurement and sampling frequency as applied to UO_2.

References:

12.1 Global Nuclear Fuel, "Additive Fuel Pellets for GNF Fuel Designs," NEDC-33406P, Revision 2, December 2009.

12.2 Global Nuclear Fuel, "Densification Testing," NEDE-33214P-A, February 2007.

NRC RAI 13

Section 5.1 - Licensing Criteria Assessment – Fuel Melting

(a) Please provide the details of the analysis procedure to determine the additive fuel pellet centerline temperature for the bounding licensed duty fuel rod using PRIME.

(b) *Explain how the fuel system damage criteria and fuel failure criteria per Standard Review Plan 4.2 (NUREG-0800, Section 4.2) are satisfied for the additive fuel.*

GNF Response

(a) For each Global Nuclear Fuel (GNF) fuel design, including the GNF2 fuel design addressed in Section 5 of NEDC-33406P, Revision 2 (Reference 13.1), thermal-mechanical operating limits are specified for each fuel rod type (UO_2 and $(U,Gd)O_2$) such that if each rod type is operated within its allowable limits all thermal-mechanical design and licensing criteria, including those which address response to anticipated operational transients, are explicitly satisfied and fuel rod integrity will be maintained. The thermal-mechanical operating limits are specified as an [[

]] During specification of the bounding GNF2 thermal-mechanical envelope, a minimum [[ ]] overpower to incipient center melting is required to be met with 95% confidence. [[

]]

The analyses summarized above were repeated for the UO_2 rod assuming the addition of additive. To reflect the statistical nature of the analysis, [[

]]

(b) Each GNF fuel design is licensed by submitting a compliance report to Amendment 22 of GESTAR II (Reference 13.2) to the Nuclear Regulatory Commission (NRC). The compliance report presents generic information on the fuel design and analyses. The fuel licensing acceptance criteria specified in GESTAR II establish the basis for evaluating new fuel designs, developing the critical power correlation for these designs, and determining the applicability of generic analyses to these designs. The criteria assure compliance with Standard Review Plan 4.2 in NUREG-0800. Compliance with the licensing acceptance criteria constitutes NRC acceptance of the design without specific NRC review.

For the GNF2 fuel design, a report confirming compliance with all GESTAR II fuel licensing acceptance criteria has been submitted to the NRC (NEDC-33270P, Reference 13.3). The intent of the Reference 13.1 is to generically license the use of additive fuel in GNF fuel designs. The approach is (1) to identify the impact of additive on limiting fuel performance characteristics, relative to standard fuel, by analyzing the limiting fuel design characteristics with the proposed range of additive and comparing the results to standard fuel with methodologies defined in GESTAR II, and (2) to show for each characteristic that additive fuel behavior and response is equivalent to or better than current UO_2 fuel. This assessment forms the basis for demonstrating that GESTAR II is applicable to additive fuel.

GESTAR II (and Standard Review Plan 4.2) both require no fuel melting as one of the fuel design criteria. The intent of the no fuel melting criterion is to assure geometric stability of the pellet and preclude migration of liquid UO_2 to the fuel cladding. As noted in the response to RAI 4, for UO_2-additive fuel, there is a liquid phase present above about [[ ]], so the requirement of no fuel melting cannot be explicitly met without overly restricting rod power. For licensing of additive fuel, GNF has introduced the concept of [[

]], and serves the same purpose, as the melting temperature for standard UO_2. Thus the intent of the GESTAR II (and Standard Review Plan 4.2) requirement of no fuel melting is satisfied.

References:

13.1 Global Nuclear Fuel, “Additive Fuel Pellets for GNF Fuel Designs,” NEDC-33406P, Revision 2, December 2009.

13.2 Global Nuclear Fuel, “General Electric Standard Application for Reactor Fuel,” NEDE-24011-P-A, Revision 20, December 2013.

13.3 Global Nuclear Fuel, "GNF2 Advantage Generic Compliance with NEDE-24011-P-A (GESTAR II)," NEDC-33270P, Revision 5, May 2013.

NRC RAI 14

Section 5.3 - Cladding Plastic Strain

Please provide details of the analysis and results that show that the cladding circumferential strain does not exceed the [[ ]] for the additive fuel.

GNF Response

As discussed in the response to RAI 13, for each Global Nuclear Fuel (GNF) fuel design, including the GNF2 fuel design addressed in Section 5 of NEDC-33406P, Revision 2 (Reference 14.1), thermal-mechanical operating limits are specified for each fuel rod type (UO_2 and $(U,Gd)O_2$) such that if each rod type is operated within its allowable limits all thermal-mechanical design and licensing criteria, including those which address response to anticipated operational transients, are explicitly satisfied and fuel rod integrity will be maintained. The thermal-mechanical operating limits are specified as an [[

]] The [[ ]] limit is applied [[

]]. The [[ ]] limit represents the cladding failure strain. For the GNF2 UO_2 rod, the minimum overpowers to [[ ]] is [[ ]]. By requiring this power margin to [[ ]], the cladding is protected from failure if an AOO was to occur, since the calculated strain would be less than the failure strain for such an event. [[

]]

For the GNF2 UO_2 rod, the MOP limits are determined using standard PRIME application methodology. In summary, one node mechanical analyses are performed for the UO_2 rod to determine cladding strain. [[

]] Calculated values of cladding strain during an AOO are shown as a function of exposure in Figure 5-3 of Reference 14.1.

The analyses summarized above were repeated for the UO_2 rod assuming the addition of additive. To demonstrate the additive concentration sensitivities, a nominal concentration of [[ ]] and an upper bound concentration of [[ ]] are applied in these analyses. The results in Figure 5-3 indicate that the addition of additive significantly reduces cladding strain during an AOO, [[

]]

These results indicate that cladding plastic strains due to AOOs for UO_2-additive fuel with additive concentration between the planned nominal concentration and upper bound concentration as used in these analyses are significantly lower than the non-additive fuel. [[

]]

The discussion in Reference 14.1 is based upon the approved cladding strain limit at the time of submission of the LTR. Although a new cladding strain limit has been approved, for clarity, the discussion above is based upon the criterion addressed in Reference 14.1. The introduction of the new strain limit has been shown to have no impact on the stated MOP limits. Based upon the results above, this conclusion will also apply to UO_2-additive fuel.

Reference:

14.1 Global Nuclear Fuel, "Additive Fuel Pellets for GNF Fuel Designs," NEDC-33406P, Revision 2, December 2009.

NRC RAI 15

Section 5.7- Impact of Nuclear Design Requirements

Please provide details of the analysis and results that show compliance with Title 10 of the Code of Federal Regulations Part 50, Appendix A, General Design Criteria (GDC) 11. GDC 11 stipulates that the reactor core and associated coolant systems shall be designed so that in the power operating range the net effect of the prompt inherent nuclear feedback characteristics tends to compensate for a rapid increase in reactivity. Discuss the impact of additive fuel on the key reactivity coefficients and confirm that there is no adverse impact on reactor operation.

GNF Response

General Design Criterion (GDC) 11 stipulates that the reactor core and associated coolant systems shall be designed so that in the power operating range the net effect of the prompt inherent nuclear feedback characteristics tends to compensate for a rapid increase in reactivity. To confirm compliance of UO_2-additive fuel at the planned concentration levels with GDC 11, it is first noted that the impacts of additive at the planned upper bound concentration on fuel temperature and cladding strain for (steady state) operation [[

]] These changes have been assessed in detail. The analyses and results are summarized below.

Global Nuclear Fuel (GNF) UO_2-additive will contain aluminosilicate additive. The additive density is approximately [[ ]] of that of UO_2. Thus the physical impact of additive addition is the displacement of uranium by the less dense additive, resulting in reduced fuel density. The reduction in density will tend to make the reactivity coefficients discussed below less negative. The planned upper bound additive concentration is [[ ]] weight percent. Even at the upper bound concentration the reduction in density will be small, as discussed in the response to RAI 11. Thus the impact on reactivity coefficients will also be small.

The absorption cross sections of the additive components (aluminum, silicon and oxygen) are at least two orders of magnitude less than those of uranium. This suggests that the impact of additive on neutron transport will be small and that the primary effect of additive on neutron transport will be the displacement of uranium by the less dense additive noted above. On this basis, [[

]].

As discussed in Section 5.7 of NEDC-33406P, Revision 2 (Reference 15.1), key nuclear dynamic response parameters (reactivity coefficients) impacted by additive addition are (1) moderator void coefficient, (2) moderator temperature coefficient, (3) Doppler coefficient, (4) power coefficient, and (5) prompt reactivity feedback. Because of the anticipated small impact of the additive on these parameters, it was assumed that the impact of additive could be adequately characterized by comparison of results for Kinf from GNF's infinite lattice code [[ ]].

On the basis of the above, infinite lattice calculations with and without additive were performed using GNF's infinite lattice code (TGBLA) to determine the impact on the reactivity coefficients noted above. In these calculations, the effect of additive was treated by [[ ]]. The analyses were performed for a GNF2 bundle for two lattices. Results are summarized below. Because the impacts are small and qualitatively similar for both lattices, only results for one lattice (denoted BASE) are included in this response.

Moderator Void Coefficient

The effect of additive on moderator void reactivity coefficient was characterized using the cold, uncontrolled, 100°C moderator temperature (infinite lattice) case at two in-channel void fractions. The moderator void coefficient (MVC) was calculated using the equation

$$MVC=1E5\ \Delta(Kinf)/(Kinf1\ \Delta V)$$

where

Kinf1=infinite lattice reactivity coefficient for [[ ]] void fraction

Kinf2=infinite lattice reactivity coefficient for [[ ]] void fraction

$\Delta(Kinf)=Kinf1-Kinf2$

$\Delta V=$[[ ]]

and 1E5 is a factor to convert MVC to units of pcm % void.

Results are presented in Figure RAI 15-1 for non-additive fuel and additive fuel with the planned upper bound additive concentration of [[ ]]. Results are presented as functions of exposure for void depletion histories of [[ ]].

Moderator Temperature Coefficient

The effect of additive on moderator temperature reactivity coefficient was characterized using infinite lattice reactivity coefficients for cold controlled and cold uncontrolled cases with moderator temperatures of 20, 100, 160, 220 and 286°C. At each temperature, the moderator temperature coefficient (MTC) was calculated using the equation

$$MTC=(dk/dT)/k$$

[[ ]]. Results are presented for the uncontrolled and controlled cases in Figures RAI 15-2 and RAI 15-3, respectively. Results are presented for exposures of 0, 20 and 35 MWd/MTU for a void depletion history of [[ ]] for non-additive fuel and additive fuel with the planned upper bound additive concentration of [[ ]]. Results were also calculated for [[ ]] void depletion histories, but because the impacts of additive were small and very similar for all three void depletion histories, only the [[ ]] results are included in this response.

Doppler Reactivity Coefficient

The effect of additive on Doppler reactivity coefficient (sometimes denoted fuel temperature coefficient) was characterized using infinite lattice reactivity coefficients for hot uncontrolled and hot uncontrolled Doppler cases to calculate a fuel temperature coefficient. The hot uncontrolled case assumes that the fuel temperature is [[ ]] and the Doppler case assumes that the temperature is [[ ]]. The Doppler reactivity coefficient (DRC) was calculated using the equation

$$DRC=\Delta(Kinf)/(Kinf1\Delta T)$$

where

Kinf1=hot uncontrolled infinite lattice reactivity coefficient

Kinf2=hot uncontrolled Doppler infinite lattice reactivity coefficient

Δ (Kinf)=Kinf1-Kinf2

ΔT=[[ ]]

Results are presented in Figure RAI 15-4 for non-additive fuel and additive fuel with the planned upper bound additive concentration of [[ ]]. Results are presented as functions of exposure for void depletion histories of [[ ]].

Power Coefficient

The power coefficient is effectively the combination of the MVC, MTC, and DRC. Therefore, [[

]].

Prompt Reactivity Feedback

The effect of additive on prompt reactivity feedback (such as during a rod drop accident) was characterized by determining the difference in infinite lattice reactivity coefficients between a perturbed cold case and the standard [[ ]] fuel/moderator cold case for both uncontrolled and controlled conditions. In the perturbed cases the fuel temperature was increased to [[ ]] and the moderator temperature was increased to [[ ]] to simulate moderator prompt heating by neutron and gamma ray energy. The water density was changed to reflect the [[ ]] moderator temperature. Results are presented for the uncontrolled and controlled cases in Figures RAI 15-5 and RAI 15-6, respectively. Results are presented as functions of exposure for void depletion histories of [[ ]] for non-additive fuel and additive fuel with the planned upper bound additive concentration of [[ ]].

In summary, infinite lattice studies have been performed to characterize the change in key reactivity coefficients associated with a change in core state due to [[

]]. The reactivity changes are negligibly small both in an absolute sense and relative to [[ ]] and confirm the conclusion that the addition of aluminosilicate additive at the planned concentrations to the GNF2 fuel assembly (1) does not impact reactor operation, and (2) more specifically does not

affect the GNF2 fuel assembly's inherent compliance with GDC 11 (particularly considering the large margins for non-additive bundles).

Reference:

15.1 Global Nuclear Fuel, "Additive Fuel Pellets for GNF Fuel Designs," NEDC-33406P, Revision 2, December 2009.

[[

]]

Figure RAI 15-1: Effect of Additive on Moderator Void Coefficient

[[

]]

Figure RAI 15-2: Effect of Additive on Moderator Temperature Coefficient

[[

]]

Figure RAI 15-3: Effect of Additive on Moderator Temperature Coefficient

[[

]]

Figure RAI 15-4: Effect of Additive on Fuel Temperature Coefficient

[[

]]

Figure RAI 15-5: Effect of Additive on Prompt Reactivity (Uncontrolled)

[[

]]

Figure RAI 15-6: Effect of Additive on Prompt Reactivity (Controlled)

NRC RAI 16

Please provide more details about how the acceptable concentration of additive from ASTM C776-00 impurity limits is derived. ASTM C776-06 specifies 250 ppm Al and 500 ppm Si.

GNF Response

The current Global Nuclear Fuel (GNF) pellet specification is based upon naturally occurring alumina-silica compounds and is intended to control unintentional inclusion of Al and Si. However, for the proposed additive fuel GNF plans to deliberately include a synthetic alumina-silica compound. The targeted nominal concentration is taken to be [[ ]] for demonstration purposes and the targeted composition is [[ ]]. If this weight and composition are converted to elemental concentrations of Si and Al, the results are [[ ]] mg/gU of Si and [[ ]] mg/gU of Al. [[ ]] Conversely, if the ASTM C776-06 levels are converted to an additive concentration level assuming the targeted [[ ]] composition, the result is an additive concentration limit of [[ ]]. For the targeted composition, the maximum additive concentration that is within the current ASTM standard for pellet Si and Al is determined by the [[ ]]. This value was rounded to [[ ]] in Table 1-1 of NEDC-33406P, Revision 2 (Reference 16.1).

Details of the determination of the maximum additive concentration based upon ASTM C776-00 are provided in Attachment 16.A.

References:

16.1 Global Nuclear Fuel, "Additive Fuel Pellets for GNF Fuel Designs," NEDC-33406P, Revision 2, December 2009.

ATTACHMENT 16.A

Calculation of Additive Concentration Corresponding to ASTM C776-00 Impurity Specification

For GNF additive fuel the nominal additive composition is [[
]]. The molar weights (gm/mol) of Al, Si, O and U are (neglecting the U^{235} enrichment) are

Al = 26.98, Si = 28.09, O = 16.00 and U = 238.03

The molar weights (gm/mol) of Al_2O_3, SiO_2 and UO_2 are then

Al_2O_3 = 101.96, SiO_2 = 60.09 and UO_2 = 270.03

For Si, the C776-00 limit is 500 ppm. Assuming that the additive concentration is X wt%, then for 1gm of fuel

gm of UO_2 = $\left(1-\frac{X}{100}\right)$∗1gm of fuel

gm of U = $\frac{238.03}{270.03}\left(1-\frac{X}{100}\right)$∗1gm of fuel

gm of SiO_2 =[[ ]]∗1gm of fuel

gm of Si =[[ ]]∗1gm of fuel

and $\frac{gm\ Si}{gm\ U}$ = [[ ]]

Assuming that the C776-00 Si limit is µgm of Si/ gm of U = 500x10^{-6} gm Si /gm U, then

$500x10^{-6}$ = [[ ]]

Solving for X yields

X = [[ ]]

For Al, the C776-00 limit is 250 ppm. Assuming that the additive concentration is Y wt%, then. for 1gm of fuel

gm of UO_2 = $\left(1-\frac{Y}{100}\right)$∗1gm of fuel

gm of U = $\frac{238.03}{270.03}\left(1-\frac{Y}{100}\right)$∗1gm of fuel

gm of Al_2O_3 =[[ ]]∗1gm of fuel

gm of Al =[[ ]]∗1gm of fuel

and $\frac{gm\ Al}{gm\ U}$ = [[ ]]

Assuming that the C776-00 Al limit is µgm of Al/ gm of U = 250x10^{-6} gm Al /gm U, then

$250x10^{-6}$ = [[ ]]
Solving for Y yields
Y= [[ ]]

The Al specification is more limiting. Thus the maximum additive concentration that is within current ASTM C776-00 limits for pellet Si and Al is [[ ]].

NRC RAI 17

The following are concerning models that are noted in the submittal to have been compared to data from fuel with additives; however, no actual data have been provided to verify that the proposed model adequately represents the additive fuel data.

(a) Please provide a comparison of yield strength data for additive fuel to the model for yield strength, identifying the concentration and ratio of $Si:Al_2O_3$. Of particular concern are the high temperature predictions. For example, the PRIME model [[ ]]. Page 2-36 states that yield strength has a strain rate dependence; however, the model provided (Equation 2-23) does not include a strain rate dependence. Please explain why this is acceptable. How does the code determine when to switch from Equation 2-28 and implement the creep model? What is the ductile brittle transition temperature assumed for additive fuel?
Additional Request per NRC-GNF Meeting August 9, 2012
Provide detailed description of the yield strength model that includes the strain rate dependency.

(b) Please provide a comparison of elastic moduli data for additive fuel to the elastic moduli model, identifying the concentration and ratio of $Si:Al_2O_3$ for each set of data.

(c) Please provide a comparison of fuel rim formation (thickness) data from high burnup additive fuel to the UO_2 model for rim formation, identifying the concentration and ratio of $Si:Al_2O_3$ for each set of data. Also, provide data to show that the structure and chemical concentration of the $Si:Al_2O_3$ does not change on the (old) grain boundaries in the rim due to restructuring.
Additional Request per NRC-GNF Meeting August 9, 2012
Discuss the impact of smaller rim size on pellet conductivity on the basis of HBEP results.

(d) Section 3.4 suggests that both in-reactor densification and swelling are expected to be same as for UO_2. Both densification and swelling are easily determined from fuel measurements. Please provide a comparison of fuel densification data at low burnups for additive fuel (both ex-reactor and in-reactor) to the UO_2 fuel densification model, identifying the concentration and ratio of $Si:Al_2O_3$ for each set of data. Please provide a comparison of fuel swelling data for additive fuel at high burnups to that for UO_2.
Supplemental Request per NRC-GNF Meeting August 9, 1012
Provide the applicable Halden data.

GNF Response

(a) Plots of calculated fuel yield strength versus temperature for UO_2 and additive fuel with concentrations of [[ ]], together with measured data for additive fuel with [[ ]] additive are presented in Figure RAI 17-1. The plots were calculated using the PRIME (Reference 17.1) relation for additive fuel yield strength; the plot for [[ ]] fits the data well. The plot for UO_2 is included to show that the reduction in yield stress with increasing temperature for additive fuel noted in the RAI does not occur due only to the additive; the yield strength of UO_2 also decreases significantly with increasing temperature. Also, as shown in Figure 17-1, [[

]]. This same limit is applied to additive fuel.

[[

]]

Figure RAI 17-1. Comparison of PRIME Yield Strength Model and Measured Yield Strength for Additive Fuel

In the Global Nuclear Fuel (GNF) model for the yield strength of $(U,Gd)O_2$, the 0.002 offset yield strength is given as an explicit function of strain rate as follows:

[[

]]

As shown in the equation, [[

]]. This is shown in Figure RAI 17-2, where plots of calculated yield strength versus temperature for UO_2 are given for three strain rates. The impact of applied strain rate [[ ]].

[[

]]

For the elastic-plastic steps, the yield strength is calculated [[

]] This rate is substituted into the yield strength relation above to obtain the following relation for $(U,Gd)O_2$ 0.002 offset yield strength:

[[

]]

This is identical to the equation given for $(U,Gd)O_2$ yield strength in Section 2.9 of Reference 17.2.

[[

]]

Figure RAI 17-2 PRIME Predicted Yield Strength for Different Strain Rates

In general, for UO_2 fuel the brittle-ductile transition temperature is not a significant factor in fuel behavior. GNF assumes that UO_2 is brittle at temperatures below [[ ]]. Pellets fracture during the initial rise to power due to differential thermal strains. Fracture occurs at [[

]].

As discussed in the response to 17c below, additive fuel consists of a combination of [[

]]. Also, as shown in Figure RAI 17-1, within the planned additive concentration range [[

]].

(b) As noted in Reference 17.2, the elastic modulus of additive fuel is derived [[
]]. The derivation, including the basis for application of [[
]], is presented in Attachment 17.A. Based upon the densities of the UO_2 and additive components, an additive concentration of [[ ]] corresponds to an additive volume fraction of [[ ]]. Then based upon the results in Attachment 17.A, even at the planned maximum additive concentration of [[ ]], below the eutectic temperature the impact of additive on the elastic modulus of additive fuel will be less than typical accuracy for measurement of elastic modulus.

(c) Irradiation to high burnup results in changes in fuel structure of UO_2 fuel pellets. Specifically, these changes begin when the local burnup exceeds ~60 GWd/MTU and occur in the lower temperature region at or near the periphery of the pellet. These changes result in a structure commonly identified as the high burnup structure (HBS) or rim structure. Formation of the HBS is attributed to recrystallization which starts at grain boundaries and propagates into the affected grains and to the formation of small pores on and within grains. Formation of the HBS is not observed at temperatures above ~1100°C. The characteristics of the HBS for UO_2 fuel and its effects on fuel performance have been the object of intensive studies since the late 1980's. These studies have explored the microstructure and porosity of the HBS, its oxidation state, lattice parameters, fission gas release (FGR), thermal conductivity and impact on pellet clad mechanical interaction (PCMI).

[[

]] Unlike UO_2-additive systems that involve soluble dopants, the GNF alumina-silica additive is essentially insoluble in the UO_2 matrix and resides on the boundaries among the as-sintered grains.

The additive consists of a combination of glassy and crystalline phases after sintering. As illustrated by creep rate versus temperature data in the response to RAI 26, [[
]], so that the as-sintered additive is essentially rigid in the temperature range of the HBS despite the presence of a glassy phase. [[

]]

The impact of the GNF alumina-silica additive effect on the HBS was evaluated relative to standard and large grain UO_2 fuel in test rods that operated to average exposures of 86 GWd/MTU (Reference 17.3). The fuel in this test was sintered to densities in the range of 96.8 – 97.8% of the respective theoretical values. The 3-dimensional grain size of the standard, large grain non-additive and additive pellets were 9–12, 51–63 and 37–58 μm, respectively. The fuel samples were irradiated in the Halden reactor at linear heat generation rates that ranged from 47 kW/m at the beginning of life to 17 kW/m at the end of life. After irradiation, the fuel was examined to characterize the resulting pellet structure. As shown in Figure RAI 17-3, the HBS formed at the edge of both standard UO_2 and additive pellets and extended radially inward to a greater extent in the standard pellet than in the additive pellet; i.e., present from the outer surface to $r/r_0 \sim 0.35$ in standard fuel with 9–12 μm as-built grains and from the surface to $r/r_0 \sim 0.73$ in additive fuel with 37-58 μm grains. Similar conditions were observed in the large grain non-additive samples.

For normal operation, including anticipated operational occurrences (AOOs), the primary concern arising from the formation of the HBS is the impact on fuel temperature. Fuel temperature in turn impacts FGR and thermal expansion, and thus rod internal pressure and cladding strain. As noted above, the thickness of the HBS is lower for additive fuel than UO_2 fuel and High Burnup Effects Program (HBEP) results indicate that the structure is similar in terms of porosity and retained fission gas. Thus the thermal impact of the HBS rim for additive fuel is expected to be lower than for UO_2 fuel. In PRIME licensing calculations, [[

]].

In summary, the GNF alumina-silica additive resides on the as-sintered boundaries of UO_2 grains and is expected to alter the formation of the HBS structure only through the presence of larger grains; i.e., suppress the formation of the HBS. The additive is insoluble in UO_2 and $(U,Pu)O_2$ that form during irradiation. The mobility of the additive is [[

]]

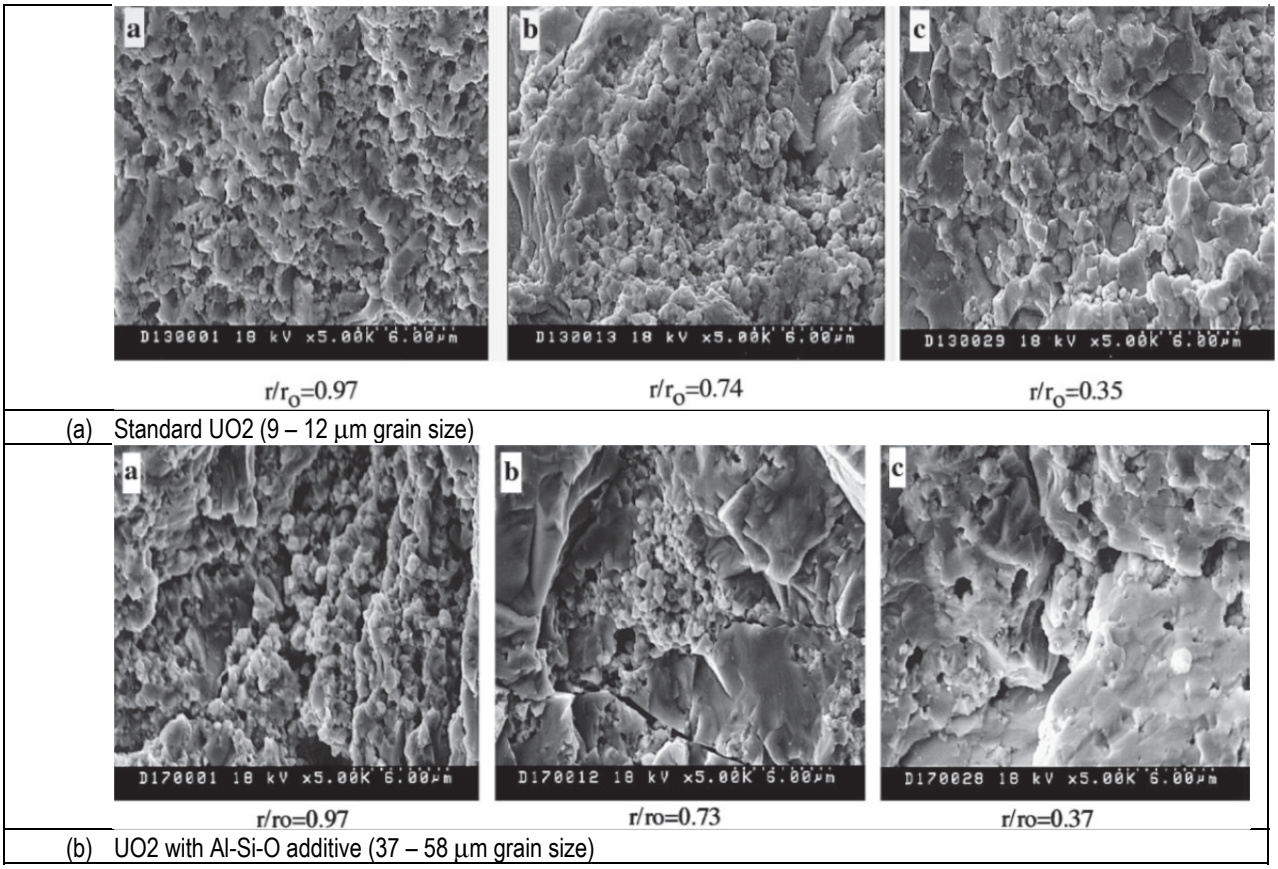

Figure RAI 17-3 Scanning Electron Microscope (SEM) Fractographs of Standard and Additive Fuel Irradiated to 86 GWd/MTU Showing the HBS at the Pellet Periphery and its Variation with Radial Position and Grain Size (Reference 17.3)

(d) In order to observe the behavior of additive fuel under controlled conditions and to obtain data required to model the response of additive fuel during BWR operation, GNF has conducted a long term (~10 year) program to irradiate additive fuel in the Halden reactor. The program included three instrumented fuel assemblies (IFAs). With the exception of how they were operated, the IFAs were identical. Each IFA contained six BWR rods. Specifically, each assembly included 2 UO_2 rods, [[

]]. The results pertaining to densification and swelling are summarized below.

Densification for the nine rods instrumented with fuel stack elongation detectors was obtained directly from periodic elongation measurements at hot standby and included maximum densification and the burnup increment required to reach maximum densification. Densification is based upon the assumption of isotropic elongation. The results are included in Table RAI 17-1 below. These results indicate that the densification response of UO_2 and additive fuel are similar; the results are within the range of data used in development and qualification of the PRIME model.

Table RAI 17-1 Densification for UO_2 and Additive Fuel (from [[ ]])

Rod	Type	Δρ/ρ (%)	ΔE (GWd/kgUO_2)
[[			
			]]

Swelling rates for the nine rods instrumented with fuel stack elongation detectors were first obtained from the slope of periodic elongation measurements at hot standby after the initial reduction in length due to densification at low exposure. The results indicated [[

]] and the swelling rates were recalculated by looking at the elongation data at a constant LHGR of [[ ]]. Results for [[ ]] are presented in Table RAI 17-2 below. These results represent the slope of the elongation versus exposure curve between [[ ]] MWd/MTU. Above this exposure, the results are confounded by the pellet-cladding mechanical interaction. The swelling rates are based upon the assumption of isotropic elongation. Very similar results were obtained for [[ ]]. Because it operated at lower power, comparable results are not available for [[ ]].

Table RAI 17-2 Fuel Swelling Rate for UO_2 and Additive Fuel
(from [[ ]])

Rod	Type	ΔV/V (% per 10 GWd/MTU)
[[		
		]]

These results indicate that the swelling response of [[

]].

Finally, the limited data above indicates [[

]]. If these trends are confirmed as additional data is obtained, the impacts on licensing analyses of additive fuel are considered negligible for the following reasons. [[

]].

On the basis of the above, it is concluded that the Halden data discussed above supports [[

]].

References:

17.1 Global Nuclear Fuel, "The PRIME Model for Analysis of Fuel Rod Thermal-Mechanical Performance, Part 1-Technical Bases," NEDC-33256P-A, Revision 1, September 2010.

17.2 Global Nuclear Fuel, "Additive Fuel Pellets for GNF Fuel Designs," NEDC-33406P, Revision 2, October 2009.

17.3 Une, K., Hirai, M., Nogita, K., Hosokawa, T., Suzawa, Y., Shimizu, S., Etoh, Y., "Rim Structure Formation and High Burnup Fuel Behavior of Large-Grained UO_2 Fuels," Journal of Nuclear Materials, Vol. 278, pp. 54 – 63, 2000.

NRC RAI 17-S01

GNF Comment regarding Additive Yield Stress Model Formulation in LTR

During preparation of the response to RAI 17a, Global Nuclear Fuel (GNF) noted an error in the listing of the additive fuel yield stress model in Section 2.9 of the additive fuel LTR (Reference 17-S01.1). The additive yield stress is given as a function of [[ ]]; however, the additive yield stress model should instead be given as a function of [[ ]], where [[ ]] are as defined in Reference 17-S01.1. The PRIME coding does not include this error and all figures based upon the PRIME additive fuel yield stress model and PRIME results provided in the additive RAI responses (and in Reference 17-S01.1) are calculated based on the PRIME coding and thus are based upon the correct additive fuel yield stress formulation. It is noted that the same error occurs in Section 4.4.3 of the PRIME LTR (Reference 17-S01.2); however, additive fuel properties were not reviewed by the NRC as part of the Reference 17-S01.2 review scope. Reference 17-S01.1 is considered the licensing basis for additive fuel. The error noted above will be corrected in the –A version of Reference 17-S01.1 (see the following for detailed changes).

Reference 17-S01.1 Section 2.9 lines requiring correction (page 2-38):

[[

]]

Corrected formulation [[ ]]:

[[

]]

GNF Comment (Definition of X_A and ρ_F)

As part of the additive yield stress error correction, GNF also noted that X_A is defined in some locations in the additive LTR (Reference 17-S01.1) as "[[ ]]" and in other sections as "[[ ]]". Additionally, during complete review of Reference 17-S01.1 for the term "[[ ]]", GNF noted that ρ_F is defined as "[[ ]]" in one location in Reference 17-S01.1 and "[[ ]]" in all others. For clarity, the definitions of X_A and ρ_F will be changed to "[[ ]]" and "[[ ]]" respectively, in all locations in Reference 17-S01.1. [[

]]

Specifically, when the –A version of Reference 17-S01.1 is published, these changes will be made to the following pages:

- Pages 2-12, 2-13, and 2-25: change the equation [[ ]] to [[ ]]
- Pages 2-10, 2-17, and 2-19: change the text "[[ ]]" to "[[ ]]"
- Page 2-25: change the equation [[ ]] to [[ ]]

References:

17-S01.1 Global Nuclear Fuel, "Additive Fuel Pellets for GNF Fuel Designs," NEDC-33406P, Revision 2, December 2009.

17-S01.2 Global Nuclear Fuel, "The PRIME Model for Analysis of Fuel Rod Thermal-Mechanical Performance, Part 1-Technical Bases," NEDC-33256P-A, Revision 1, September 2010.

ATTACHMENT 17.A

[[

]]

[[

]]

Figure RAI 17-A1

NRC RAI 18

The following are related to licensing analyses with additive fuel.

(a) What grain size (identify whether 3-D or mean linear intercept (MLI)) is assumed for additive fuel in relation to fission gas release and cladding strain for licensing analyses? [[

]] Please confirm that this is the case for additive fuel. Page 2-28 states that a much larger limiting grain diameter is set in PRIME. Please provide a description of how the fission gas release model is applied for additive fuel.
Additional Request per NRC-GNF Meeting August 9, 2012
For the additive fuel fission gas release qualification data, show the impact of [[
]] on predicted fission gas release.

(b) Does the grain growth model impact licensing analyses? If so, what grain growth coefficients are used for additive fuel? Are they the coefficients for $(U,Gd)O_2$? If grain growth impacts licensing analyses, please provide a comparison of grain growth data to PRIME predictions from power ramped rods. (Grain growth is easily measured from micrographs).
Additional Request per NRC-GNF Meeting August 9, 2012
Provide the grain growth model, including coefficients, that was used to calculate the grain growth in Figure 18.1. Discuss how the equation relates to the grain growth equation in the LTR.

(c) Section 5.6 provides difference in licensing predictions between additive and non-additive fuel. Please provide comparisons of stored energy for a plant where loss-of-coolant-accident peak cladding temperatures are limiting due to stored energy and/or where stored energy is high.
Additional Request per NRC-GNF Meeting August 9, 2012
Provide the impact for the upper bound additive concentration ([[ ]]) as well as the nominal concentration ([[ ]]).

GNF Response

(a) Global Nuclear Fuel (GNF) has historically reported 3-D (rather than MLI) grain size for GNF fuel pellets, and has continued to do so for additive fuel. Production experience has shown that additive fuel has an initial 3-D grain size of [[
]] for non-additive fuel. As described in Reference 18.1, the PRIME fission gas release model includes [[ ]], as follows:

- [[

]]

The [[ ]] and were calibrated (and qualified) by comparison to a fission gas release database that included a range of (initial) grain sizes and operating conditions. The [[ ]] was also calibrated (and qualified) by comparison to a fission gas release database that included a range of (initial) grain sizes and operating conditions and [[

]].

On the basis of the discussion above, it is expected that for similar temperatures and exposures that [[
]]. However, this expectation neglects possible effects of [[

]]. However, licensing analyses for additive fuel will be [[

]] This limit is applied to both additive and non-additive fuel. The impact of the use of licensing basis grain size relative to as-fabricated grain size on predicted fission gas release for additive fuel qualification data is presented in the response to RAI 20.

(b) In the PRIME licensing methodology, the primary calculated parameters of interest are rod internal pressure [[ ]] for operation on the linear heat generation rate (LHGR) limit curve and the fuel centerline temperature and cladding plastic strain during an overpower event. As discussed in the response to (a), [[

]].

On the basis of the discussion above, it is concluded that [[

]]; the model, including constants, is given in Section 2.6 of Reference 18.2 and is given below for completeness. This model addresses [[ ]] of grain growth.

[[

]]

The experimental basis for the model is given in Reference 18.1. A comparison of predicted to measured grain growth taken from Reference 18.1 is presented in Figure RAI 18-1 for UO_2 fuel. In Figure RAI 18-1, the triangles represent UO_2 ramp test data.

[[

]]

Figure RAI 18-1: Predicted vs. Measured Grain Growth

(c) For loss-of-coolant accident (LOCA) events, BWR/2 plants are [[
]] and BWR/3-6 plants are limited by peak cladding temperatures (PCT). In these plants, there are typically two cladding temperature peaks during the LOCA event: the first occurs early in the event and is dependent upon boiling transition, which in turn is dependent upon the stored energy at the start of the event; the second occurs later in the event and is dependent upon uncovering the fuel. [[
]] From the same analyses performed to assess the impact of additive on fuel rod internal pressure and discussed in Section 5.2 of Reference 18.2, calculated values of stored energy at the peak power node at [[ ]] for UO_2 and additive fuel with additive concentration of [[ ]], respectively. The corresponding value of stored energy for additive fuel with additive concentration of [[
]]. These results confirm that the effect of additive on fuel stored energy is [[
]].

References:

18.1 Global Nuclear Fuel, "The PRIME Model for Analysis of Fuel Rod Thermal-Mechanical Performance, Part 1-Technical Bases," NEDC-33256P-A, Revision 1, September 2010.
18.2 Global Nuclear Fuel, "Additive Fuel Pellets for GNF Fuel Designs," NEDC-33406P, Revision 2, December 2009.

NRC RAI 19

Section 6.2, page 6-3 suggests that fuel relocation (or residual remaining gap after relocation) is significantly different (factor of 2) for additive fuel than for UO_2, however, no additive fuel relocation model is provided. Does this mean PRIME utilizes the UO_2 relocation model? If so please explain why this is acceptable given the discussion that relocation is significantly different between these two fuel types. Could the difference in gap size be due to fuel densification and/or swelling?

Additional Request per NRC-GNF Meeting August 9, 2012

Clarify how much of the [[
]].

GNF Response

The data in question was obtained from lead use assemblies (LUAs) which were irradiated at low power to minimize pellet-cladding mechanical interaction that could impact subsequent ramp tests. For such irradiations [[

]]

As noted in the response to RAI 17(d), [[

]]

On the basis of the discussion above, [[

]] The impact of additive fuel on cladding circumferential strain and the comparison of predicted and measured cladding circumferential strains is discussed further in the response to RAI 21.

References:

19.1 Global Nuclear Fuel, "The PRIME Model for Analysis of Fuel Rod Thermal-Mechanical Performance, Part 1-Technical Bases," NEDC-33256P-A Revision 1, September 2010.

[[

]]

Figure RAI 19-1. Relocation at a High Power Node during Steady-State Operation at the Peak Power followed by a Thermal Overpower Event

NRC RAI 20

The LTR states that: "The additive fission gas release (FGR) data are well within the scatter of the non-additive data." [[

]]. Fuel rods with high release are those of primary concern in a core because these rods are those with limiting rod internal pressure. [[

]]. Please provide the terminal ramp powers for the IFA-635 rods. Also, for the non-power ramped rods (NFD [Nippon Fuel Development] Halden and NUPEC [Nuclear Power Engineering Corporation] Step 3 lead use assembly tests tests) provide the maximum rod power (peak and average) at beginning, middle and latter one third of irradiation.

Additional Request per NRC-GNF Meeting August 9, 2012

Regenerate Figures 20.1 and 20.2. For the additive cases use [[

]]. Provide as-fabricated grain sizes and terminal powers for the ramped additive FGR qualification cases.

GNF Response

As noted in RAI 20, [[

]]. Reviewing these data sets in more detail shows the following.

There are only [[

]]. As discussed in Section 3.1 of Reference 20.1 and in the response to RAI 25, [[

]]. Additionally, in preparing this response, it was noted that the coolant temperature used in the analyses of these rods was incorrect (too low). Corrected results for the PRIME (Reference 20.2) analyses are included in Table RAI 20-1 below (Reference 20.1 results are included in parenthesis). [[

]]

Table RAI 20-1. Corrected PRIME Predicted FGR from [[ ]]

Segment Serial Number	Pre/Post Ramp Test Exposure, GWd/tU	Additive Concentration, ppm	Measured FGR, %	PRIME03 FGR, (%)
[[				
				]]

There are [[

]]. Side by side tests of the grain size effect on FGR for UO_2 fuel indicates that the FGR for large grain size is initially lower than for smaller grain size. [[

]].

There are [[

]].

For all three of the data sets discussed above, it is noted that additive pellets were produced by different processes (and for the NFD and NUPEC data with different additive composition) than for the planned GNF additive fuel. The fabrication processes may have impacted pellet microstructure and composition in such a way as to impact FGR. For this reason, the FGR predictions for the [[ ]] lead use assembly (LUA) data assume increased significance. The rods were prototypical of current (GE14) GNF fuel designs, and included the planned additive at concentrations that bound the planned concentration. They were produced in the GNF production facility by a more mature production

process with less variability than earlier LUA pellets and operated in a commercial reactor. [[
]].

Finally, as noted in the response to RAI 21a, subsequent to the submittal of Reference 20.1, PRIME analyses were performed for several of the Segmented Rod Program (SRP) rods discussed in the response to address the concern expressed in RAI 21a about the PRIME capability to predict cladding strain during AOOs for additive fuel. These rods also had measured FGR. Because these rods were ramped to high powers, the FGRs were high. [[
]] The PRIME FGR predictions are compared to the measured values in Table RAI 20-2 below. [[
]]

In Figures RAI 20-1 and RAI 20-2 below, Figures 4-3 and 4-4 from Reference 20.1 are revised to reflect the corrections and additions to the additive fuel FGR data discussed above. Figures RAI 20-3 and RAI 20-4 are included to illustrate PRIME fission gas prediction of the data in Figures 4-3 and 4-4 from Reference 20.1 with [[
]]. Additionally, since GNF [[

]]. The as-fabricated grain sizes and ramp terminal powers for the ramp test additive fuel data in these figures are presented in Table RAI 20-3 below.

Table RAI 20-2. PRIME Predicted and Measured FGR for SRP Additive Rods (As-fabricated Grain Size)

Tests	Exposure, MWd/MTU	Additive Concentration, w/o	Measured FGR[%]	Predicted FGR[%]
[[				
				]]

Table RAI 20-3. As-fabricated Grain Size and Terminal Power for Additive Fuel Data

Rod Designation	As-Fabricated Grain Size (µm)	Terminal Power (kW/ft)
[[		
		]]

[[

]]

Figure RAI 20-1. Updated Predicted versus Measured FGR
([[ ]])

[[

]]

Figure RAI 20-2. Updated Predicted/Measured FGR versus Exposure ([[ ]])

[[

]]

Figure RAI 20-3. Updated Predicted versus Measured FGR ([[ ]])

[[

]]

Figure RAI 20-4. Updated Predicted versus Measured Fission Gas Release ([[ ]])

As noted in the response to RAI 18, [[

]].

[[

]]

Figure RAI 20-5.Updated Additive Predicted FGR [[
]]

[[

]]

Figure RAI 20-6. Updated Predicted versus Measured FGR ([[ ]])

[[

]]

Figure RAI 20-7. Updated Predicted versus Measured FGR ([[ ]])

[[

]]

Figure RAI 20-8. Updated Predicted versus Measured FGR ([[ ]])

[[

]]

Figure RAI 20-9. Updated Predicted versus Measured FGR ([[ ]])

On the basis of the results in Figures RAI 20-1 through RAI 20-9 and the discussion above, particularly considering [[

]].

References:

20.1 Global Nuclear Fuel, "Additive Fuel Pellets for GNF Fuel Designs," NEDC-33406P Revision 2, December 2009.

20.2 Global Nuclear Fuel, "The PRIME Model for Analysis of Fuel Rod Thermal-Mechanical Performance, Part 1-Technical Bases," NEDC-33256P-A Revision 1, September 2010.

NRC RAI 20-S01

Responses to PNNL Comments/Questions and Requests on GNF Responses to Round 02 RAIs Sent October 31, 2012 on Additive Fuel Pellet

NRC Comment

The [[ ]]. The fission gas release (FGR) UO_2 model prediction using [[ ]]. However, the predictions [[ ]]. This is also evident in the [[ ]]. For this small FGR database for additive fuel the code [[ ]] This suggests that [[ ]]. As noted in RAI 20 the limiting rod pressure analysis usually predicts FGR values [[ ]], therefore, this is the range of interest for rod pressure licensing analyses.

NRC Request

Please provide the mean of the predicted-minus-measured and standard deviation for the UO_2 data [[ ]] FGR, provide the number of data points based on these values of mean and σ. Please provide the mean of the predicted-minus-measured and standard deviation for additive fuel data [[ ]] FGR, provide the number of data points based on these values of mean and σ. The probability that these two populations of additive and UO_2 fuel are similar or different can be determined, however, the probability analysis needs to consider that the number of data points are significantly different for the two populations. It appears that [[ ]].

GNF Response

To better address the Pacific Northwest National Laboratory (PNNL) concerns about possible PRIME underprediction of fission gas release for additive fuel, Figures RAI 20-6, RAI 20-7, RAI 20-8 and RAI 20-9 from Response 20 are replotted below as Figures RAI 20S-6, RAI 20S-7, RAI 20S-8 and RAI 20S-9, respectively. In these figures, the additive data are identified by the source of the data. Figures RAI 20S-6 and RAI 20S-8 present the predicted versus measured PRIME nominal and [[ ]] fission gas release results and Figures 20S-7 and 20S-9 present the predicted/measured PRIME nominal and [[ ]] fission gas release results versus exposure. [[ ]].

Based upon Figures RAI 20S-6 and RAI 20S-8, [[

]]. The impact of these data sets on the statistics is explicitly included in the tables.

Table RAI 20S-4. Nominal P-M Summary Statistics

Dataset (Measured FGR > 5%)	Mean	SD	Count
[[ ]]			

Table RAI 20S-5. [[ ]] P-M Summary Statistics

Dataset (Measured FGR > 5%)	Mean	SD	Count
[[ ]]			

Based upon the summary statistics for the nominal results, [[

]], the NFD Halden data was obtained from irradiation of rods in the Halden reactor. The design of the rods included high enrichment and small diameter in order to accumulate exposure quickly. At the time of the irradiation of these rods, light water reactor (LWR) operating conditions were not as closely simulated as in later tests. For these reasons, differences in prediction of fission gas release for these rods relative to prototypical boiling water reactor (BWR) UO_2 rods operated under BWR operating conditions are possible. On the basis of the differences noted above and [[

]].

As shown in Table RAI 20S-4 (and Table RAI 20S-5), [[

]]. These rods are irradiated at low power to high exposure. The primary contribution to predicted fission gas release for these rods is [[
]] in the PRIME fission gas release model. In addition to [[

]].

As noted above, the PNNL request to evaluate the P-M fission gas release statistics for additive data with fission gas release [[

]]. For this reason GNF concludes that use of all the additive fission gas release data is valid. This applies specifically to the [[
]] LUA data, which is most prototypical of current additive fuel fabrication and operation. Therefore, GNF has also evaluated the P-M fission gas release statistics for all additive data in Figures RAI 20S-6 and RAI 20S-8. The results are summarized in Tables RAI 20S-6 and RAI 20S-7 below. As in Tables RAI 20S-4 and RAI 20S-5, the [[
]] is explicitly included in Tables RAI 20S-6 and RAI 20S-7.

Table RAI 20S-6. Nominal P-M Summary Statistics

Dataset	Mean	SD	Count
[[ ]]			

Table RAI 20S-7. 2σ Model P-M Summary Statistics

Dataset	Mean	SD	Count
[[ ]]			

As shown in these tables, including all measured additive fission gas release data increases the number of additive fission gas release data points to [[ ]], even when [[ ]], increasing confidence in the statistical assessment of the adequacy of the PRIME model for application to additive fuel. The results of the summary statistics when all additive data is included [[

]].

In summary, on the basis of the discussion and results above, GNF concludes that the PRIME nominal predictions for additive fuel [[

]]

[[

]]

Figure RAI 20S-6. Updated Predicted versus Measured Fission Gas Release with Additive Programs Labeled ([[ ]])

[[

]]

Figure RAI 20S-7. Updated Predicted/Measured vs. Exposure Fission Gas Release with Additive Programs Labeled ([[ ]])

[[

]]

Figure RAI 20S-8. Updated Predicted versus Measured Fission Gas Release with Additive Programs Labeled ([[ ]])

[[

]]

Figure RAI 20S-9. Updated Predicted/Measured vs. Exposure Fission Gas Release with Additive Programs Labeled ([[ ]])

NRC RAI 20-S02

Based on evaluation of responses please provide the following information.

The PRIME predicted and measured FGR values and their operating power histories for those data [[

]]. Identify the Halden test assembly if the data came from a Halden test. This will also determine whether or not the code covers the proposed operating range required for additive fuel. The additive fuel FGR data that [[

]]. PNNL [[

]] based on PRIME FGR predictions for additive fuel in Figure 20S.6 of response.

Response

As discussed in the response to RAI 20-S01, [[

]]. In the response, it is postulated that [[

]]. The basis for the postulation is as follows. [[

]].

Based on the discussions above, [[

]]. It is noted that the provided figures/data include the requested [[ ]] releases ([[ ]] FGR data); thus, the smaller subset of data requested by the NRC is contained in the figures.

The results are presented in terms of the datasets discussed in the response to RAI 20-S01 and a short assessment of each dataset is contained in the notes following the figures. An example [[ ]] illustrating representative operation is shown on each plot for reference[2]. Summarizing the results illustrated in the figures, [[

]].

In summary, based upon the entire preceding discussion (and the assessment of each dataset following each corresponding figure in Figures RAI 20S-10 through RAI 20S-16), GNF concludes [[

]].

[1] As requested by the NRC, the operating history for each of the additive test programs is provided. The figures illustrate the nodal power-exposure history in a single chart and the rod average power history in a separate single chart or multiple charts. Along with the operating history, measured and predicted FGR are provided for best-estimate and model perturbation including P/M and P-M for convenience in review.

[2] For plots of rod average power history, an example [[ ]] is shown only for FLR rod comparisons.

Data Set	Rod	[[ ]]
[[		
		]]

[[

]]

Figure RAI 20S-10. [[ ]] **Halden Ramp Test FGR and Power History Data**

Figure notes: [[ ]]

[[

]]

Figure RAI 20S-11. Halden Steady-State Thermal Rig FGR and Power History Data

Figure notes: [[

]]

[[

]]

Figure RAI 20S-12. [[ ]]**-Halden Ramp Test FGR and Power History Data**

Figure notes: [[

]]

[[

]]

Figure RAI 20S-13. SRP Ramp Test FGR and Power History Data

Figure notes: [[

]]

[[

]]

Figure RAI 20S-14. NFD-Halden Steady-State Thermal Rig FGR and Power History Data

Figure notes: [[

]]

[[

]]

Figure RAI 20S-15. NUPEC STEP3 LUA FGR and Power History Data

Figure notes: [[

]]

[[

]]

Figure RAI 20S-16. [[ ]] **LUA FGR and Power History Data**

Figure notes: [[

]]

NRC RAI 20-S03

This supplement addresses the status of GNF additive fuel LTR RAI 20 following the June 25, 2013 NRC/PNNL/GNF conference call. The conference call was held to resolve final NRC/PNNL RAIs. The focus of the call relative to RAI 20 scope was in regards to PNNL proposed application of [[

]].

Response

The proposed Pacific Northwest National Laboratory (PNNL) penalty is based upon 1) a PNNL proposed mechanism for increased FGR for additive relative to UO_2 discussed during the call and subsequently transmitted to Global Nuclear Fuel (GNF), and 2) PNNL focus on specific additive FGR datasets [[

]].

After consideration of the basis of the proposed PNNL penalty, including assessment of the proposed mechanism for increased release, GNF's position continues to be that the FGR from GNF additive fuel [[ ]]; and thus that the [[

]]. The GNF position is based upon GNF's mechanistic understanding of FGR in UO_2 fuel and the [[

]] and upon assessment of GNF's additive fuel FGR data relative to PRIME predictions when all data is considered.

The GNF position relative to both of the PNNL concerns which lead to the proposed PRIME FGR model penalty for additive fuel is detailed below.

1) Mechanistic understanding of Additive FGR relative to UO_2 (addresses PNNL concern 1)

The GNF mechanistic understanding of FGR from UO_2 nuclear fuel rods is summarized as follows:

a) Fission gas (FG) atoms are generated within grains due to the fission process.
b) The FG atoms diffuse to grain boundaries and collect to eventually form bubbles on the grain boundaries. The rate of diffusion is controlled by the intragranular FG atom concentration gradient and the intragranular FG atom diffusion coefficient (which is highly temperature dependent).
c) FG bubbles formed on grain boundaries grow and eventually interlink to provide FG transport paths to the rod void volume. Before interlinkage, release is controlled primarily by recoil and knockout and is low. After interlinkage and release of the FG in the interlinked bubbles to the rod void volume, FG atoms arriving at grain boundaries are released to the rod void volume. The rate of arrival of FG atoms at the grain boundaries depends upon the diffusion coefficient and the diffusion distance. Diffusion distances are on the order of the grain size, thus grain size has an effect on interlinkage and FGR.

This understanding is generally accepted in the nuclear industry.

[[

]]

The PNNL proposed mechanism for increased FGR from additive fuel relative to UO_2 fuel is summarized as follows: [[

]]. PNNL also notes that at temperatures below T_{eut} some of the mechanical and chemical properties of the additive phase, such as viscosity and diffusivity of FG atoms/bubbles, begin to change and suggests that [[

]].

GNF concludes that the proposed mechanistic basis for increased FGR for GNF additive fuel relative to UO_2 fuel is not supported for the following reasons:

- The proposed mechanistic basis for increased FGR for additive fuel is not supported by historical industry programs focused on fission gas release, in particular in high burnup additive fuel (Reference 20-S03. 1).
- Recent SCIP results to be presented at the 2013 ANS TOPFUEL meeting (Reference 20-S03.2) indicate that additive pellets release [[ ]] of fission product gases during a power ramp (and 12 hour hold) as compared to standard UO_2 fuel (where the standard fuel was ramped to much lower power). Detailed PIE by SCIP revealed that this is due to 1) the additive microstructure after ramp, which shows evidence of [[

  ]] and 2) the additive pellets also show [[ ]] compared to the UO_2 fuel, resulting in lower release from interlinkage.
- The proposed mechanistic basis for increased FGR for additive fuel is not supported based on a review of the GNF additive fuel FGR measurement database (detailed in Appendix A of this supplemental response).

[3] Additive mechanical and chemical properties are functions of temperature and could change at temperatures below T_{eut}; however, the significance of the changes below T_{eut} will be much less than the changes at or above T_{eut}. [[

]]

Additionally, even if the proposed [[ ]] is accepted, the impact of such a mechanism is not consistent with the application of the proposed FGR penalty at high exposure, where the most limiting SAFDL is related to rod internal pressure. At high exposure ([[ ]]) where fuel temperatures are below T_{eut}, FGR is controlled by diffusion to grain boundaries and is a function of grain size. Additive fuel will have [[ ]], FGR at high exposure will not be increased relative to UO_2. Finally it is noted that in actual fuel rod operation, temperatures above (or close to) T_{eut} are not expected, rendering the concern about [[ ]] minimal for actual operation.

2) *Basis for Including all GNF Additive FGR data in assessing the adequacy of the PRIME UO2 FGR Model for Licensing Analyses of GNF Additive Fuel (addresses PNNL concern 2)*

As noted above, the proposed [[ ]] appears to be due in large part to the fact that PNNL has neglected a significant fraction of the additive FGR data with measured release [[ ]] in the assessment of the adequacy of the PRIME UO_2 model. Thus, the penalty resulting from the assessment is based primarily on [[ ]]. For both [[ ]], GNF contends that the high release should not be attributed [[ ]]; but agrees with PNNL that both [[ ]] datasets should be included in the PRIME additive FGR qualification database. GNF thus believes that all additive FGR data (including [[ ]]) should be used in assessing the adequacy of [[ ]] (P-M for all additive data is shown in Figure 20-S03-1); and that, when all data is considered, no FGR penalty is required for the following reasons:

- GNF has historically used [[ ]] as a threshold for graphical presentation of FGR data. For measured FGR less than [[ ]] the data has been presented as P-M and for measured FGR greater than [[ ]] the data has been presented as P/M. The [[ ]] threshold was selected to avoid the large scatter that would have resulted if all data was presented using either P-M or P/M only. GNF did not assign any fuel performance significance to the threshold.
- GNF contends that the use of an arbitrary threshold for whether FGR measurements are relevant for evaluating model prediction adequacy is not generically applicable since it does not consider operating history or rod characteristics which are considered explicitly in licensing analyses (i.e., large grain size fuel will release less than smaller grain size fuel for similar operation as is the case for many of the additive datasets).
- Specifically, use of the [[ ]] threshold results in 3 datasets with low measured FGR being neglected in the PNNL assessment of the PRIME adequacy and resulting penalty. Based upon review of the rod characteristics, comparisons to

similarly operated UO_2 rods, and comparison to the TMOL, GNF contends that the three datasets are relevant to assessing the adequacy of the PRIME UO_2 FGR model for applicability to additive fuel licensing. Details of the assessment are contained in Appendix B to this supplemental response.

- P-M results are presented in Figure 20-S03-2 for [[ ]] additive rods and UO_2 rods with the same or similar fuel design and produced by the same manufacturer and GNF UO_2 rods with the same fuel design (9X9). All rods were irradiated in commercial reactors. Based on Figure 20-S03-2, [[ ]] P-M additive FGR results are within the experience base for UO_2 FGR. Therefore, the higher than expected FGR for [[ ]] should not be attributed to the presence of additive; and the [[ ]] additive results should not be overemphasized in determining the adequacy of PRIME additive FGR predictions. As previously noted in prior supplements to this RAI, the [[

  ]]. However, as noted above, the [[ ]] data will be retained in the PRIME additive FRG database.
- [[ ]] tests are NFD sponsored tests carried out in the Halden reactor as part of a program to support new fuel development, programs. The tests consisted of two different rod types, one with small diameter ([[ ]]) with five rod segments measured and one with typical BWR dimensions ([[ ]]) with four rod segments measured. Both [[ ]] had the same additive concentration and grain size. [[ ]] operated at higher power (LHGR) than [[ ]] for most of the operating history; however, [[

  ]]. These results demonstrate the basis for the GNF concern about the [[ ]]. Because the operating histories were similar and since [[ ]] contained similar additive content, and [[

  ]]. From the P-M results in Figure 20-S03-1 it is noted that all [[

  ]]. However, the [[

  ]]. As noted above, the [[ ]] data will be retained in the PRIME additive FGR database.
- The PRIME methodology (NEDC-33258P-A) will be applied to additive fuel licensing. PRIME licensing analyses to demonstrate compliance with SAFDL's related to rod internal pressure and temperature are performed statistically by applying the [[ ]] to the results of a PRIME nominal analysis and multiple single parameter perturbation analyses that account for design, operational, and model uncertainties. The perturbation analyses are

performed on a 2σ basis and the results of the statistical treatment are used to ensure that the associated SAFDL's are met at a [[ ]] confidence level. Operation [[ ]] is assumed for these analyses. The PRIME model uncertainty is derived via statistical evaluation of predicted vs. measured results for the GNF qualification database. Specifically, the adequacy of PRIME predictions for application to fuel rod licensing is based upon the requirement that the application of the 2σ model uncertainty results in ~98% of the data being bounded by the predictions. A detailed review of the PRIME UO_2 and additive FGR database shows that PRIME nominal predictions result in overprediction of [[ ]] of UO_2 and additive FGR measurements, respectively, indicating the PRIME nominal predictions are slightly conservative in both cases. Application of the PRIME 2σ model uncertainty (consists of [[ ]] as defined in NEDC-33258P-A) results in [[ ]] of FGR measurements being overpredicted for both UO_2 and additive fuel. Based upon these essentially equivalent statistical results for UO_2 and additive fuel, GNF contends that the PRIME UO_2 FGR model and licensed statistical application methodology are adequate for additive fuel licensing without a penalty.

In summary, on the basis of the discussion above, GNF contends that: (a) the mechanistic basis proposed by PNNL for increased FGR for additive fuel relative to UO_2 fuel is not supported by results from additive fuel experimental programs and is not supported by FGR data for GNF additive fuel operated in commercial reactors; (b) application of a penalty to the PRIME UO_2 FGR model for additive fuel based upon the proposed PNNL basis is inconsistent on a mechanistic basis with the PNNL concern about underprediction of FGR at high exposure; (c) FGR for additive and UO_2 fuel is similar over the entire operating regime defined by the TMOL when design features and operation are considered; and (d) the PRIME UO_2 FGR model (and associated PRIME model uncertainty) can be applied to licensing analyses for GNF aluminosilicate additive fuel without application of a FGR penalty.

References:

20-S03.1. SCIP PRG/2012/2, "Summary Record of the Seventeenth Meeting of the Program Review Group of the OECD-NEA SCIP Project," Section 5.2.1, November 13-15, 2012.

20-S03.2. D. Jãdernas et al., "Microstructural and Chemical Characterization of Ramp Tested Additive Fuel," (to be presented at) Proceedings of 2013 LWR Fuel Performance Meeting, TopFuel/WRFPM, Charlotte, NC, 2013.

[[

]]

Figure 20-S03-1. P-M for All GNF Additive FGR Data

[[

]]

Figure 20-S03-2. P-M for [[ ]]Additive and [[ ]]UO_2 (plus GNF 9X9 UO_2 LUAs)

Appendix 20-S03-A

This appendix details a review of the GNF additive fuel FGR measurement database for the purpose of determining if the PNNL proposed basis for increased FGR for additive fuel is supported by measurement data. Since the PNNL concern with FGR is primarily the impact on licensing analyses to confirm compliance with the SAFDL that addresses rod internal pressure, the focus of the review was steady-state additive fuel FGR data Steady-state data reviewed included FGR data from the Halden test reactor, i.e., [[ ]], the Halden steady-state thermal rig tests (HSSTR), and from LUAs operated in commercial reactors, i.e., [[ ]] and GUNC LUAs.

Data from [[ ]] are the most relevant data for determining the effects of operation close to or above T_{eut} on FGR since they operated at very high linear heat generation rate LHGR and had (predicted) sustained temperatures close to or above T_{eut} from the start of irradiation to approximately [[ ]]. Peak node LHGR and centerline temperature (TCL) vs. exposure for some of the highest LHGR [[ ]] rods are shown in Figure 20-S03-A1. From Figure 20-S03-A1, it is noted that [[

]]. Based upon the temperature results in Figure 20-S03-A1, [[

]].

Peak node LHGR and predicted TCL vs. exposure for the highest LHGR rods from the HSSTR test program are shown in Figure 20-S03-A2. From Figure 20-S03-A2, it is noted that these rods operated at high LHGR early in life and had peak TCLs close to T_{eut} from the start of operation to [[ ]] GWd/MTU; the measured FGR data was as expected based upon UO_2 rods with similar operation. As a result, measured FGR data from this test program does not support the proposed basis for increased FGR for additive fuel.

Peak node LHGR and predicted TCL vs. exposure for the [[ ]] and GUNC LUAs (excluding GUNC segmented rods) are shown in Figure 20-S03-A3. As shown in Figure 20-S03-A3, peak TCL for the [[ ]] rods remains well below T_{eut} from the start of irradiation to very high exposure. [[

]]

[[

]]

Figure 20-S03-A1. Max LHGR and Max (predicted) TCL at Each Time Step for [[ ]] High LHGR Rods

[[

]]

Figure 20-S03-A2. Max LHGR and Max (predicted) TCL at Each Time Step for HSSTR Rods 2 and 5

[[

]]

Figure 20-S03-A3. Max LHGR and Max (predicted) TCL at Each Time Step for All [[ ]] and GUNC LUA Rods (Excluding Segmented GUNC Rods)

Appendix 20-S03-B

This appendix details additional review of the measured FGR data from the steady-state HSSTR tests and GUNC LUAs; and ramp tests of Duane Arnold (DA) which were all neglected in the development of the PNNL proposed FGR penalty on PRIME prediction of additive fuel. This additional review was conducted to confirm the relevance of this data in assessing the adequacy of the PRIME UO2 FGR model for application to additive fuel licensing.

Figure 20-S03-B1 shows a plot of peak node LHGR vs. exposure for the highest LHGR HSSTR tests and a similarly operated UO_2 rod with an overlaid example TMOL. Figure 20-S03-B1 also includes a plot of the ratio of LHGR to TMOL for these HSSTR rods. From Figure 20-S03-B1, the measured FGR for the HSSTR tests is as expected based upon the similarly operated UO_2 rod when the differences in grain size ([[ ]]) and operating history are considered. It is noted that the LHGRs for these HSSTR rods are close to the example TMOL up to [[ ]]GWd/MTU after which the LHGR decreases. GNF contends that the HSSTR data is relevant in assessing PRIME UO_2 FGR applicability to additive fuel due to operation near the TMOL (during some part of operation) and due to the comparison to similarly operated UO_2 at or near T_{eut} (i.e., shows that increased FGR does not occur in additive fuel due to early interlinkage from operation at or near T_{eut} and if HSSTR would have had similar grain size to UO_2 then the [[ ]] arbitrary threshold would have been exceeded).

Similar information for the GUNC LUA rods ([[ ]]) is shown in Figure 20-S03-B2. From Figure 20-S03-B2, considering differences in grain size ([[ ]]), the GUNC FGR is well within the expected range based on the UO_2 rod included for comparison and shows much lower release compared to [[ ]] data. It is noted that the LHGRs for GUNC are very similar to the [[ ]] LHGRs up to [[ ]] GWd/MTU; after this point the GUNC LHGRs are significantly higher than the [[ ]] rods and extend to higher exposure. This is evident also from the second plot of Figure 20-S03-B2, which shows the ratio of peak LHGR/TMOL (close to or above 1.0 at high exposure). GNF contends that the GUNC LUA data is relevant in assessing PRIME UO2 FGR applicability to additive fuel due to similar operation to [[ ]] rods (which are included in PNNLs current assessment), due to operation near the TMOL at EOL (where FG inventories are high and rod internal pressure SAFDLs are of concern), and due to the comparison to similarly operated UO_2. This comparison shows that additive and UO_2 FGR are similar and that if GUNC would have had similar grain size to UO_2 then the [[ ]] arbitrary threshold would have been exceeded.

Figure 20-S03-B3 shows a plot of peak node LHGR vs. exposure for the DA ramp rests with an overlaid example TMOL. From Figure 20-S03-B3 it is noted that the LHGR during the ramp exceeds the TMOL at [[ ]] GWd/MTU. [[

]] Thus, GNF contends that the DA ramp test data is relevant in assessing PRIME UO_2 FGR applicability to additive fuel due to operation on (or above) the TMOL for sufficient time

following the ramp to achieve steady-state release and since the [[ ]] arbitrary threshold would have likely been exceeded if the DA rods would have had grain size typical of UO_2.

Based upon the review of fuel rod characteristics and operating histories and measured from similar UO_2 rods, GNF contends that FGR data for GNF additive fuel from the HSSTR tests, GUNC LUAs and ramp tests of DA segments are relevant to the assessment of the adequacy of the PRIME UO_2 FGR model for application to additive fuel licensing analyses.

[[

]]

Figure 20-S03-B1. HSSTR Peak LHGR vs. Exposure relative to example TMOL and the Ratio of Peak LHGR to Example TMOL (Including a Similarly Operated UO_2 Rod for Comparison)

[[

]]

Figure 20-S03-B2. GUNC (Excluding Segmented Rods) Peak LHGR vs. Exposure Relative to Example TMOL and the Ratio of Peak LHGR to Example TMOL (Including the [[ ]] Data and a Similarly Operated UO_2 Rod for Comparison)

[[

]]

Figure 20-S03-B3. DA Peak LHGR vs. Exposure Relative to Example TMOL

NRC RAI 21

The following are related to demonstrating that pellet-clad interaction (PCI) and cladding strain criteria are met for additive fuel.

a. *There is very little cladding strain data from additive fuel, particularly for power ramped rods which are of interest for verifying cladding strain predictions during anticipated operational occurrence (AOO) events. [[*

]]. This makes it difficult to assess the appropriateness of the calculations in Section 5.3 that show a large margin to the mechanical overpower (MOP) limit with additive fuel, when there are no assessments of ramped rods where large strains are measured, and those that are provided are underpredicted. Please identify each ramp tested data provided on Figure 6-2 with additive concentration and Si:Al_2O_3 ratio and terminal power hold times. Are the ramp terminal powers rod average or axial peak powers? Please provide measured (usually measured following a ramp test) and predicted plastic strains for these ramped rods (Figure 6-2). Are the axial locations provided in Table 6-1 axial peak locations?

Additional Request per NRC-GNF Meeting August 9, 2012

For the additive fuel cladding strain qualification data, quantify the impact of the use of [[ ]] on predicted cladding strain. Provide additional details for the parameters in Tables 21.1 and 21.2

b. *Please provide a plot of delta power change at the terminal power versus exposure for the data presented in Figure 6-2 (peak terminal power plotted) because PCI thresholds have been shown to also be dependent on delta power change.*

c. *Will additive fuel with and without barrier cladding have different LHGR operating limits than non-additive fuel with and without barrier cladding to prevent PCI failures?*

d. *Pages 6-6 and 6-7 suggest that PCI resistance of additive fuel as compared to UO_2 is due to the increased retention of fission products on the grain boundaries and further notes that this is confirmed from electron probe micro-analysis (EPMA) data. Please provide this EPMA data for cesium and cadmium comparing it to UO_2 EPMA data with similar in-reactor operation. Also, provide krypton-85 EPMA data for additive and non-additive fuel, if measured. Was any micro-gamma scanning performed across the fuel radius of irradiated additive pellets? If so, please provide this data.*

e. *Was the amount of dish filling or axial fuel column increase measured in the power ramped rods with additive and non-additive fuel? If so please provide this data as this provides a measure of the amount of fuel creep experienced during these tests that can be used to confirm fuel creep model differences between additive and non-additive fuel for an AOO event.*

f. *What was the assumed grain size for PRIME cladding strain analyses of the ramped rods?*

g. Permanent strain values for setting the MOP limit provided in Figure 5-3 do not reflect the differences in [[ ]]. Please provide a figure of margin to strain limit for a given MOP limit as a function of exposure.
Additional Request per NRC-GNF Meeting August 9, 2012
Provide the strain evolution [[ ]] showing the details of elastic/plastic response during power ramp and the hold time. Provide inputs for FRAPCON audit calculations.

GNF Response

a. The results in Figure 6-2 of Reference 21.1 were obtained from ramp tests of rods from the Segmented Rod Progam (SRP) and the [[ ]] lead use assembly (LUA) program. The SRP rods were base irradiated in a United States commercial reactor and ramp tested in either the R2 or Halden test reactor. The [[ ]] LUA rods were base irradiated in the [[ ]] reactor and ramp tested in the Halden test reactor. Requested details for the rods in Figure 6-2, including rod identification, additive concentration and composition, ramp terminal power and hold time, and measured and predicted cladding plastic strain, are presented in Tables RAI 21-1 and RAI 21-2. In Table RAI 21-2, the values of predicted diametral strain have been updated to reflect strains accumulated during the ramp tests. These values were also updated in Figure RAI 21-1b.

At the time that Reference 21.1 was submitted, PRIME (Reference 21.2) predictions for the ramped additive rods had not been performed. To address the concern expressed in the RAI about the PRIME capability to predict cladding strain during AOOs for additive fuel, PRIME analyses were performed for several ([[ ]]) of the SRP rods. These results are included in Table RAI 21-1. The results are plotted in Figure RAI 21-1a (Nominal) and superimposed on the PRIME cladding diametral strain qualification given in Figure 4.7 of Reference 21.1 in Figure RAI 21-1b. In Figure RAI 21-1a, the circles and triangles denote A ramp and C ramp tests, respectively. In A ramp tests, [[ ]]; in C ramp tests, [[ ]]. In Table RAI 21-1, all initial ramps are A ramps and all second ramps are C ramps. In Table RAI 21-2, all ramps are A ramps. The measured diameter changes or strains are generally [[ ]] corresponding to the stated test power and are incremental strains occurring during the ramp test. The PRIME predicted cladding strains for the newly included SRP ramp tested rods with positive measured strains are [[ ]] the measured values.

Table RAI 21-1. Segmented Rod Program Ramp Test Results (with PRIME Predictions)

			Initial Ramp				Second Ramp			
SRP number	**Additive content [wt%]**	**SiO2:Al2O3 ratio**	**Peak power reached in test [KW/ft]**	**Hold time minutes**	**Average diameter change [mil]**	**Predicted diameter change [mil]**	**Peak power reached in test [KW/ft]**	**Hold time minutes**	**Average diameter change [mil]**	**Predicted diameter change [mil]**
[[										
										]]

[[

]]

Figure RAI 21-1a Segmented Rod Program Predicted vs. Measured Strain

Table RAI 21-2. [[ ]] Program Ramp Test Results

Halden NDT Rod Designation	Additive Content, ppm by Weight				Maximum diametral strain %	Predicted Diametral Strain (%)
		SiO_2:Al_2O_3 ratio	Peak Power During Ramp kW/ft	Hold time minutes		
[[						
						]]

[[

]]

Figure RAI 21-1b Predicted vs. Measured Diametral Strain ([[ ]])

As noted in the response to RAI 18, licensing analyses for additive fuel will be performed [[

]]. The additive fuel qualification cases were rerun [[

]]. The PRIME non-additive cladding strain qualification cases and the additive fuel qualification cases above were reanalyzed [[

]]. The perturbations are defined in Table RAI 21.3. The [[
]] results are shown in Figure RAI 21-1a (WSTOL) and Figure RAI 21-1c. As intended, use of [[
]].

Table RAI 21-3. Perturbations for [[ ]] Cladding Strain Analyses

Parameter	Perturbed Value
[[	
	]]

[[

]]

Figure RAI 21-1c Predicted vs. Measured Diametral Strain ([[ ]])

To further address [[
]], measured cladding permanent strain for non-additive and additive fuel [[ ]] are presented in Figure RAI 21-2. The results in Figure RAI 21-2 indicate [[
]]. These results help explain [[ ]] results presented in the response to RAI 21(g) below.

[[

]]

Figure RAI 21-2 Measured Cladding Permanent Strain versus Exposure for [[ ]]

b. The power at the start of the test and the ramp terminal power for each of the rods in Figure 6-2 of Reference 21.1 are shown as a function of nodal exposure in Figure RAI 21-3. It is noted that both delta power and terminal power for the non-additive rods which failed during ramp testing [[
]].

[[

]]

Figure RAI 21-3 Ramp Terminal Power vs. Exposure

c. Currently, linear heat generation rate (LHGR) operating limits for non-additive fuel are identical for barrier and non-barrier cladding. Because of the susceptibility of fuel with non-barrier to PCI failures during rapid power increases, GNF provides operating recommendations for fuel with non-barrier cladding to minimize the risk of PCI failures. [[ ]] operating guidelines are offered for barrier fuel for those utilities that choose to apply them to improve the already high reliability of GNF fuel. To improve reliability even further, GNF is currently offering additive fuel. The LHGR limits for additive fuel [[ ]]. However, based upon additive ramp test results currently available, [[

]].

d. Data confirming [[ ]] of additive fuel was a major finding of the EPMA analyses of additive pellets from the [[ ]] Halden ramp tests (Reference 21.3). In GNF additive fuel, [[ ]]. Trapping of [[ ]] was observed for all additive concentrations ([[ ]]) tested.

Similar results were reported by the SCIPII Project (Reference 21.4), where results of EPMA analyses indicated the existence of [[ ]] in the center region of the pellet. The Post Irradiation Examination (PIE) of rods from the [[ ]] Halden ramp tests also included EPMA analyses for the inner cladding surface. The inner cladding surfaces [[

]].

There is no data from EPMA analyses of [[

]].

e. Experimental data that directly confirms fuel movement for GNF additive fuel, such as filling of dishes or axial column elongation, is not available. The basis for such movement is based upon the expectation that GNF additive pellets [[ ]] than non-additive pellets; the basis is discussed in the response to RAI 26c. Indirect confirmation of additive movement is provided [[ ]], for additive fuel relative to non-additive fuel for comparable ramps. Such data is shown in Figure RAI 21-2.

f. For the PRIME cladding strain analyses of the newly added SRP rods discussed in the response to RAI 21a above, for 2-56, 2-57 and 2-97 the grain size was assumed to be [[ ]] microns and for 3-90 and 3-91 the grain size was assumed to be [[ ]] microns. These assumptions were based upon available pre-characterization data. It should be noted that for PRIME qualification, it is standard GNF practice to use the best available input data, since PRIME is intended to be a best estimate model. As discussed in the response to RAI 21a, for PRIME licensing analyses of additive fuel, the grain size [[ ]].

g. In Figure 5-3 of Reference 21.1, the calculated cladding permanent circumferential strain is shown as a function of exposure for [[ ]]. At the time that Reference 21.1 was prepared, the PRIME code and methodology were being reviewed

by the NRC, and the [[ ]]. As part of the PRIME approval, [[ ]]. The results in Figure 5-3 have been modified to reflect this change; the modified results are presented in Figure RAI 21-4 below. In this figure the limit is [[ ]], so the margin is equal to the difference between [[ ]] and the calculated strain. As shown in Figure RAI 21-4, the revised limit [[ ]].

The [[ ]] licensing analysis is performed by assuming an [[ ]]. The results in Figure RAI 21-4 show [[ ]]. To show the evolution of this strain [[ ]] are presented in Figure RAI 21-5. Figure RAI 21-5 shows [[ ]] at the top of the power increase. The difference is due to the large contribution of elastic strain to total strain at the start of the hold.

As noted above, Reference 21.1 was prepared before the PRIME and GNF2 licensing reviews were completed and the [[ ]] assumed for the licensing calculations were preliminary. The current GNF2 [[ ]] is less limiting, so the results in Reference 21.1 are conservative [[ ]].

[[

]]

Figure RAI 21-4 Calculated Cladding Strain for [[ ]]

[[

]]

Figure RAI 21-5 Cladding Strain Components for [[ ]]

Inputs for FRAPCON analyses are in Attachment 21.A[4].

References:

21.1 GNF, "Additive Fuel Pellets for GNF Fuel Designs," NEDC-33406P, Revision 2, October 2009.

21.2 GNF, "The PRIME Model for Analysis of Fuel Rod Thermal-Mechanical Performance, Part 1-Technical Bases," NEDC-33256P-A, Revision1, September 2010.

21.3 EPRI and Vattenfall Bränsle AB Report, "Post-irradiation Examination of GNF Rods Ramped in Halden," 2004.

21.4 Ella Ekeroth, "SCIPII Subtask2.1 SEM/EPMA after Ramp on Rodlet Ga (GNF Additive)," Presentation at SCIPII Meeting," November 3-5, 2010.

21.5 S. B. Wisner et al., "Embrittlement of Irradiated Zircaloy by Cadmium and Iodine," Embrittlement by Liquid and Solid Metals, M. H. Kamdar, Ed., Metallurgical Society of AIME, 437-456, 1982.

21.6 J. Matsunaga et al., "Chemical Trap Effect of Aluminosilicate Additive Fuel," Proceedings of 2010 LWR Fuel Performance Meeting, TopFuel/WRFPM, Orlando, Florida, 2010.

[4] Reference 21.1 was prepared before the PRIME and GNF2 licensing reviews were completed and the [[ ]] assumed for the licensing calculations were preliminary. The current GNF2 [[ ]] is less limiting in terms of both LHGR and exposure, however, to maintain a consistent basis, the [[ ]] used in Reference 21.1 is provided in Attachment 21.A. Therefore, the provided [[ ]] is conservative [[ ]]

NRC RAI 21-S01

Resolution of PNNL Comments/Questions and Requests on GNF Responses to Round 02 RAIs Sent October 31, 2012 on Additive Fuel Pellet

NRC Comment

There appears to be [[ ]] in Figure 21.1b. The [[ ]] Halden power ramped rods are [[ ]]. In addition the three SRP rods with measured positive strains on the first power ramp are [[ ]], there is a much better prediction on the second power ramp but AOO events only consist of one power transient not two consecutive transients. The first transient could be considered more prototypical of an AOO power transient with the exception that the first SRP power ramp was [[ ]]. The [[ ]] in Figure 21.1c for measured positive strains. Figure 21.2 demonstrates that [[ ]].

NRC Request

Please provide the mean of the predicted-minus-measured and standard deviation for the UO_2 data for measured positive strains, provide the number of data points based on these values of mean and σ. Please provide the mean of the predicted-minus-measured and standard deviation for additive fuel data for measured positive strains for power ramped rods, provide the number of data points based on these values of mean and σ. The probability that these two populations of additive and UO_2 fuel are similar or different can be determined, however, the analysis needs to consider that the number of data points is significantly different for the two populations. It appears that [[ ]]. Also, how were the [[ ]] applied in Figure 21.1c compared to how [[ ]] are applied in licensing analyses of cladding strain for an AOO event?

GNF Response

The comment [[ ]]. As discussed in the response to RAI 21, GNF-A [[

]], as shown in Figure RAI 21-2 of Response 21. As noted in the comment above, Pacific Northwest National Laboratory (PNNL) agrees qualitatively with this conclusion. In consideration of the very limited additive ramp test data available, at this time [[

]]

Additionally, the comment [[

]] The comparison of predicted and measured cladding strains for these ramps is very good. Although data is limited, the results confirm the adequacy of the PRIME code for analyses of AOOs for additive fuel.

Finally, the question is posed [[

]] was not included in the reanalysis of the qualification results.

ATTACHMENT 21.A

Fuel Rod Dimensions:

Parameter	Nominal Value
[[	
	]]

Plenum Spring Dimensions:

Parameter	Nominal Value
[[	
	]]

Pellet Isotopics:

Parameter	Nominal Value
[[	
	]]

Pellet Fabrication:

[[	
	]]

Cladding Fabrication:

[[	

[5] [[ ]]

	]]

Rod Fill Conditions:

[[	
	]]

Reactor Conditions:

[[	
	]]

Power History:
Power histories are provided in PRIME input format. [[

[6] The range of basal pole texture factors in the longitudinal, circumferential and radial directions were provided in the LTR. Based upon FRAPCON-3 documentation, the nominal texture factor in the longitudinal direction (fraction of basal poles parallel to the longitudinal axis) is provided for use in FRAPCON-3 benchmarking.

]]

NRC RAI 22

The following are related to clarifying the equations given in the LTR.

a. The PRIME thermal conductivity model does not appear to be valid for the case with no Gd_2O_3 and zero burnup. In this case, the parameter χ is 0, which leads to undefined values for K in equation 2-11 and 2-12. Please provide details for how the thermal conductivity of unirradiated UO_2 is calculated.

b. The value of thermal conductivity calculated by the PRIME model appears to [[ ]]. Please confirm this behavior of the model and explain how this is acceptable.

c. The variable, ρ , in the equation on Page 2-42 is not defined. Based on its use, it is assumed that this variable is the percent theoretical density (as-fabricated?) of the fuel pellet. Please confirm this assumption.

d. *The value of the modulus of elasticity of $(U,Gd)O_2$ at room temperature, E_U, in equation 2-26 is not provided. Please provide this value.*

GNF Response

a. [[

]]

[[

]]

Figure RAI 22-1. [[ ]] **from PRIME Thermal Conductivity Model**

b. Plots of thermal conductivity versus temperature for UO_2 and the maximum additive concentration of [[ ]] are shown in Figure RAI 22-2. The thermal conductivity for the additive fuel [[

]]

[[

]]

Figure RAI 22-2. PRIME Thermal Conductivity versus Temperature

The [[

]], which is indicated in Figure RAI 22-2.

c. The equation referred to is used to calculate cumulative exposure in f/cc The NRC's assumption is correct. The variable ρ represents fuel pellet density (%TD).
d. In the PRIME code the modulus of elasticity for $(U,Gd)O_2$ fuel is given by the equation.

[[

]]

Assuming an initial density of [[ ]], applying this equation to calculate Eu at room temperature yields

Eu = [[ ]]

Reference:

22.1 GNF, 'The PRIME Model for Analysis of Fuel Rod Thermal-Mechanical Performance, Part 1-Technical Bases', NEDC-33256P-A Rev. 1, September 2010.

NRC RAI 23

Section 2.14, Page 2-44 and Section 3.3 suggest that the existence of Si:Al_2O_3 on grain boundaries will result in similar behavior to non-additive fuel in a reactivity insertion accident (RIA). It appears that the RIA tests provided in Figure 3-6 for additive fuel utilized fresh fuel (no base irradiation, essentially zero burnup). Is this interpretation correct? It is known that the increase fission gas bubbles on the grain boundaries with burnup has a significant impact on fuel dispersal when the cladding fails during a RIA. Because the Si:Al_2O_3 also exists on the grain boundaries and weakens this boundary there may be some interaction of the fission gas/products with Si:Al_2O_3 that could impact the strength of the grain boundaries, which in turn may lead to an increase in additive fuel dispersal. This scenario is reasonable considering that EPMA measurements suggest that cesium is retained in larger amounts on the grain boundaries than for UO_2 due to the presence of Si:Al_2O_3 on the grain boundaries of additive fuel. In addition, Electric Power Research Institute (EPRI) December 2010 technical report number 1021036, "Fuel Reliability Program: Proposed RIA Acceptance Criteria", suggests that mixed oxide (MOX) fuel has a significant amount of gaseous swelling during a RIA that reduces the RIA failure threshold compared to that for UO_2. MOX fuel has a similar situation to additive fuel where a significant number of gas bubbles exist within a matrix (PuO_2) of MOX that has a higher creep rate than UO_2. The EPRI report suggests will lead to greater gaseous swelling than for UO_2.] The additive fuel has a significant amount of gas bubbles on the grain boundaries with Si:Al_2O_3 that also exhibits a high creep rate. Have out-of-reactor fast heating tests been performed on high burnup additive and non-additive fuel to demonstrate similarities or differences in grain boundary strength? Are there other tests that could be used to examine grain boundary strength of high burnup additive fuel?

<u>Additional Request per NRC-GNF Meeting August 9, 2012</u>
Provide details of the temperature ramp testing for the high burnup additive fuel.

<u>GNF Response</u>

The results in Figure 3-6 are for unirradiated fuel. The RAI [[

]]

First, the similarities between additive fuel and MOX noted above occur by different mechanisms. The increased release for MOX results from regions of high fissioning rate due to the non-homogeneous structure of MOX fuel, which consists of Pu rich regions surrounded by $(U,Pu)O_2$ solid solution. The result is regions with increased fission gas bubbles, high creep rate and high gaseous swelling. The increased fission gas release resulting from the non-homogeneous structure of MOX, and the increased gaseous swelling, [[

]].

Next, since the high burnup structure (HBS) at the pellet periphery of the high burnup fuel has the potential to affect pellet fragmentation and fuel dispersal, the impact of additive on the thermal and mechanical properties of the HBS are considered. The development of the HBS is summarized in the response to RAI 17c. As noted in the response, the GNF additive is [[

]] The impact of additive on HBS structure has been studied by Post Irradiation Examination (PIE) of 9x9 LUAs. [[

]] Additional fission product release, thermal diffusivity and heat capacity data was obtained by heating specimens from pellet peripheral regions with (local) burnups of 30, 60, 74 and 86 GWd/MTU to temperatures between 600 and 1800 ^{o}C at heating rates between 1.7 and 4600 ^{o}C/sec. Details of both the pellet cracking tests and the tests on pellet rim specimens are provided in Reference 23.1. From the results of these tests, it is concluded that no major impacts of the additive on the HBS have been observed to date.

Finally, the effect of the GNF additive on pellet microstructure at the start of an RIA at high burnup is considered through comparison of PIE of pellet microstructure for UO_2 and additive rods included in the [[ ]] Halden ramp tests described in Section 4.1.3 of Reference 23.2. [[

]] The regions near the center of the pellets contained both intra- and intergranular pores. The size, number and relative frequency of such pores changed with increasing pellet radius. From the results of PIE of pellets subjected to ramp tests, it is concluded that [[ ]].

References:

23.1 K. Une et al., J. Nucl. Sci. Technol., 1161-1171, 43(9), 2006.
23.2 Licensing Topical Report, 'Additive Fuel Pellets for GNF Fuel Designs', NEDC-33406P Rev. 2, October 2009.
23.3 Post-irradiation Examination of GNF Rods Ramped in Halden', EPRI and Vattenfall Bränsle AB Report, 2004.

NRC RAI 23-S01

Responses to PNNL Comments/Questions and Requests on GNF Responses to Round 02 RAIs Sent October 31, 2012 on Additive Fuel Pellet

NRC Comment

PNNL has performed an evaluation of the UO_2 and MOX pellet clad mechanical interaction (PCMI) failure thresholds for RIA and determined that there is no significant difference. PNNL has concluded that the difference in gas on the grain boundaries of UO_2 versus MOX fuel has no impact on the PCMI failure threshold because the strength of the cladding during the early part of the RIA is strong enough to contain the gas on the grain boundaries for this very fast RIA transient (because cladding temperatures are relatively low early in the tranisent). The NEA/OECD report (ISBN 978-92-64-99113-2, NEA/CSNI/R,2010) also came to a similar conclusion for MOX fuel. This conclusion is also likely to apply to additive fuel. [[

]] It is known that the FGR during a RIA event is due to fracturing of the grain boundaries that contains gas bubbles. Therefore, if [[ ]] more will be released when they are fractured during a RIA. It is difficult to determine the impact of additive fuel on the radiological release without FGR data.

NRC Request

This issue of radiological release needs to be addressed.

GNF Response

The comment notes the increased fission gas retention on grain boundaries for MOX fuel relative to UO_2 fuel and the concerns about possible reduced pellet clad mechanical interaction (PCMI) failure thresholds and increased radiological release during an reactivity insertion accident (RIA) due to the increased retention. The comment then expresses similar concerns for additive fuel [[

]]. As discussed in the response to RAI 23, the size and distribution of grains and subgrains and of grain boundary bubbles in additive fuel is expected to be different than for MOX fuel and the grain boundary bubbles are expected to have little impact of dispersal of additive fuel relative to UO_2 fuel. More specifically, because the additive phase is non-fissioning and uniformly distributed, regions with increased fission gas bubbles observed in MOX fuel will not occur for additive fuel. Additionally, as noted in Reference 23-S01.1, the Global Nuclear Fuel (GNF) alumina-silica additive has negligible effect on the diffusivity of fission gas atoms within pellet grains, so that except for differences due to different grain sizes, the fission gas atoms arriving at grain boundaries will be similar for additive and UO_2 fuel. This fission gas is either retained in fission gas bubbles on the grain boundaries or released to the rod void space. If more gas was being retained on grain boundaries for additive fuel relative to UO_2 fuel, the retained gas would result in increased swelling of additive fuel relative to UO_2 fuel. However, as noted in Response 17d, [[ ]],

indicating similar fission gas retention on grain boundaries for additive fuel relative to UO_2 fuel. Scanning Electron Microscope (SEM) images in Reference 23-S01.2 confirm similar retention for additive and UO_2 fuels [[ ]]. Thus available information suggests that gas retention on grain boundaries [[ ]]. Also, as discussed in Response to RAI 20, fission gas release is similar for UO_2 and additive fuel, which also indicates [[ ]]. Finally, from Reference 23-S01.1, the increased PCI resistance of GNF alumina-silica additive fuel relative to UO_2 fuel is attributed to the trapping of iodine on pellet grain boundaries by Cs-Al-Si-O compounds and not by the trapping of more abundant fission gases, including Xe and Kr.

Based upon the above, GNF concludes that [[ ]]. However, GNF recognizes the Pacific Northwest National Laboratory (PNNL) concerns regarding increased retention of fission gas on grain boundaries on RIA response; these concerns are addressed below.

The licensing basis of boiling water reactor (BWR) fuel includes consideration of several design basis accidents. The licensing basis BWR RIA is the Control Rod Drop Accident (CRDA). The primary concerns for a CRDA are the release of fission gas and the dispersal of fuel to the coolant. To address these concerns, failure threshold and design limit energy deposition limits are applied to the CRDA. The failure threshold is applied to determine the number of fuel rod failures during the event, as an input to the radiological consequence assessment of the event; the design limit is imposed to ensure core coolability and provide protection to the reactor system by avoiding the generation of damaging pressure pulses that might result from energetic fuel dispersal from the fuel rods to the reactor coolant. Using the failure criterion, the licensing basis analysis of the CRDA conservatively calculates the number of rods that fail due to the transient conditions resulting from rapid removal of a control rod, including fuel melting in approximately [[ ]]. The analysis then confirms that the resultant fission gas release can be processed by the plant offgas system and released off-site without violating Tech Spec limits for that plant. Because of the local nature of the CRDA and thus the limited number of rods impacted, the fission gas release due to a CRDA [[ ]]. For additive fuel, even if the release in the impacted rods was significantly higher than predicted [[ ]], the impact relative to the capacity of the offgas system would be small. The dispersal of fuel from rods that exceed the design limit depends upon the range of particle sizes, which can range from subgrain size in the high burnup rim to grain size to fragments due to pellet fracture due to differential thermal expansion. The distribution depends upon the extent of high burnup structure, initial grain size and fracture strength of the fuel. The bundles impacted by a CRDA will include a range of burnups. Thus fuel dispersion and the resulting pressure pulse is extremely variable. For this reason, [[ ]]. As noted in Response 17c, [[

]]

In summary, potential radiological release impacts of additive fuel relative to UO_2 are expected to be negligible in terms of the CRDA licensing basis analysis.

References:

23-S01.1 Proceedings of 2010 LWR Fuel Performance/ TopFuel/ WRFPM, "Chemical Trap Effect of AluminoSilicate Additive Fuel," Paper 024, September 2010.

23-S01.2 Journal of Nuclear Materials, "EPMA and SEM of Fuel Samples from PWR Rods with an Average Burn-up of Around 100 MWd/kgHM," Manzel, R. and Walker, C.T., Vol. 301, pp. 170 – 182, 2002.

NRC RAI 24

Please provide the radial volume fraction of additive fuel melt versus fuel radius at the peak axial temperature locations for thermal overpower and MOP limits. The weight of the fuel column is significant for a 12-foot length. Has fuel slumping for additive fuel been examined for full-length (12-foot) fuel columns?

Additional Request per NRC-GNF Meeting August 9, 2012
Provide eutectic volume fraction as a function of active fuel length.

GNF Response

As discussed in Section 2.2 of Reference 24.1 and Response to RAI 4 of Additive RAIs, the concept of slump temperature has been introduced for additive fuel to assure geometric stability of additive fuel at high temperature. [[

]] The intent of the 'no fuel melting' regulatory criterion is to assure geometric stability of the pellet and preclude radial migration of liquid fuel to the fuel cladding. The criterion is also intended to preclude axial migration of liquid fuel. [[

]]

[[

]]

On the basis of the discussion above, the requested radial volume fractions are calculated on the basis of the radius at which the fuel temperature is equal to the slump temperature. The calculations are based upon results from the same analyses performed to determine the [[ ]] responses discussed in Sections 5.1 and 5.3 respectively of Reference 24.1. Results for additive fuel with additive concentration of [[ ]]) are given in Table RAI 24.1 below. Results are given at [[

]]. Also included in the table are the radial volume fractions corresponding to [[ ]]. Between the [[

]].

Table RAI 24-1: Slump Temperature and [[ ]] Radii and Volume Fractions for Additive Fuel

	[[ ]]/R_p	Radial Volume Fraction	R_{eut}/R_p	Radial Volume Fraction
[[				
				]]

In Table RAI 24-1 R_{eut} is the radius at which the pellet temperature is equal to the eutectic temperature, [[
]] and R_p is the pellet radius.

[[

]]

The results in Table RAI 24-1 are for a single axial node. To determine the axial distribution of pellet volume above the eutectic temperature during an anticipated operational occurrence (AOO), [[

]] The results are shown in Table RAI 24-2. As indicated in the table, node 1 is the bottom node. The results for node 3 correspond to [[
]].

Table RAI 24-2: Axial Distribution of Eutectic Temperature Radius and Volume Fraction for Additive Fuel

Axial Node	OP (%)	R_{eut}/R_p	Radial Volume Fraction
[[			
			]]

Combining the results for all axial nodes, the calculated eutectic volume fraction for the rod is [[ ]]. Thus [[ ]] of the fuel will be above the eutectic temperature. [[ ]] This indicates that for the assumed AOO [[ ]], but that 100% of the fuel is geometrically stable.

GNF has not examined full length rods for fuel slumping. However, it is noted that slumping would not be expected for rods that did not experience an OP event and slumping would not be expected for an event satisfying [[ ]]. Even if [[ ]] were exceeded the full length of the rod would not be impacted. Any tendency for axial slump in the impacted region would be constrained by the fuel with no axial slump in the non-impacted zone below the impacted zone (such as node 1 in Table RAI 24-2). Similarly, even if the lower portion of the rod were to exceed [[ ]], unlike for the case of isotropic heating where the entire pellet exceeds the slump temperature, the radial volume fraction of the pellet above the slump temperature would be limited to a small fraction at the center of the pellet. The weight of the fuel stack above the pellet would be supported by the outer region of the pellet and geometric instability or collapse of the pellet due to the weight of the fuel column would not occur.

References:

24.1 Global Nuclear Fuel, “Additive Fuel Pellets for GNF Fuel Design,” NEDC-33406P, Revision 2, December 2009.

24.2 Global Nuclear Fuel, “The PRIME Model for Analysis of Fuel Rod Thermal-Mechanical Performance, Part 1-Technical Bases,” NEDC-33256P-A, Revision 1, September 2010.

NRC RAI 24-S01

Responses to PNNL Comments/Questions and Requests on GNF Responses to Round 02 RAIs Sent October 31, 2012 on Additive Fuel Pellet

NRC Comment

Probably want to limit the amount of time with a significant fraction of fuel above the eutectic temperature.

NRC Request

Please propose a time limit.

GNF Response

As clarified in the December 13, 2012 call between Pacific Northwest National Laboratory (PNNL), the Nuclear Regulatory Commission (NRC), and Global Nuclear Fuel (GNF), the expressed concern is with the slump temperature rather than the eutectic temperature. This concern is addressed below.

One objective of the current GNF-A fuel rod and core design methodologies is to assure that the licensing requirement of no fuel melting during normal operation, including anticipated operational occurrences (AOOs), is satisfied. To meet this objective, [[ ]] is defined on the basis of a limiting slow transient. The duration of the transient is assumed to be [[ ]] and is based upon the expected spectrum of slow boiling water reactor (BWR) transients.

As discussed in the response to RAI 3, for additive fuel [[ ]] The same transient duration is assumed for additive fuel as for UO_2 fuel. To confirm [[ ]], Table 2-1 from the additive fuel LTR is reproduced below and expanded to include both the additive concentration and the time at temperature. The planned test time was [[ ]]; test temperatures were near the liquidus temperature and were specified prior to testing [[ ]]. The two very short tests were terminated due to capsule breaching. The other tests that were less than [[ ]] were terminated due to increased possibility of breaching.

Additive Concentration (wt%)	Time at Temperature (minutes)	Liquid Volume (%)	[[Evidence]]
[[			
			]]

[[

]]

NRC RAI 24-S02

PNNL recommends [[

]] analysis of additive fuel rod. These time and liquid volume fraction limits apply to individual axial nodes within an additive fuel rod.

PNNL also recommends [[

]]

Response

As described in Reference 24-S02.1, [[ ]] behavior was investigated experimentally by holding additive pellets at elevated temperatures near the liquidus temperature to assure a significant liquid volume fraction (isothermal heating of entire pellet) for a prescribed amount of time ([[ ]]) and observing pellet [[ ]] behavior. Based on these experiments, it was determined that the condition of [[ ]] can conservatively be ensured by [[ ]]. Thus, in additive fuel licensing analysis, the fuel melting temperature is replaced by the [[ ]]. Thermal-mechanical design and licensing analyses will be performed to ensure pellet temperatures do not exceed the [[ ]].

As noted in the NRC request for this supplement, [[ ]]. For normal (steady-state) operation, due to the conservative nature of the Global Nuclear Fuel (GNF) thermal-mechanical analyses, where [[ ]], the temperature of peak power nodes can exceed the eutectic temperature of additive fuel ([[ ]]) in a very limited fashion for some portion of fuel life. For these peak power nodes, the pellet region above the eutectic is confined to a small fraction of the overall pellet volume (pellet central region), while the outer, cooler, region of the pellet remains fully solid, including the additive phase. Additionally, the pellet temperatures above the eutectic temperature would occur only in the highest power nodes axially and, thus axial nodes above and below high power nodes would also remain fully solid, including the additive phase. As a result, these lower temperature radial and axial portions provide mechanical support to the fuel column (see Figure 3-5 of Reference 24-S02.1).

As noted above, the slump tests were conducted on isothermally heated pellets. Thus these pellets did not contain the cooler outer portion without liquid (and did not contain the cooler pellets located axially above and below without liquid) that would be present during normal operation and that would constrain the liquid phase. It is anticipated that slump tests conducted with a radial temperature distribution such as occurs in normal operation would not exhibit slumping, even at temperatures of the magnitude tested in the additive slump tests (at or near liquidus temperature). At lower temperatures, such as those during steady-state operation, with

the very small percent of liquid volume shown in Figure RAI 24S-1, a change in pellet overall geometry (slumping) is considered extremely unlikely even for long durations.

Additionally, the geometric stability of additive pellets with very small percent of liquid volume is considered to be very high during normal operation for the following reason. [[

]] As discussed above, during steady-state operation a significant fraction of the outer region of the pellet remains below the eutectic temperature (discussed below and shown in Figure RAI 24S-2) and there are pellets completely below the eutectic temperature above and below the pellet with liquid phase. If any liquid phase was extruded, it would revert to solid phase upon reaching the cooler regions, and the pellet would be stable in terms of overall geometry. Additionally, it is noted that PCMI stresses during steady-state operation are lower than during power ramp testing, so the extrusion forces are lower than during ramp testing.

As an example of the limited extent of liquid phase, the total liquid volume percent for the peak power node was determined as a function of exposure (based on the example case in Section 3.2 of Reference 24-S02.1) and plotted in Figure RAI 24S-1; the corresponding fractional radius above the eutectic temperature is plotted in Figure RAI 24S-2 As illustrated, the total liquid volume fraction of fuel predicted during steady-state operation, [[

]] and is only be predicted to occur for a fraction of fuel rod lifetime. Figure RAI 24S-1 reinforces the assertion that additive fuel will remain geometrically stable during steady-state operation.

Finally, it is emphasized again that the results in Figures RAI 24S-1 and RAI 24S-2 are for [[ ]]. The actual (normal) operation of GNF fuel is specified to [[ ]]. Examination of fuel temperature for rods which operated normally in commercial reactors in the PRIME database shows that the fuel temperature did not exceed the additive eutectic temperature

[7] Reference 24-S02.1 was prepared before the PRIME and GNF2 licensing reviews were completed and the [[ ]] assumed for the licensing calculations were preliminary. The current GNF2 [[ ]] is less limiting in terms of both LHGR and exposure, however, to maintain a consistent basis, the [[ ]] used in Reference 24-S02.1 is used in this RAI response. Therefore, the results are conservative [[ ]]

([[ ]]) in any of the rods. It should be acknowledged that [[ ]]. However, the difference in thermal conductivity, and thus temperature, [[ ]] (Reference 24-S02.1). In this regard, it is also noted that the temperature review included the [[ ]] additive rods. The power histories for these rods are included in the response to RAI 20-S02 and [[ ]]. Thus these results indicate that no liquid phase would be present during actual operation of additive fuel.

Based on this discussion, GNF contends that the fuel column for additive fuel will remain geometrically stable during steady-state operation. Therefore, [[ ]] the total liquid volume percent predicted is very small, is confined to a small fraction of the overall pellet radius (volume), and will not impact overall pellet geometry/geometric stability.

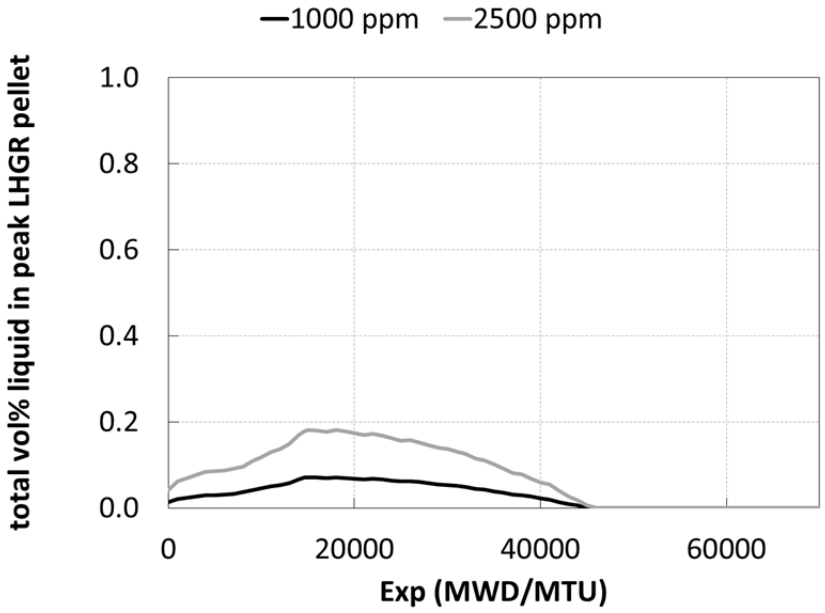

Figure RAI 24S-1. Example Total Liquid Volume Percent for Peak Power Node Operating along Bounding LHGR vs. Exposure Envelope

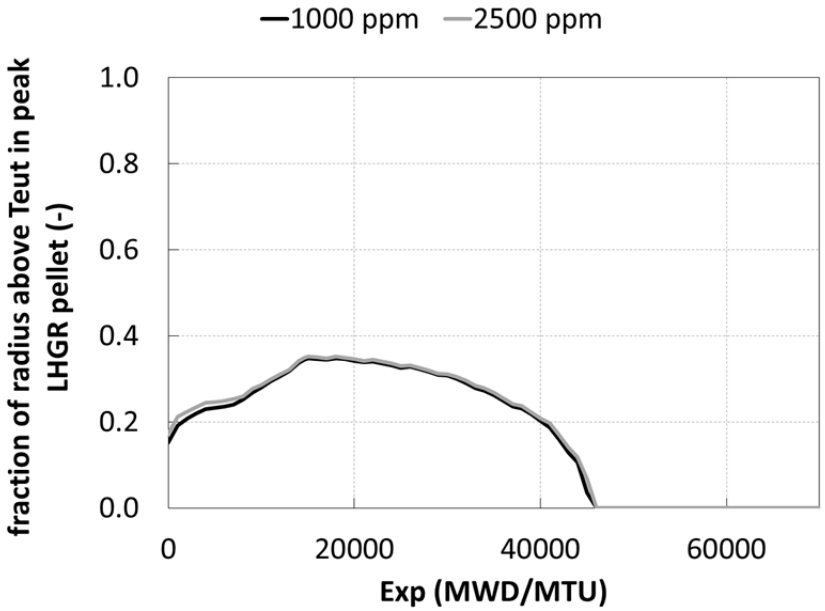

Figure RAI 24S-2. Example Fraction of Radius ≥ Teut for Peak Power Node Operating along Bounding LHGR vs. Exposure Envelope

Reference:

24-S02.1 Global Nuclear Fuel, "Additive Fuel Pellets for GNF Fuel Design," NEDC-33406P Rev. 2, December 2009.

NRC RAI 25

Page 3-3 notes that corrections were made to the fuel oxidation data to account for the effect of surface defects. Please explain how this was done. How many additive pellets prototypic of those for commercial reactor operation have been examined for surface defects to confirm that no surface defects exist in production additive fuel? It appears that the cause of the surface defects is unknown. Will sampling be performed on production fuel batches of additive fuel to confirm that no surface defects exist?

Additional Request per NRC-GNF Meeting August 9, 2012

Explain how the production qualification and on-going quality monitoring performed for additive pellets will ensure that the pellets meet specifications. Also address whether the qualification and on-going quality monitoring will be sufficient to detect [[

]].

GNF Response

As discussed in Section 3.1 of Reference 25.1, [[

]]

Reference:

25.1 Global Nuclear Fuel, "Additive Fuel Pellets for GNF Fuel Designs," NEDC-33406P, Revision 2, December 2009.

NRC RAI 25-S01

Responses to PNNL Comments/Questions and Requests on GNF Responses to Round 02 RAIs Sent October 31, 2012 on Additive Fuel Pellet

NRC Comment/Request

Is the [[ ]] of pellet volume correct because this seems very low? Is there a specification on [[ ]] and, if so, what is the specification? If not how will the [[ ]] be determined to be outside of normal fabrication?

GNF Response

As noted in the response to RAI 25, [[

]]

The specified [[ ]] limits for GNF additive (and UO_2) fuel pellets are as follows:

a. [[

]]

Project size can range from a limited number of LUAs to a full reload (~100-200 bundles).

To assure compliance with pellet specifications, including [[

]]

As discussed above, [[

]]

NRC RAI 26

The following are related to the fuel creep model and how it is applied in the code.

a. *It is noted that a large increase in the magnitude of creep model predictions exist between fuel with no additives and fuel with additives. This difference is especially large at large stress values relevant to AOO conditions. For example, at high stress and high temperature the model predicts a [[*

]] Please provide data to justify the use of [[

]]

b. *Please provide measured creep strains versus time for temperatures of 1673K at approximately 4 kilo-pounds per square inch (ksi) stress ([[ ]]), 1573K at approximately 6 ksi stress [[ ]] 1473K at approximately 9 ksi [[ ]], and 1673K at approximately 5 ksi stress [[ ]] Also provide the model predictions for this data.*

c. *In order to conserve fuel mass, where does the code assume the fuel moves if it does not expand in the radial or hoop directions when hard contact is established between the fuel and cladding? Does it expand in the axial direction or by dish filling once a fraction of the as-fabricated porosity is filled? Has this movement of the fuel been confirmed experimentally?*

<u>Additional Request per NRC-GNF Meeting August 9, 2012</u>

Explain why the cladding strain in Figure 26.3 does not agree with the strain for the same case shown in Table 21.1. Also, explain [[

]].

<u>GNF Response</u>

a. Large creep rates for additive fuel, such as shown in Figure 2-15 of Reference 26.1, do not occur in PRIME (Reference 26.2) calculations, since the applied stress in PRIME creep calculations is limited by pellet yield and as a result the applied stress at high temperature, specifically temperatures above the eutectic temperature, do not reach the levels shown in Figure 2-15. As shown in the response to RAI 17a, the yield stress at the eutectic temperature ([[ ]]) is less than [[ ]] for additive (and non-additive) fuel .

b. Subsequent to the development of the PRIME creep model for additive fuel, Global Nuclear Fuel (GNF) conducted creep tests on [[ ]] additive (and non-additive) archive fuel pellets for a range of temperature, stress and additive concentrations (Reference 26.3). Comparison of measured and calculated creep strains at 1813K for 1.7 ksi and [[ ]] is presented in Figure RAI 26-1. This figure was generated by superimposing calculated steady-state creep strain on the trace of measured strain versus time. Other results are available in Reference 26.3. In a creep test, the measured strain consists of an initial strain at the start of the test (time=0) due to application of the load, a primary creep strain component and a steady-state creep strain component for which the creep rate is constant. In Figure RAI 26-1, the initial strain is negligible (since the applied

stress is low); primary creep occurs between [[ ]] and is followed by steady-state creep. As indicated in Figure RAI 26-1, the PRIME creep model predicts the steady-state creep rate well [[

]] For normal boiling water reactor (BWR) operation, power increases occur as a result of startup or control blade withdrawal [[ ]]. Thus [[

]]

[[

]]

Figure RAI 26-1 Predicted and Measured Creep Strain versus Time

c. In PRIME, during a power increase pellet thermal expansion causes closure of the pellet-cladding gap. Initial pellet-cladding interaction is [[

]]

Direct data to confirm [[

]]. However, as discussed in the response to RAI 21a, measured permanent cladding strains for additive and non-additive fuel ramped to [[

]]. The results are shown in Figure RAI 21-2. Since the ramp terminal powers and hold times are identical for the results in Figure RAI 21-2, increasing exposure corresponds approximately to increased PCMI. [[

]]

To further address the effect of the GNF additive on fuel movement during a power ramp, a parametric study on additive concentration was performed with PRIME for one of the rods included in the SRP ramp tests discussed in the response to RAI 21a. The rod was SRP2-97 with additive concentration of [[ ]]. The ramp was an A ([[ ]]) ramp to [[ ]]. Full details are included in Table RAI 21-1. For the parametric study, PRIME analyses were performed for additive concentrations of [[ ]] and compared to the results for the actual concentration.

Based upon the discussion of fuel movement above, it is anticipated that [[

]] Calculated hot void volume and cladding diametral strain at the ramped node from the PRIME parametric cases are presented as functions of time in Figures RAI 26-2 and RAI 26-3 below. From these figures it is noted that [[

]].

Concerning cladding strains, it is noted that Figure RAI 26-3 in the draft response reviewed with the Nuclear Regulatory Commission (NRC) during the August 9, 2012 meeting did not have the correct cladding strains. Figure RAI 26-3 below contains the correct strains. Additionally, it is noted that the cladding strains contained in Table RAI 21-1 are [[ ]] and the strains in Figure RAI 26-3 are [[ ]]. [[

]] Finally, it is noted that the cladding strains for the cases in Figure RAI 26-3 decrease by [[

]]

[[

]]

Figure RAI 26-2 Hot Void Volume (SRP2-97)

[[

]]

Figure RAI 26-3 Cladding Diametral Strain (SRP2-97)

References:

26.1 Global Nuclear Fuel, "Additive Fuel Pellets for GNF Fuel Designs," NEDC-33406P, Revision 2, December 2009.
26.2 Global Nuclear Fuel, "The PRIME Model for Analysis of Fuel Rod Thermal-Mechanical Performance, Part 1-Technical Bases," NEDC-33256P-A, Revision 1, September 2010.
26.3 EPRI Research Project, "Power Ramp Test of Additive Fuel Rods: Results of Ramp Tests in the Halden Reactor," WO 3564-06, Global Nuclear Fuel, 2002.